Polycyclic indole derivatives as novel structures for neuroprotection

Dissertation submitted in partial fulfilment of the requirements for the degree

MAGISTER SCIENTIAE

in

the Department of Pharmaceutical Chemistry

at the North-West University, Potchefstroom Campus

By

Armand de Vries

December 2006

Supervisor: Prof S.F. Malan
Co-supervisor: Prof D.W. Oliver

Table of contents

Abbreviations

PD	-	Parkinson's disease
SAR	-	Structure-activity relationships
O_2	-	Oxygen
ROS	-	Reactive oxygen species
LMWA	-	Low molecular weight antioxidants
SOD	-	Superoxide dismutase
OS	-	Oxidative stress
NADPH	-	Nicotinamide adenine dinucleotide phosphate
CNS	-	Central nervous system
BBB	-	Blood-brain barrier
NMDA	-	N-methyl-D-aspartate
nNOS	-	Neuronal nitric oxide synthase
MAO-B	-	Monoamine oxidase oxidase B
MPTP	-	1-methyl-4-phenyl-1,2,3,6-tetrahydropyridine
MPP^+	-	1-Methyl-4-phenylpyridinium
7-NI	-	7-nitroindazole
$MPDP^+$	-	1-methyl-4-phenyl-1,2,3,6-tetrahydropyridine
DA	-	Dopamine
ATP	-	Adenosine triphosphate
TBA	-	Thiobarbituric acid
NOS	-	Nitric oxide synthase
3-NP	-	3-nitropropionic acid
MA	-	Malonic acid
HD	-	Huntington's disease
EAA	-	Excitatory amino acid
RNS	-	reactive nitrogen species
AMPA	-	α-Amino-3-hydroxy-5-methylisoxazole-4-propionic acid
KA	-	Kainate
NO	-	nitric oxide
mGluR	-	metabotropic glutamate receptor
PL	-	phospholipidsPLA_2 - phospholipase A_2

DAG	-	diacylglycerol
PLC	-	phospholipase C
PKC	-	protein kinase C
G	-	G protein
PIP_2	-	phosphatidylinositol 4,5-bisphosphate
IP_3	-	inositol 1,4,5-trisphosphate
H_2O_2	-	hydrogen peroxide
VSCC	-	voltage-sensitive Ca^{2+} channel
•OH	-	hydroxyl radical
$ONOO^-$	-	peroxynitrite
DNA	-	Deoxyribonucleic acid
PARS	-	poly ADP ribosyl synthase
PARP	-	poly ADP ribosyl polymerase
NAD	-	Nicotinamide adenine dinucleotide
HNE	-	4-hydroxynonenal
SNO	-	cysteine sulfhydryl group
CTD	-	carboxyl terminal domain
PCP	-	phencyclidine
TBI	-	traumatic brain injury
CDPC	-	Cytidine 5'-diphosphocholine
eNOS	-	Endothelial nitric oxide synthase
iNOS	-	Inducible nitric oxide synthase
H_4B	-	Biopterin
TRIM	-	1-(2-trifluoromethylphenyl) imidazole
DDAH	-	dimethylarginine dimethylaminohydrolase
AD	-	Alzheimer's disease
3-Br-7-NI	-	3-bromo-7-nitroindazole
L-Arg	-	L-arginine
SD	-	Structural data
L-NHA	-	N^{ω}-Hydroxy-L-arginine
EI	-	Electron ionisation
HRMS	-	High resolusion mass spectrometry
IR	-	Infrared
TLC	-	Thin layer chromatography

Abbreviations

NBT	-	Nitro blue tetrazolium
OxyHb	-	Oxyhemoglobin
metHb	-	Methemoglobin
PUFAs	-	Polyunsaturated fatty acids
MDA	-	Malondialdehyde
PBS	-	Phosphate-buffered saline

Abstract

The lethal triplet of metabolic compromise, excitotoxicity and oxidative stress causes neuronal cell death that is both necrotic and apoptotic in nature. Aspects of each of these mechanisms are believed to play a role in the neurodegeneration that occurs in both Parkinson's and Huntington's diseases.

The overstimulation of the *N*-methyl-D-aspartate (NMDA) subtype of glutamate receptors is involved in excitotoxicity, a process in neurodegeneration that characterises some neurological disorders and acute cerebral insults. In this process excess NO formation and oxidative stresses are key factors. In searching for compounds with neuroprotective properties, a series of tryptamine derivatives were synthesised and their effects were evaluated on both NOS and lipid peroxidation activity.

Computer modelling was performed using Catalyst 4.9® and the Ligandfit module of Cerius²® to determine the feasibility for synthesis and biological evaluation of the novel compounds. The hydrogen bond network formed in the enzyme was used as an indication for possible inhibitory activity. H-bonds with Tpr587, Glu592 and heme were taken as essential for NOS activity. Hydrogen bonds with Tyr588, Gln478 and Asp597 could also be important, since these amino acids play a role in the stabilisation and orientation of ligands in the cavity. The molecular modelling study indicated that the novel compounds were potential candidates for future investigation in view of their interaction at the NOS active site.

Compounds were synthesised by reductive amination or activation chemistry with various linkers. Novel rearranged polycyclic structures were obtained when linkers were applied. Difficulties were experienced with yields, purification and isolation of the compounds and could be attributed to solubility and multiple reactions taking place. Selected compounds were characterised and evaluated for NOS and antioxidative properties.

The oxyhemoglobin assay was employed to determine the NOS activity of the polycyclic indole derivatives. Results from the assay showed that four compounds, containing the indole moiety, 8-[3-(2-aminoethyl)indole]-pentacyclo[5.4.0.$0^{2,6}$.$0^{3,10}$.$0^{5,9}$]undecane-11-one (**1**), 3-hydroxy-4-[3-(2-aminoethyl)indole]-azahexacyclo[5.4.1.$0^{2,6}$.$0^{3,10}$.$0^{5,9}$.$0^{8,11}$]dodecane (**3**), 8-[3-(2-aminoethyl)indole]-pentacyclo[5.4.$0^{2,6}$.$0^{3,10}$.$0^{5,9}$]undecane (**4**) and 8-[3-(2-

aminoethyl)indole]-pentacyclo[5.4.$0^{2,6}$.$0^{3,10}$.$0^{5,9}$]undecane (**5**) displayed potencies in the sub millimolar range. Compounds such as **19** and **21** that do not possess an indole moiety, were poor inhibitors of NOS.

From the lipid peroxidation study, compounds **1**, **2**, **3**, **4** and **5** showed antioxidative properties comparable to that of trolox.

The results obtained in this study clearly indicate the potential of these novel indole cage structures as NOS inhibitors and anti-oxidants.

Taking the above aspects into account, together with the described calcium channel activity of the cage structures, these novel compounds may find applications as multipotent drugs in neuroprotection.

Uittreksel

Die letale triplet bestaande uit metaboliese afwyking, eksitotoksisiteit en oksidatiewe skade lei tot seldood wat nekroties en/of apoptoties van aard is. Elkeen van hierdie drie meganismes speel 'n rol in neurodegenerasie en kom voor in Parkinson en Huntington se siekte.

Oorstimulasie van die M-metiel-D-aspartaat (NMDA) reseptore is betrokke by eksitotoksisiteit, 'n proses in neurodegenerasie wat sommige neurologiese siektes en akute serebrale skade karakteriseer. Oormatige produksie van stikstofoksied (NO) en oksidatiewe skade is sleutelfaktore tydens hierdie proses. In die soeke na verbindings met neurobeskermende eienskappe is 'n reeks tryptamienderivate gesintetiseer en geëvalueer vir inhibisie van stikstofoksiedsintetase (NOS) en lipiedperoksidase.

Molekulêre modellering is uitgevoer met Catalyst 4.9® en die Ligandfit-module van Cerius$^{2®}$ om te bepaal of dit sinvol sou wees vir die sintese en biologiese evaluering van die nuwe verbindings. Die waterstofbindingsnetwerk wat gevorm het in die ensiem is gebruik as 'n indikasie vir moontlike inhibitatoriese aktiwiteit. Waterstofbindings met Tpr587, Glu592 en heem is as essensieel geag vir NOS-aktiwiteit. Waterstofbindings met Tyr 588, Gln 478 en Asp 597 is ook van belang, aangesien dié aminosure 'n rol speel by die stabilisering en oriëntasie van ligande in die aktiewe setel. Na aanleiding van hul interaksies by die NOS ensiem, toon hierdie verbindings potensiaal as NOS inhibeerders.

Die verbindings is gesintetiseer deur reduktiewe aminering of aktiveringschemie met verskeie skakels. Nuwe herrangskikte polisikliese strukture is verkry in die geval. Probleme is ondervind met die opbrengste, suiwering en isolering van die verbindings en kan toegeskryf word aan oplosbaarheid en meervoudige reaksies wat plaasgevind het.

Die oksihemoglobientoets is gebruik om die NOS aktiwiteit van die polisikliese indoolderivate te bepaal. Die resultate het getoon dat vier verbindings wat die indoolentiteit besit, 8-[3-(2-amino-etiel)indool]-pentasiklo[5.4.0.0^{2,6}.0^{3,10}.0^{5,9}]undekan-11-oon (**1**), 3-hidroksi-4-[3-(2-amino-etiel)indool]-azaheksasiklo[5.4.1.0^{2,6}.0^{3,10}.0^{5,9}.0^{8,11}] dodekan (**3**), 8-[3-(2-amino-etiel)indool]-pentasiklo[5.4.0^{2,6}.0^{3,10}.0^{5,9}]undekan (**4**) en 8-[3-(2-amino-etiel)indool]-pentasiklo[5.4.0^{2,6}.0^{3,10}.0^{5,9}]undekan (**5**), aktiwiteit in millimolêre konsentrasie besit. Verbindings soos **19** en **21** wat nie die indoolentiteit besit nie, is swak inhibeerders van NOS.

Die lipiedperoksidasiestudie het getoon dat die indoolverbindings **1**, **2**, **3**, **4** en **5** anti-oksidatiewe eienskappe besit wat vergelykbaar is met trolox.

Die resultate verkry in hierdie studie beklemtoon die potensiaal van die nuwe indoolhokverbindings as NOS inhibeerders en anti-oksidante. Met die bekende kalsiumkanaal aktiwiteit van die hokstrukture en die bogenoemde aktiwiteite kan die nuwe verbindings toepassings as multipotente middels in neurobeskerming vind.

Chapter 1 Introduction

1.1. Background

Neurodegeneration and subsequent neuronal death account for the clinical manifestations of many different neurological disorders of aging, including Alzheimer's disease, Parkinson's disease and stroke. These disorders are of vast concern for the modern population and have thus raised great interest in this field.

Drug design plays a pivotal role in the attenuation of these disorders due to the fact that the cause of neurodegeneration in PD remains unresolved and debatable. Computer modelling has been developed to increase the likelihood of discovering new potential pharmacologically active compounds. Rational drug design is based on the principle that biological properties of molecules are related to their actual structure. SAR evaluation of a series of homologous compounds, derived from a lead compound, may uncover a desired pharmacologically active compound that can be used as drug or lead in further studies.

Most diseases are induced by more than one pathogenic factor and therefore the current drug discovery paradigm is shifting from addressing single molecular targets to multiple ones (Keith *et al.*, 2005). Because nitric oxide synthase and various free radicals are implicated in the initiation and progression of neurodegenerative disorders, more attention is currently being paid to finding multipotent drugs that can surpass the therapeutic effects of selective drugs (Mencher & Wang, 2005).

1.2. Antioxidants

Antioxidants are exogenous (natural or synthetic) or endogenous compounds acting in several ways including removal of O_2, scavenging reactive oxygen species (ROS) or their precursors, inhibiting ROS formation and binding metal ions needed for catalysis of ROS generation. The natural antioxidant system can be classified into two major groups, enzymes and low molecular weight antioxidants (LMWA). The enzymes include SOD, catalase, peroxidase, and other supporting enzymes. The LMWA can be further classified into directly acting antioxidants (e.g., scavengers and chain breaking antioxidants) and indirectly acting antioxidants (e.g., chelating agents). The former

subgroup is extremely important in defence against oxidative stress (OS) and currently contains several hundred compounds. Most of them, including ascorbic and lipoic acids, polyphenols and carotenoids are derived from dietary sources (Shohami *et al.*, 1997).

The cell itself synthesises some biological molecules, such as glutathione and NADPH. The distribution of protective antioxidants in the body has some interesting features. For instance, there is a relatively high concentration of the water soluble antioxidant, vitamin C in the brain. However, vitamin E concentrations in the CNS are not remarkably different from those in other organs. The concentrations of antioxidants also vary within the different regions of the brain itself and the lowest concentration of vitamin E is found in the cerebellum (Vatassery, 1992). It has also been shown that enzymatic antioxidants, such as catalase, are in lower concentrations in the brain than in other tissues.

Melatonin (*N*-acetyl-5-methoxytryptamine; fig. 1.1) is an indoleamine secreted by the pineal gland and shows structural similarities to serotonin. Melatonin, a biological modulator of many physiological mechanisms (e.g., circadian rhythms and sleep), is highly lipophilic and when administered exogenously, can readily cross the BBB and gain access to neurons and glial cells. There is experimental evidence that melatonin influences aging and age-related processes and disease states. These effects are apparently related to its activity as a free radical scavenger (Beyer *et al.*, 1998).

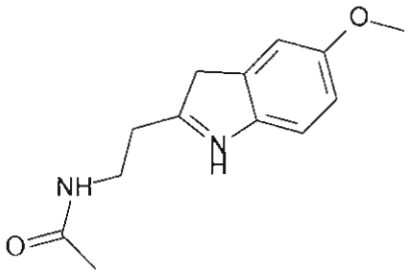

Figure 1.1: Melatonin

Electrophysiological experiments have revealed that melatonin inhibits NMDA-induced activity in several brain areas, including the striatum (El-Sherif *et al.*, 2002; León *et al.*, 1998). Melatonin also has anxiolytic actions and anticonvulsant activity against seizures induced by glutamate, NMDA, quinolinate, kainate and pentylenetetrazole in animals (Bijkdaouene *et al.*, 2003; Chung & Han, 2003). Some of these effects have also been shown in humans (Cajochen *et al.*, 2003; Muñoz-Hoyos *et al.*, 1998).

An important consequence of NMDA receptor activation is the production of free radicals and neuronal oxidative damage (Gunasekar *et al.*, 1995) and melatonin has been shown to counteract brain oxidative damage in NMDA and kainate models of excitotoxicity (Reiter, 1998; Giusti *et al.*, 1996). The protective effects of melatonin against brain oxidative stress have also been shown in neurodegenerative diseases such as Alzheimer's and Parkinson's diseases, where NMDA receptor activation is involved (Acuña-Castroviejo *et al.*, 1995; Reiter, 1998; Brusco *et al.*, 1998; Khaldy *et al.*, 2003). Melatonin also reduces NMDA-dependent nNOS activation in rat cortical cells, cerebellum and striatum (El-Sherif *et al.*, 2002; Yamamoto & Tang, 1998). Conversely, melatonin-deficient rats display increased brain damage after stroke or excitotoxic seizures (Manev *et al.*, 1996). An important part of the brain melatonin action is thus related to inhibition of NMDA-dependent excitation, and this might be correlated to antioxidant activity and/or inhibition of nNOS. Melatonin also controls important neuroendocrine functions by mechanisms involving specific receptors (Acuña-Castroviejo *et al.*, 1995; Dubocovich *et al.*, 2003). However, to date, little is known regarding the exact mechanism of NMDA inhibition by melatonin and the role of melatonin receptors in this effect.

1.3. Enzyme inhibition

The selective inhibition of MAO-B has been shown to have neuroprotective effects in MPTP animal models (Bach *et al.*, 1988). MAO-B inhibition prevents the formation of the toxic MPP^+ species by inhibiting the bioactivation of MPTP. There is also evidence that the inhibition of nNOS protects against MPTP mediated neurotoxicity in animals (Cawthon *et al.*, 1981). The potential roles of MAO–B and nNOS in neurodegenerative processes and their selective inhibition are areas of intense investigation. Only a few studies have however considered these two enzymes together. There are also only a few compounds which have been reported both for their MAO-B and nNOS inhibiting properties as well as neuroprotective activity. One of these compounds is 7-nitroindazole (7-NI; fig. 1.2; Mizuno *et al.*, 1987).

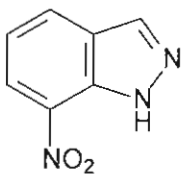

Figure 1.2: 7-Nitroindazole (7-NI)

7-NI is a selective inhibitor of nNOS (Berry *et al.*, 1994) and treatment of animals with 7-NI protects against MPTP neurotoxicity (Sket & Pavlin, 1985. These neuroprotective effects were not associated with decreased MPP^+ production since 7-NI did not inhibit the MAO-B catalysed oxidation of benzylamine by mouse brain mitochondrial preparations. In another study, striatal levels of MPP^+ in MPTP-treated mice were compared between 7-NI injected and control mice (Westlund *et al.*, 1988). The authors reported that the striatal MPP^+ levels were unaffected by neuroprotective doses of 7-NI, leading to the conclusion that the neuroprotective effect of 7-NI was mainly due to nNOS inhibition. However, several studies show that planar heterocyclic compounds are inhibitors of MAO-B (Tipton, 1973; Kalaria & Harik, 1987), suggesting that 7-NI, also a planar heterocyclic compound could inhibit MAO-B. This led Castagnoli's group to investigate the MAO-B inhibiting properties of 7-NI (Glover & Sandler, 1986). The effect of different 7-NI concentrations on the MAO-B catalysed oxidation of MPTP to its metabolite $MPDP^+$ was studied *in vitro*. The results showed that 7-NI had activity as a competitive inhibitor of MAO-B.

7-NI was also found to protect against the MPTP induced depletion of nigrostriatal DA in mice (Lewinsohn *et al.*, 1980). This effect was accompanied by a significant decrease in the striatal levels of MPP^+ showing that the neuroprotective effect of 7-NI is at least partly mediated through the inhibition of MAO-B. Similar striatal MPP^+ levels were obtained for both 7-NI together with MPTP and MPTP only treated mice by injecting a higher dose of MPTP in the 7-NI treated mice. In this case, a modest (20 %) protection of DA depletion was observed suggesting that the inhibition of MAO-B may not be the only mechanism mediating the protection against MPTP induced neurotoxicity. According to these results, the neuroprotective effects of 7-NI may be due to MAO-B inhibition, nNOS inhibition or inhibition of both enzymes. The effect of 7-NI and N^G-nitro-*L*-arginine, another NOS inhibitor, was also studied on MPTP-induced striatal ATP depletion (Kalaria *et al.*, 1988). The results showed that 7-NI prevented the striatal ATP loss in mice after MPTP administration. However, N^G-nitro-*L*-arginine didn't have any effect on MPTP induced ATP loss, suggesting the importance of MAO-B inhibition rather than NOS inhibition in 7-NI mediated neuroprotection. Another group investigated the effect of 7-NI on 3-nitrotyrosine immunoreactivity in the substantia nigra, which is considered a marker for peroxynitrite mediated neurotoxicity (Konrodi *et al.*, 1989). An increase in 3-nitrotyrosine immunoreactivity was reported in MPTP treated baboons, which was blocked by 7-NI, providing further evidence for the involvement of nNOS

inhibition in protection against MPTP induced neurotoxicity (Fowler *et al.*, 1980). In order to understand the role of 7-NI in neuroprotection better, additional animal studies will have to be done with this compound. However, the low aqueous solubility of 7-NI at pH 7.4 limits its utility *in vivo* studies and a prodrug approach has been suggested as an avenue to overcome this problem.

1.4. Compounds for synthesis

From the above data it was decided to synthesise a series of polycyclic indole and other polycyclic derivatives (table 1.1). Combinations of the pentacycloundecyl and indole moieties were included to determine the effect it will have on the potency and activity of NOS inhibition and lipid peroxidation.

Table 1.1: Compounds evaluated and synthesised in this study.

Compound	Name	Structure
1	8-[3-(2-aminoethyl)indole]-pentacyclo[5.4.0.0^{2,6}.0^{3,10}.0^{5,9}]undecane-11-one	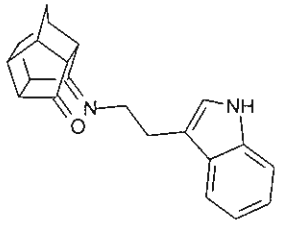
2	8-[3-(2-aminoethyl)indole]-8,11-oxapentacyclo[5.4.0.0^{2,6}.0^{3,10}.0^{5,9}] undecane	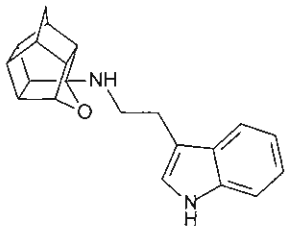
3	3-hydroxy-4-[3-(2-aminoethyl)indole]-azahexacyclo[5.4.1.0^{2,6}.0^{3,10}.0^{5,9}.0^{8,11}] dodecane	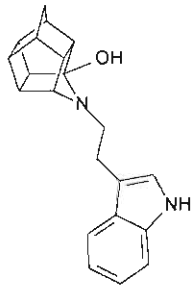

4	8-[3-(2-aminoethyl)indole]-pentacyclo[5.4.$0^{2,6}$.$0^{3,10}$.$0^{5,9}$]undecane	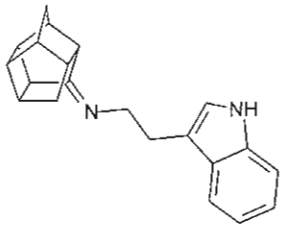
5	8-[3-(2-aminoethyl)indole]-pentacyclo[5.4.$0^{2,6}$.$0^{3,10}$.$0^{5,9}$]undecane	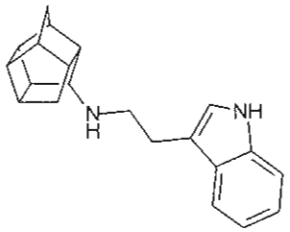
6	3-hydroxy-4,5-(1,3-oxazinane)-4-azahexacyclo[5.4.1.$0^{2,6}$.$0^{3,10}$.$0^{5,9}$.$0^{8,11}$] dodecane	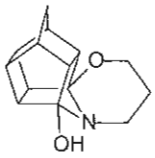
7	8-Ethoxy-8-ethylamino-pentacyclo[5.4.$0^{2,6}$.$0^{3,10}$.$0^{5,9}$]undecane-11-one	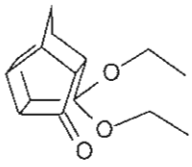

1.5. Aim of study

The aim of this study was to design and synthesise a series of polycyclic indole derivatives and to evaluate these compounds for neuroprotective activity. A decrease in the production of free radicals due to the inhibition of NOS or direct antioxidant activity, was indicative of neuroprotective potential. This study included:

- Computer modelling to justify the synthesis and biological evaluation of these compounds,
- Synthesis of selected polycyclic indole derivatives and
- *In vitro* evaluation employing the oxyhemoglobin (NOS inhibition) and TBA (lipid peroxidation) assays.

Mechanisms in neurodegeneration

Chapter 2

2. Introduction

Physiological cell death is generally regarded as apoptotic and is mediated by active, intrinsic mechanisms. Pathological (or accidental) cell death is regarded as necrotic, resulting from extrinsic insults to cells (e.g. osmotic, thermal, toxic, traumatic). The process of cellular necrosis involves disruption of membrane structural and functional integrity with rapid influx of Ca^{2+} and water, resulting in the dissolution of the cell. Cellular necrosis is thus induced by an abrupt environmental perturbation and departure from physiological conditions (Martin *et al.*, 1998).

In this review relevant neurodegenerative aspects and various neurodegenerative strategies, including N-methyl-D-aspartate (NMDA) antagonists, antioxidants and NOS inhibitors will be discussed.

2.1. The lethal triplet

There are three critical mechanisms of neuronal cell death which may act separately or cooperatively to cause neurodegeneration. This lethal triplet of metabolic compromise, excitotoxicity and oxidative stress (Greene and Greenamyre, 1996a; Alexi *et al.*, 1998) causes neuronal cell death that can be classified as being either apoptotic or necrotic (Hughes *et al.*, 1997; Tatton & Chalmers-Redman, 1998). Aspects of each of these three mechanisms are believed to play a role in the neurodegeneration that occurs in Parkinson's disease (fig. 2.1).

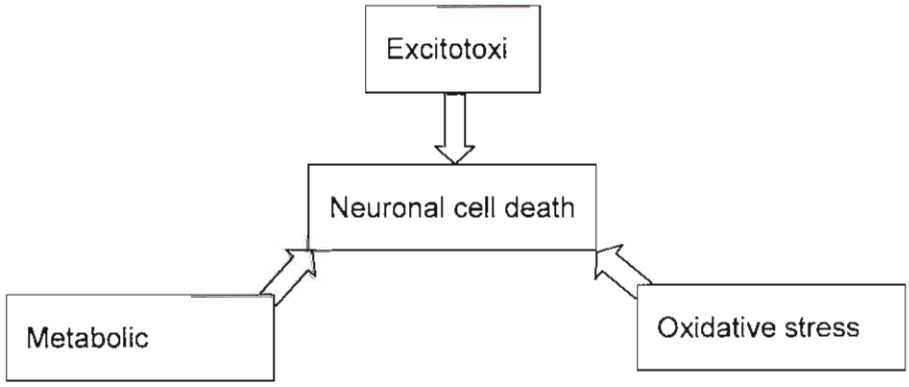

Figure 2.1: Lethal triplet in neuronal cell death.

2.1.1. Metabolic compromise

Metabolic compromise of neurons (bioenergetic impairment) can be caused by stroke, asphyxiation, hypoglycemia and certain respiratory poisons. These neurotoxic poisons are mainly mitochondrial poisons and include cyanide, carbon monoxide, 1-methyl-4-phenyl-1,2,3,6-tetrahydropyridine (MPTP), 3-nitropropionic acid (3-NP), malonic acid (MA) and rotenone. As the synthesis of ATP for energy in neurons occurs mainly in the mitochondria via the Krebs-cycle and the electron transport chain, mitochondrial poisoning results in a cytotoxic depletion of ATP.

Both Parkinson's disease (PD) and Huntington's disease (HD) show evidence of deficits in mitochondrial enzymes. Metabolic injuries result in a loss of mitochondrial function leading to a depletion of ATP which causes preferential neurodegeneration in the basal ganglia. Bioenergetic failure causes both a depletion of ATP and deregulates mitochondrial function. Dysfunctioning of mitochondria results in a loss of intracellular calcium buffering capacity and in an increase in the production of damaging oxygen and nitrogen free radicals, leading to oxidative stress. Both these processes can be cytotoxic.

The depletion of ATP causes failure of ATP-dependent ion pumps which results in depolarisation of neurons (Greene and Greenamyre, 1996b). This results in a loss of ionic integrity and an accumulation of intracellular Ca^{2+}. The accumulation of Ca^{2+} in mitochondria rather than in the cytoplasm may be more critical in determining cell death (Stout *et al.*, 1998). Intracellular Ca^{2+} further induces mitochondrial strain and free radical generation and increases the neurotoxic processes by activation of Ca^{2+}-dependent proteases and lipases.

2.1.2. Excitotoxicity

Excitotoxicity is the second aspect of neurotoxicity and occurs due to a dysfunction of excitatory amino acid (EAA) neurotransmission - usually stimulation of glutamate receptors that becomes pathological (Olney *et al.*, 1971). Glutamate is a very important neurotransmitter and controls several functions in the central nervous system (CNS). It is the main excitatory signalling mediator and is implicated in functions such as memory and learning. Nevertheless, glutamate can also produce neurotoxicity and consequently, the glutamate homeostasis must be carefully regulated (Danbolt, 2001).

N-Methyl-D-aspartate (NMDA) receptors are a subtype of glutamate receptors that, upon activation by glutamate can lead to potentially lethal intracellular ionic derangements, in particular, intracellular Na^+ and Ca^{2+} overload (Dingledine *et al.*, 1999). Excitotoxic neuronal cell death, which tends to occur by necrosis, correlates well with total Ca^{2+} influx, and removal of extracellular Ca^{2+} attenuates glutamate-induced neuronal death.

Sustained elevation in intracellular Ca^{2+} initiates toxic cascades, which ultimately leads to cell death (fig. 2.2). These cascades include activation of catabolic enzymes, such as proteases, phospholipases and endonucleases (Choi, 1995). Elevated concentrations of intracellular Ca^{2+} can further lead to initiation of protein-kinase and lipid-kinase cascades, impairment of metabolism and generation of reactive oxygen species (ROS) and reactive nitrogen species (RNS) responsible for the neuronal damage (Herrling, 1994; Meldrum & Garthwaite, 1990; Sattler & Tymianski, 2000). While many of these events occur early and can result in rapid cell death, others, such as energy compromise and ROS formation, may initiate a more delayed death processes. Most of these Ca^{2+}-dependent events may be prevalent to both NMDA and AMPA/KA receptor-mediated excitotoxicity.

Ca^{2+} cytotoxicity follows a complex mechanism and may involve not only Ca^{2+} overloading but also disruption of intracellular Ca^{2+} dynamics and mitochondrial ATP synthesis (Castilho *et al.*, 1998). NMDA has been shown to increase not only cytosolic levels of Ca^{2+} but also mitochondrial Ca^{2+} concentration (Peng *et al.*, 1998).

An especially important detrimental consequence of Ca^{2+} overload following excitotoxic glutamate receptor activation is the formation of ROS. Free radical production is linked to elevated [Ca^{2+}] in several ways: (i) Ca^{2+}-dependent activation of phospholipase A_2, with liberation of arachidonic acid and further metabolism, leading to free radical production and lipid peroxidation; (ii) activation of nitric oxide synthase (NOS) and the release of nitric oxide (NO), which can then interact with ROS from other sources to generate highly reactive peroxynitrite (Beckman & Koppenol, 1996) and (iii) uncoupling of mitochondrial electron transport, enhancing mitochondrial production of free radicals (Dykens, 1994).

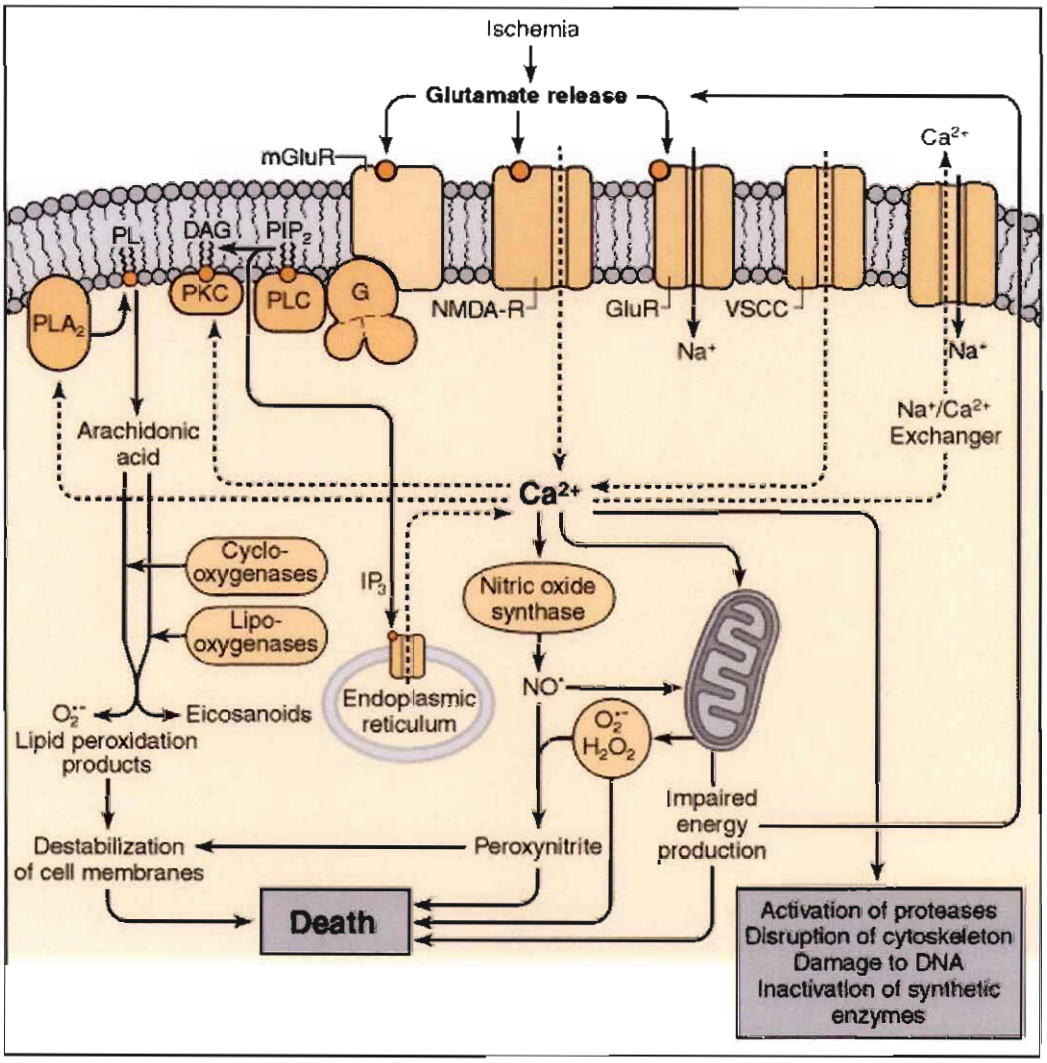

Figure 2.2: Mechanisms contributing to neuronal injury during ischemia-reperfusion.

Simplified diagram showing several pathways believed to contribute to excitotoxic neuronal injury in ischemia. *mGluR*, metabotropic glutamate receptor; *NMDA-R*, *N*-methyl-D-aspartate receptor; *GluR*, AMPA/Kainate type of glutamate receptors; *PL*, phospholipids; *PLA_2*, phospholipase A_2; *DAG*, diacylglycerol; *PLC*, phospholipase C; *PKC*, protein kinase C; *G*, G protein; *PIP_2*, phosphatidylinositol 4,5-bisphosphate; *IP_3*, inositol 1,4,5-trisphosphate; *NO*, nitric oxide; *$O_2^{\bullet-}$*, superoxide radical; H_2O_2, hydrogen peroxide; VSCC, voltage-sensitive Ca^{2+} channel (Taken from Dugan &

VSCC, voltage-sensitive Ca^{2+} channel (Taken from Dugan & Choi, 1999).

Simplified diagram showing several pathways believed to contribute to excitotoxic neuronal injury in ischemia. *mGluR*, metabotropic glutamate receptor; *NMDA-R*, *N*-methyl-D-aspartate receptor; *GluR*, AMPA/Kainate type of glutamate receptors; *PL*, phospholipids; PLA_2, phospholipase A_2; *DAG*, diacylglycerol; *PLC*, phospholipase C; *PKC*, protein kinase C; *G*, G protein; PIP_2, phosphatidylinositol 4,5-bisphosphate; IP_3, inositol 1,4,5-trisphosphate; *NO*, nitric oxide; $O_2\bullet^-$, superoxide radical; H_2O_2, hydrogen peroxide; VSCC, voltage-sensitive Ca^{2+} channel (Taken from Dugan & Choi, 1999).

In cell cultures, ROS production is stimulated by concentrations of NMDA which are not neurotoxic, and in conscious rats, NMDA receptors are responsible for a low baseline production of ROS, suggesting that even "physiological" NMDA receptor activity may trigger production of ROS. However, cell culture studies suggest that substantially greater quantities of mitochondrial ROS are generated when NMDA receptors are sufficiently over-stimulated to produce excitotoxicity. Since AMPA/KA receptor activation, possibly in conjunction with the group 1 metabotropic glutamate receptors, may also elicit enhanced mitochondrial ROS production, it is likely that excitotoxicity may be an important trigger for mitochondrial free radical production in ischemia-reperfusion injury. The concept that free radicals are important downstream mediators of excitotoxicity is supported by the fact that treatment with free radical scavengers can attenuate NMDA or AMPA receptor-mediated neuronal death.

2.1.3. Oxidative stress

Oxidative stress on the other hand can be defined as the disruption of the equilibrium between the factors that promote free radical formation and the anti-oxidant defence mechanisms (Olanow, 1993). This process is characterised by the actions of highly reactive free radicals such as the ROS, superoxide anion ($\bullet O_2^-$) and hydroxyl radical ($\bullet OH$) and the RNS peroxynitrite ($ONOO^-$) (Simonian and Coyle, 1996; Cassarino and Bennett, 1999). The oxidising actions of these reactive species destroy membrane lipids, proteins and DNA, and can be detrimental to cells if they accumulate at high levels or if deficits in cellular antioxidant defence systems occur. ROS and RNS are generated under normal cellular functioning, mainly during mitochondrial respiration and are deactivated by endogenous antioxidants and scavengers. Various substances in high

concentration can enhance the production of toxic free radicals, such as intracellular Ca^{2+}, DA and nitric oxide synthase (NOS) (Dykens, 1994; Dawson *et al.*, 1991).

Activation of NOS results in the increased formation of nitric oxide (NO), which can then react with superoxide anion ($\bullet O_2^-$) to form peroxynitrite ($ONOO^-$). Peroxynitrite can activate the enzyme poly ADP ribosyl synthase (PARS), also called poly ADP ribosyl polymerase (PARP) that goes on to polyribosylate proteins with ADP and which can lead to the depletion of ATP and NAD (Zhang *et al.*, 1994; Szabo *et al.*, 1996). If mitochondrial activity is impaired, the cell cannot replace these energy substrates (NAD and ATP) and the cell subsequently dies. The oxidation of membrane lipids (lipid peroxidation) by free radicals produces a cytotoxic byproduct, 4-hydroxynonenal (HNE), which has recently been identified as a mediator of oxidative stress-induced neuronal cell death (Kruman *et al.*, 1997; Pedersen *et al.*, 1999). Oxidative stress occurs in various neurodegenerative disorders as shown by increases in measures of oxygen and nitrogen free radicals and deficits in antioxidant substances.

The lethal triplet of metabolic compromise, excitotoxicity and oxidative stress may also act cooperatively in causing neuronal cell death. For example, metabolic impairment may elicit secondary excitotoxicity. The depolarisation of neurons and the loss of ionic integrity caused by bioenergetic impairment releases the voltage-dependent block on the NMDA receptor thus activating it and causing secondary excitotoxicity in neurons that possess these receptors (Zeevalk and Nicklas, 1990). The striatum is an example of a glutamaceptive region (receives glutamatergic inputs and has glutamate receptors) and is thus prone to excitotoxic mechanisms. Blockade of excitatory transmission by NMDA receptor antagonists such as MK801 largely prevents striatal damage due to energetic inhibition *in vivo*, suggesting that toxicity due to metabolic compromise involves an excitotoxic component. However, while metabolic impairment may lead to secondary excitotoxicity, these two neurotoxic events share only partial overlapping mechanisms, as each leads to somewhat different patterns of neuropathology and locomotor dysfunction (Nakao & Brundin, 1997). Metabolic compromise may also cause oxidative stress by inducing the production of free radicals both from the electron transport chain and due to the burden of increased intracellular Ca^{2+} on mitochondrial function. The reverse interaction may also occur, as oxidative stress may cause metabolic impairment and initiate excitotoxic pathways. For example, oxidative stress can cause lipid peroxidation which yields the byproduct HNE (Morel *et al.*, 1999; Pedersen *et al.*, 1999).

HNE impairs glucose transport which can lead to energetic failure. HNE also renders neurons more sensitive to excitotoxicity as it inhibits Na^+/K^+-ATPase activity which is necessary for maintaining neuronal polarisation and therefore the voltage-dependent Mg^{2+} block of the NMDA receptor channel. Also, NO, which promotes the formation of the free radical peroxynitrite, causes mitochondrial depolarisation and depletes ATP (Brorson *et al.*, 1999). Depolarisation of mitochondria impairs the transport of electrons along the mitochondrial matrix during ATP synthesis. This inhibition of metabolic function by NO is partially due to PARS/PARP activation (which causes depletion of ATP by accelerated ATP consumption) via peroxynitrite (Zhang *et al.*, 1994). Excitotoxicity can also contribute to oxidative stress due to the detrimental cascades of events described above. Intrastriatal injection of NMDA ligands results in increases in markers of reactive oxygen species while free radical scavengers and inhibitors of oxidative stress attenuate the neuropathology.

In summary, biological injuries that cause neuronal cell death generally occur through one or more mechanisms of the lethal triplet: metabolic compromise, excitotoxicity and oxidative stress. These events cause a series of intracellular responses which either promote the recovery of the cell or cause cell death. The neuronal cell death that occurs is most likely along an apoptotic and necrotic continuum (Portera-Cailliau *et al.*, 1997).

2.2. NMDA receptor in neurodegeneration

The NMDA receptor (fig. 2.3a) is unique among ligand-gated ion channels in that it requires two co-agonists: glutamate and glycine (Kornhuber & Weller, 1997). Normal physiological stimulation of the NMDA receptor has been found to promote survival, maturation and neuronal outgrowth of cultured neurons isolated from the cerebellum, hippocampus or spinal cord (Williams *et al.*, 1991).

The NMDA receptor is complex in that it contains at least five modularly, distinct binding sites:

(i) a site that binds glutamate (or NMDA),
(ii) a regulatory allosteric glycine site,
(iii) a Mg^{2+} binding site, where Mg^{2+} blocks the channel in a voltage-dependent way,
(iv) a PCP or MK-801 binding site and
(v) a site that is modulated by Zn^{2+} binding and the polyamines such as spermine.

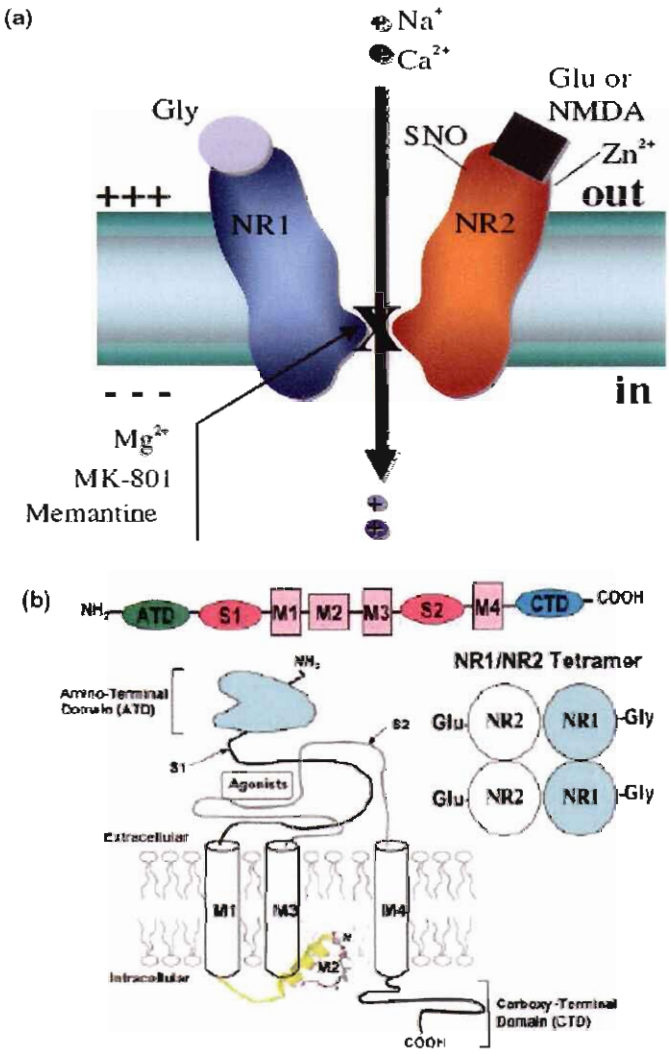

Figure 2.3: NMDA receptor model illustrating important binding and modulatory sites.

(a) Glu or NMDA: glutamate or NMDA binding site. Gly, glycine binding site; Zn^{2+}, zinc binding site; NR1, NMDAR subunit 1; NR2, NMDAR subunit 2A; SNO, cysteine sulfhydryl group (–SH) reacting with nitric oxide species (NO); X, Mg^{2+}, MK-801, and memantine binding sites within the ion channel pore region. (b) Schematic representation of various domains of the NMDAR subunit. Top, linear sequence; bottom left, proposed 3-D folding; bottom right, proposed tetrameric structure of the classical NMDAR. ATD, amino terminal domain; S1 and S2, agonist binding domains; M1–4, the four transmembrane domains; CTD, carboxyl terminal domain (Taken from Chen & Lipton, 2006).

The NMDA receptor ion channel has a very high Ca^{2+} conductance and Ca^{2+} is thought to be the primary mediator of both physiological and toxic properties of the NMDA receptor. In addition to this, the channel can also transport Na^{+}.

The following membrane topology has been proposed for the NMDAR (fig. 2.3b, Wollmuth & Sobolevsky, 2004):

(i) the N-terminal domain contains 380 amino acids that are related to the bacterial periplasmic binding protein sequence designated leucine/isoleucine/ valine-binding protein (LIVBP), the Zn^{2+} binding site, the proton site, and other modulatory sites;
(ii) four transmembrane domains (M1–M4) are present, and the selectivity filter of the channel pore is formed by M2 (a P-loop region);
(iii) the ligand-binding domains are formed by the pre-M1 (S1) and M3-M4 linker region (S2);
(iv) a cytoplasmic C-terminal domain interacts with intracellular proteins (Dingledine *et al.* 1999); and
(v) the pre-M1 segment, the C-terminal portion of the M3 segment, and the N-terminal region of the M4 segment form the channel outer vestibule (Beck *et al.* 1999).

In general, NMDAR antagonists can pharmacologically divided into four major groups according to site of action on the receptor-channel complex (Wong and Kemp 1991). Drugs acting at the

(i) NMDA (agonist) recognition site,
(ii) glycine (co-agonist) site,
(iii) channel pore, and
(iv) modulatory sites, such as the redox modulatory site, the proton-sensitive site, the high-affinity Zn^{2+} site, and the polyamine site.

The degree of NMDAR activation and consequent influx of Ca^{2+} and Na^{+} into the cell can be altered by higher levels of agonists and by substances binding to one of the modulatory sites on the receptor. The two modulatory sites that are most relevant are open-channel blocker sites within the ion channel pore and the S-nitrosylation site located towards the N-terminal of the receptor. S-nitrosylation reactions represent transfer of NO to a thiol or sulfhydryl group (–SH) of a critical cysteine residue (Lipton *et al.* 2002).

Other modulatory sites also exist on the NMDA receptor and may in the future prove to be of therapeutic value. These include binding sites for Zn^{2+}, polyamines, the drug ifenprodil and a pH (i.e. proton) sensitive site (Kemp & McKernan, 2002). Additionally,

three pairs of cysteine residues at extracellular domains contribute to the redox sites and can modulate NMDAR function by virtue of their redox sensitivity (Lipton *et al.* 2002). These redoxsensitive cysteine residues may constitute a unique NO reactive molecular oxygen sensor' in the brain, enhancing the degree of down-regulation of NMDA receptor function by S-nitrosylation in the presence of low pO_2 levels, and thus dictating the pathological effects of hypoxia that are mediated via the receptor (Chen & Lipton, 2006).

2.3. Neuroprotective strategies

The initiation and duration of a neuroprotective treatment depends on the animal model, the neuroprotective agent and the method of delivery of the agent (Emborg & Kordower, 2000). Prevention of nigral dopaminergic cell loss in PD or animal models of PD requires delivery of neuroprotective agents when there are still cells to be protected. Ideally, neuroprotective substances are administered before the onset of parkinsonian signs. However, we currently lack the tools to preclinically diagnose PD and our best alternative is to start neuroprotective interventions early after the diagnosis of PD (Montgomery *et al.*, 2000a, 2000b).

Several neuroprotective strategies have been suggested and a brief discussion will follow.

2.3.1. Attenuation of excitotoxicity

Attenuation of glutamate-mediated excitotoxicity includes the inhibition of two major classes of glutamate receptors, ionotropic (NMDA, KA and AMPA) and metabotropic (Groups I-III) receptors, coupled to intracellular second messengers (Pitkänen *et al.*, 2005). Many reports have targeted the NMDA receptor (table 2.1), where MK-801, phencyclidine (PCP) and ketamine showed strong psychomimetic effects. The occurrences of adverse effects were diminished in later generations of NMDA receptor antagonists such as NPS 1506 and NPS 846. To date, magnesium, HU-211 (dexanabinol), memantine and Cp-101,606 have generated clinical interest because of improved functional and histological outcomes (Morales *et al.*, 2005). In addition to antagonism of excitatory amino acid (EAA) receptor function, modulation of EAA receptor activity might also be accomplished by inhibition of EAA release. Examples include the compound riluzole which is currently in Phase III clinical trials. Despite promising preclinical documentation, all glutamate blockers evaluated to date, have shown to be ineffective in Phase III clinical trials (Marklund *et al.*, 2004; table 2.1).

Table 2.1: Targets of neuroprotection in traumatic brain injury (Taken from Pitkänen *et al.*, 2005).

Pharmacological target	Examples of compounds
EAA[1] modulation	
NMDA[2]	Mg^{2+},CPI 101-606[6],MK-801[7], HU-211[8], Memantine[9]
AMPA[3]/KA[4]	RPR117824[10], YM872[11], NBQX[12]
Metabotropic	MCPG[13], AIDA[14], CPCCOet[15], LY-367385[16], MPEP[17], DCG-IV[18], LY354740[19]
EAA release inhibition	BW1003C87[20], 619C89[21], Riluzole
ROS[5] scavenging	PBN[22], S-PBN[23], Vitamin E, L-NAME[24], CDPC[25], PEG-SOD[26]
Calcium-mediated damage	LOE908[27], SNX-111[28]
Modulators of inflammation	IA29[29], Ibuprofen, HU-211, CP-0127[30]
Miscellaneous	GPI 6150[31], CsA[32], CCPA[33], Lactate
Neurotrophic factors	NGF[34], GDNF[35], BDNF[36]
Inhibitors of apoptosis	Z-VAD-fmk[37], Z-DEVD-fmk[38]
Endocrinology	TRH[39] analogs, IGF-I[40], DHEAS[41], progesterone

[1]EAA: excitatory amino acid; [2]NMDA: N-methyl-D-aspartate; [3]AMPA: α-amino-3-hydroxy-5-methyl-4-isoxazole propionic acid; [4]KA: kainate receptors 1 and 2; [5]ROS: reactive oxygen species; [6]CPI 101-606: (1S,2S)-1-(4-hydroxyphenyl)-2-4-hydroxy-4-phenylpiperidino)-1-propanol; [7]MK-801: dizocilpine maleate; [8]HU-211: (+)-(3S,4S)-7-hydroxy-D-6 tetrahydro-cannabinol 1,1-dimethylheptyl; [9]Memantine: 3,5-dimethyl-l-adamantanamine; [10]RPR117824: 9-carboxymethyl-imidazo-[1-2α]indenol[1-2e]; [11]YM872: zonampanel monohydrate; [12]NBQX: 6-nitro-7-sulfamoylbenzo (F) quinoxaline-2,3-dione; [13]MCPG: (S)-α-4-carboxyphenylglysine; [14]AIDA: (RS)-L-iaminoindan-1,5-dicarboxylic acid; [15]CPCCOet: 7-(hydroxyimino)cyclopropa[b]chromen-1a-carboxylate ethyl ester; [16](S)-(+)-a-amino-4-carboxy-2-methylbezeneacetic acid; [17]MPEP: 2-methyl-6-(phenylethynyl)-pyridine; [18]DCG-IV: 2, (2',3')-dicarboxycyclopropylglycin; [19]LY354740: (1S,2S,5R,6S)-(+)-2-aminobicyclo[3.1.0]hexane-2,6-dicarboxylic acid; [20]BW1003C87: 5-(2,3,5-trichlorophenyl) pyrimidine 2,4-diamine ethane sulfonate; [21]619C89: [4-amino-2-(4-methyl-1-piperazinyl)-5-(2,3,5-trichlrophenyl)pyrimidine mesylate monohydrate]; [22]PBN: α-phenyl-N-tert-butyl-nitrone; [23]S-PBN: sodium 2-sulfophenyl-N-tert-butyl nitrone; [24]L-NAME: nitro-L-arginine methyl ester; [25]CDPC: cytidine 5'-diphosphocholine; [26]PEG-SOD: polyethylene glycol-conjugated superoxide dismutase; [27]LOE908: (R,S)-(3,4-dihydro-6,7-dimethoxy-isoquinoline-1-yl)-2-phenyl-N,N-di[2-(2,3,4-trimethoxyphenyl)ethyl]-acetamide; [28]SNX-111: Ziconotide; [29]IA29: anti-ICAM-1 monoclonal antibody; [30]CP-0127: Bradycor or deltibant, bissuccimidohexane (L-Cys6)-1; [31]GPI 6150: (1,11b-dihydro-[2H]bezopyrano[4,3,2-de]isoquinolin-3-one; [32]CsA: cyclosporin A; [33]CCPA: 2-chloro-N(6)-cyclopentyladenosine; [34]NGF: nerve growth factor; [35]GDNF: glial cell-derived neurotrophic factor; [36]BDNF: brain-derived neurotrophic factor; [37]Z-VAD-fmk: acetyl-Tyr-Val-Ala-Asp-chloromethyl-ketone; [38]Z-DEVD-fmk: N-benzyloxycarbonyl-Asp-Glu-Val-Asp-fluoromethyl ketone; [39]TRH: thyrotropin-releasing hormone; [40]IGF-1: insulin-like growth factor-1; [41] DHEAS: dehydroepiandrosterone sulfate.

2.3.2. Calcium channel blockage and calpain inhibition

Several Ca^{2+} blockers such as (S)-emopamil, LOE 908, S100B, BMS-204352 and SNX-111 have been shown to attenuate neurological motor and cognitive deficits following experimental traumatic brain injury (Morales *et al.*, 2005). Much clinical interest, to date,

has focused on the Ca^{2+}-channel blocker nimodipine, but considerable uncertainty remains as to its efficacy (Langham *et al.*, 2003).

Downstream inhibition of calpains (Ca^{2+}-dependent proteases) might also be of therapeutic value. The calpain inhibitor AK295 has shown to reduce both motor and cognitive deficits, while the calpain inhibitor MDL-28170 reduced the damage of brainstem fiber tracts. However, its efficacy as calpain inhibitors need to be further investigated (Pitkänen *et al.*, 2005).

2.3.3. Reactive oxygen and nitrogen scavengers

Tirilazad mesylate and its related pyrrolopyrimidines, including U-101033E, showed promising effects in a series of traumatic brain injury (TBI) studies, but Phase III clinical trials have failed to show a positive outcome (Roberts *et al.*, 2000). Inhibition of lipid peroxidation and/or attenuation of hydroxyl radicals are of clinical interest and further evaluation are ongoing.

Cytidine 5'-diphosphocholine (CDPC), or citicoline, compounds that attenuate the activation of phospholipase A_2, have shown to be neuroprotective and possess neurobehavioral efficacy (Dempsey & Raghavendra, 2003). CDPC improved the motor and cognitive outcome, implying a potential role for CDPC in the treatment of human TBI.

2.3.4. Superoxide scavenging

Administration of the antioxidant enzyme superoxide dismutase (SOD) conjugated to enhance blood-brain barrier penetration (PEG-SOD, pegogortein) improved survival and neurological recovery, attenuated cerebral edema and decreased hippocampal cell loss across TBI models. PEG-SOD failed in the randomised, Phase III multicenter trail and the reason for this failure are probably multifactorial but might be related to the inclusion of many severely brain-injured patients (Young *et al.*, 1996).

2.3.5. Pharmacological inhibition of caspases and pro-apoptotic cascades

Another strategy to prevent acute cell death after TBI might be to inhibit caspases, the enzymes involved in the process leading to apoptosis. Several caspase inhibitors have been successfully evaluated in TBI models including ketones such as the pan-caspase inhibitor z-VAD-fmk, the caspase-1 specific inhibitor acetyl-Tyr-Val-Ala-Asp-chloromethyl ketone and the caspase-3-specific z-DEVD-fmk (Raghupathi, 2004). However, the role

of anti-apoptotic compounds in TBI is controversial and more preclinical research is necessary to evaluate their clinical potential.

Several studies have demonstrated that exogenously administered progesterone or its metabolite allepregnanolone reduced post-traumatic increase in cerebral edema, improved cognitive performance and functional deficits and reduced lesion volume and apoptotic cell death (Djebaili *et al.*, 2005).

2.4. Enzyme inhibition

2.4.1. Nitric oxide synthase

There is evidence that not only reactive oxygen species but also nitric oxide (NO), a free radical, may play a role in oxidative damage in PD (Gerlach *et al.*, 1999). Nitric oxide (NO) has a broad range of biological activities and acts as cell messenger with important regulatory functions in the nervous, immune and cardiovascular systems (Moncada *et al.*, 1991). Overproduction of NO however, plays a role in a variety of disorders such as septic shock, pain, ischemia and several neurodegenerative diseases (Dawson & Dawson *et al.*, 1996).

NO is formed via the nitric oxide synthase (NOS) catalysed conversion of L-arginine (**27**) to L-citrulline (**29**; Kerwin *et al.*, 1995), a process that leads to the formation of free radical nitric oxide (NO).

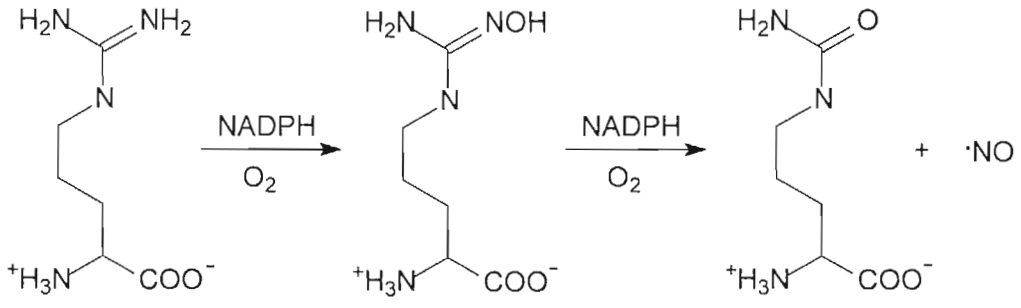

27 **28** **29** **30**

Scheme 2.1. NOS catalysed conversion of L-arginine (**27**) to L-citrulline (**29**) and NO (**30**).

The development of neuroprotective agents is orientated toward the synthesis of novel structures that interfere with some step of the complex chemical signaling system involving NOS, including the inhibition of the enzyme itself.

2.4.2. Structure

Nitric oxide synthases (NOS), the enzymes responsible for synthesis of NO consists of homodimers whose monomers are two fused enzymes themselves: a cytochrome reductase and a cytochrome that requires three co-substrates (L-arginine, NADPH and O_2) and five cofactors or prosthetic groups (FAD, FMN, calmodulin, tetrahydrobiopterin and heme (fig. 2.4).

This enzyme is comprised of an N-terminal oxidase domain with binding sites for L-arginine and tetrahydrobioprotein (H_4B) and a C-terminal reductase domain with binding sites for FMN, FAD, and NADPH (fig. 2.5). The domains are connected by a Ca^{2+}/ calmodulin binding region that allows electron transport through the enzyme (Marletta, 1993; Roman *et al.*, 2002). In its functional state, NOS is a dimer in which electrons from one subunit of the oxygenase domain accepts electrons from FMN of the reductase domain of the other subunit (Siddhanta *et al.*, 1998). This unique enzyme catalyses a two-step monooxygenase reaction, converting L-arginine to N^{ω}-hydroxyl-L-arginine, as an intermediate and then to L-citrulline and NO (Stuehr *et al.*, 1991; Rosen *et al.*, 2002).

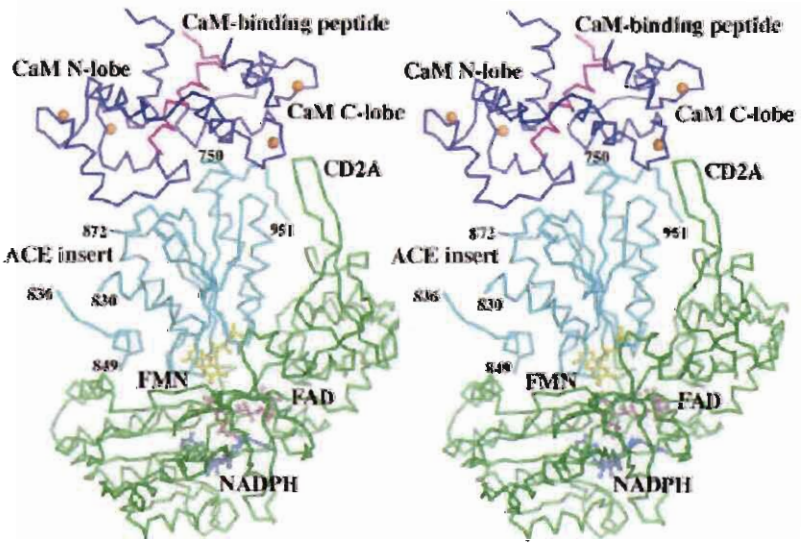

Figure 2.4: A manually constructed docking model showing possible interactions between CaM complexed with a helical peptide from human eNOS (1N1W) and the rat nNOS reductase domain (1TLL). The C-terminal helix is hidden behind the FMN binding domain. Cofactors FMN, FAD, and NADPH are shown as ball-and-sticks, while Ca^{2+} ions in CaM are represented as gold spheres (Taken form Li & Poulos, 2005).

Neuronal nitric oxide synthase also generates superoxide ($O_2^{\bullet -}$) and hydrogen peroxide (H_2O_2) during enzymatic cycling (Pou *et al.*, 1992). There are a number of control mechanisms that regulate nNOS production of NO, $O_2^{\bullet -}$, and H_2O_2. For instance, H_4B appears to play a critical role in the NOS oxidation of L-arginine to NO and L-citrulline (Presta *et al.*, 1998). Similarly, this pterin, in the absence of L-arginine, promotes direct generation of H_2O_2 at the expense of $O_2^{\bullet -}$ (Rosen *et al.*, 2002). Finally, L-arginine, by binding to nNOS, shifts electron transport away from O_2, increasing NO production at the expense of $O_2^{\bullet -}$ (Pou *et al.*, 1999), since NO, $O_2^{\bullet -}$, and H_2O_2 initiate different cell signaling pathways (Wolin, 2000; Dröge, 2002), such as lipid peroxidation (fig. 2.2).

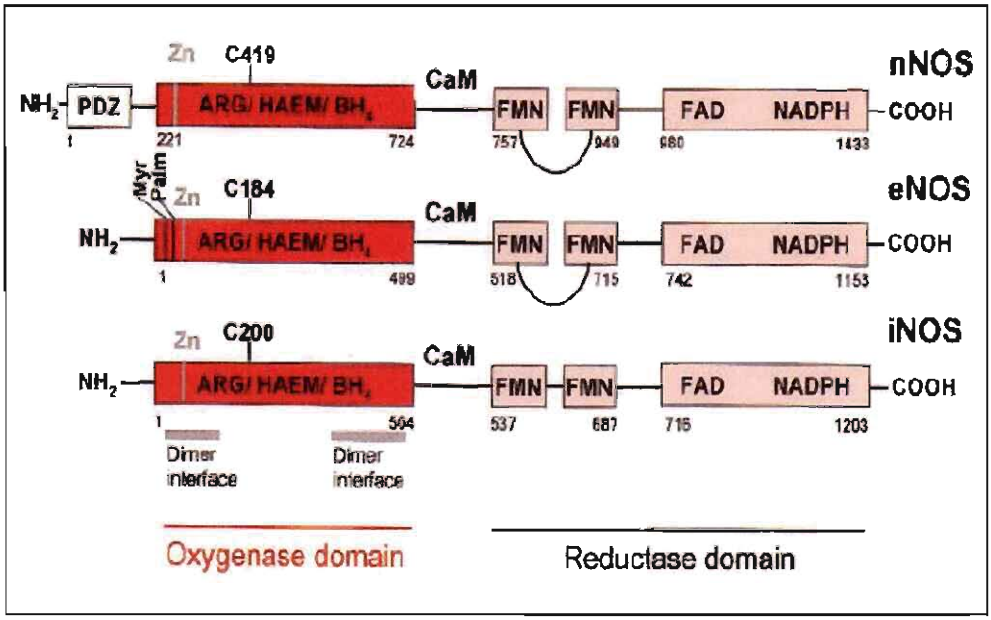

Figure 2.5: Domain structure of human nNOS, eNOS and iNOS.

Oxygenase, reductase and PDZ domains are denoted by solid boxes and the amino acid residue number at the start/end of each domain is shown. The cysteine residue which ligates the heme and the CaM-binding site is indicated for each isoform, myristoylation (Myr) and palmitoylation (Palm) sites on eNOS are shown, as is the location of the zinc-ligating cysteines (Zn in grey). The auto inhibitory loop within the FMN regions of nNOS and eNOS are also shown and grey bars indicate the dimer interface in the oxygenase domain (Taken from Alderton *et al.*, 2001).

2.4.3. NOS isoforms

Several distinct NOS isoforms are expressed from three distinct genes. These include two constitutive Ca^{2+}/CaM-dependent forms of NOS: neuronal nitric oxide (nNOS) whose activity was first identified in neurons, and endothelial nitric oxide synthase (eNOS) first identified in endothelial cells. These two isoforms are physiologically activated by steroid hormones or neurotransmitters such as NO, DA, glutamate and glycine that increase the intracellular calcium concentrations. In contrast, the inducible form of nitric oxide synthase, iNOS, is Ca^{2+} independent and is expressed in a broad range of cell types. This form of NOS is induced after stimulation with cytokines and exposure to microbial products. After permanent activation, it continuously produces high concentrations NO.

Since these isoforms possess a distinct cellular localisation and are differentially regulated, they represent specific targets for potential therapeutical approaches (table 2.2).

Table 2.2: Postulated roles for NO synthesised by three NOS isoforms (Knowles, 1996).

nNOS	eNOS	iNOS
Central nervous system Neurotransmitter/ neuromodulator	Cardiovascular system	Nonspecific immunity
Responses to glutamate	Relaxation of vascular smooth muscle: regulation of • tissue conductance • blood flow • blood pressure	Resistance to infection by • Protozoa • Fungi • Bacteria • Viruses
Nociception	Inhibition of platelet aggregation and reactivity	Pathological roles
Peripheral nitrergic nerve neurotransmitter • GI Tract • Penile erection • Sphincter relaxation • Blood flow	Protection of the vasculature from atherosclerosis	Inflammatory/autoimmune diseases • Acute inflammation • Ulcerative colitis • Asthma • Transplant rejection • Arthritis, prosthetic joint failure • Multiple sclerosis? • Dementias (Alzheimer's, Lewy body, viral)
Pathological roles • Ischaemic brain damage • Hyperalgesia • Epilepsy • Parkinson's disease		Tumours • Promotion of vascularisation, growth and metastasis

2.4.4. NOS Inhibitors

Since the development of selective inhibitors only a few specific isoforms are of considerable interest, both for therapeutic purposes and for their use as specific pharmacological tools. For example, NO of neuronal origin is involved in pain transmission (Moore *et al.*, 1991; Moore *et al.*, 1993) and thus constitutes a potential target for antinociceptive drugs. However, such a drug needs to be selective for nNOS, i.e., leaving the eNOS unaffected, to avoid hypotensive side effects. Though there is a low homology between the three human NOS primary sequences (approximately 50%), the active site of the enzymes seems to be relatively conserved (Li *et al.*, 1999), presumably explaining the difficulty to obtain selective inhibitors.

Several nNOS inhibitors have been developed over the last decade but only few present both potency and a clear selectivity toward this isoform. The first inhibitors developed belong to the L-arginine analogue family (Dwyer *et al.*, 1991) and are mostly not selective for the neuronal isoform. Another series of inhibitors is constituted by heterocycles such as substituted indazole and imidazole. It has been reported that 1-(2-trifluoromethylphenyl) imidazole (TRIM) has a relative selectivity for nNOS in comparison to eNOS but its potency is rather weak (IC_{50}=30 mM for nNOS) (Handy *et al.*, 1996). The nitroindazole family (with 7-nitroindazole as the lead compound) are more potent nNOS inhibitors but their selectivity over the other isoforms remain low, at least *in vitro* (Moore *et al.*, 1991; Babbedge *et al.*, 1993). It has also been reported that melatonin (fig. 2.6), a compound secreted by the pineal gland, can inhibit the nNOS activity in rat striatum in a dose-dependent manner (León *et al.*, 1998).

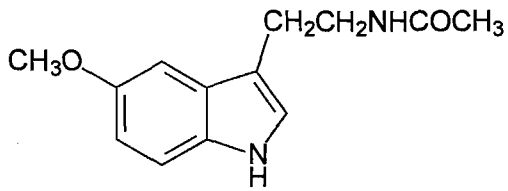

Figure 2.6: Melatonin

It is important to note that while some compounds are apparently selective for one or other isoform *in vivo*, they may show no real selectivity at the enzyme level. For example, 7-nitroindazole (7-NI) has been shown to be a selective nNOS inhibitor *in vivo* but when studied at the isolated enzyme level it is in fact equally effective as an inhibitor of all three NOS enzymes.

2.4.4.1. Endogenous inhibitors

L-NMMA (N^G-monomethyl-L-arginine) and asymmetric dimethylarginine (ADMA) are synthesised by methylation of arginine residues in proteins (Leiper and Vallance, 1999) and act as endogenous inhibitors of NOS (fig. 2.7, table 2.3). Methylarginines are released into the cell cytosol on degradation of the protein where they can act as competitive inhibitors of all three isoforms of NOS.

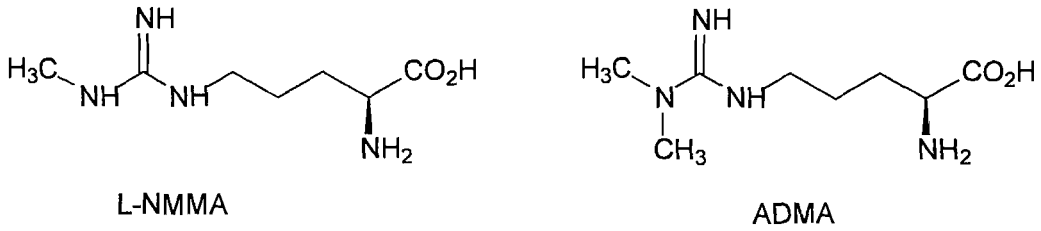

Figure 2.7: Structures of naturally occurring NOS inhibitors.

An alternative therapeutic approach to regulate NO synthesis could thus be by the manipulation of endogenous NOS inhibitors. These naturally occurring NOS inhibitors are metabolised to citrulline by the action of the enzyme dimethylarginine dimethylaminohydrolase (DDAH; Vallance & Leiper, 2002; Vallance, 2003). Inhibition of this enzyme leads to accumulation of methylarginines inhibiting NO production. Two isoforms of DDAH have been identified (Leiper *et al.*, 1999); one of which is expressed mainly in nerve tissue and another which is widely expressed in vascular and other tissues. This differential tissue distribution of DDAH could potentially be used as a method to manipulate NO overproduction by regulating endogenous NOS inhibitors in a specific cell type or tissue. An advantage of this would be that these NOS inhibitors would only accumulate to levels that partially inhibit NOS and the detrimental effects of complete NOS inhibition could probably be avoided.

2.4.4.2. Substrate analogues for NOS enzymes

The first described inhibitors of NOS were analogues of the substrate L-arginine. These compounds are thought to bind competitively at the arginine-binding site, a fact that has been confirmed for aminoguanidine (fig. 2.8), S-ethylisothiourea and thiocitrulline (Alderton *et al.*, 2001). For many of the arginine-site NOS inhibitors there are however other mechanisms involved in their mode of action that cannot be explained by simple competition with L-arginine.

There is a whole series of substrate analogues and these are shown in fig. 2.8 and table 2.3 and include aminoguanidine, L-NMMA, 1400W, (N-[3-(aminoethyl) benzyl]acetamidine), L-NIL (N^6-iminoethyl-L-lysine), L-NIO (N^5-iminoethyl-L-ornithine), GW273629 (S-[2-[(1-iminoethyl)-amino]ethyl]-4,4-dioxo-L-cysteine), GW274150 (S-[2-[(1-iminoethyl)-amino]ethyl]-L-homocysteine). Aminoguanidine has been shown to be beneficial in rodent models of stroke but its selectivity for NOS should be taken in context with its inhibitory effects on advanced glycosylation end-product formation, diamine oxidase and polyamine metabolism.

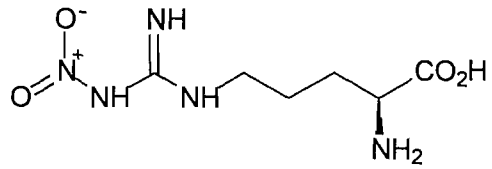

L-NNA

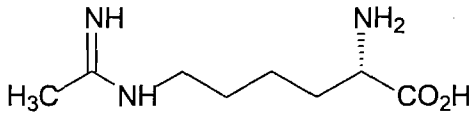

L-NIL

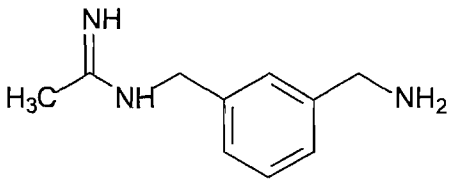

1400W

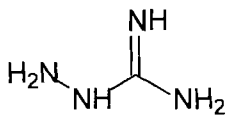

Aminoguanidine

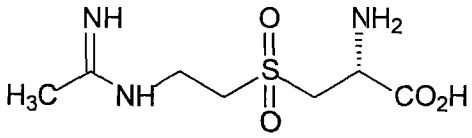

GW273629

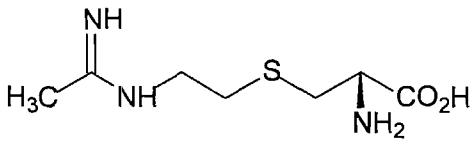

GW274150

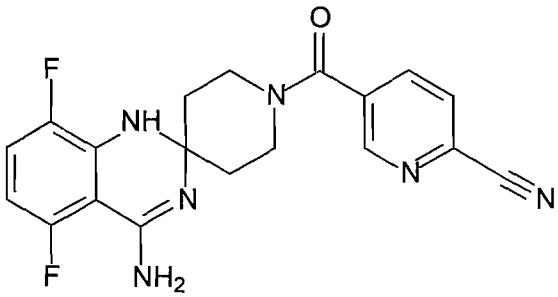

AR-C102222

Figure 2.8: Selected substrate analogues as NOS inhibitors.

The first highly selective iNOS inhibitors described were the bis-isothioureas (e.g. PBTIU or S,S-1,3-phenylene-*bis*(1,2-ethanediyl)*bis*-isothiourea (fig. 2.9). Although these compounds have some selectivity for iNOS over eNOS, their development as potential drugs was limited due to their toxic effects, that includes action at Na^+/K^+ ATPase. Binding studies with more bulky ligands led to the construction of a set of criteria by which an isoform-selective inhibitor could be developed. These are as follows:

- A structural scaffold that provides a guanidino, amidino or ureido group that donates hydrogen bonds to the glutamate residue in the NOS active site is required. There should also be a small hydrophobic group, such as an alkyl or thienyl group, to provide further non-polar interactions with the protein opposite to the glutamate residue.
- An isoform-selectivity-conferring functional group bearing hydrogen-bonding capability that can reach into the substrate-access channel remote from the active site. Such a group could take advantage of the amino acid differences in this channel between isoforms.
- A linker between the scaffold and the functional group of appropriate length and flexibility to reach isoform-specific regions.

In patients with septic shock the nonselective NOS inhibitor, L-NMMA, restored blood pressure and seemed to improve haemodynamics (Petros *et al.*, 1991, 1994). However, one of the largest clinical trials involving the use of NOS inhibitors, showed adverse effects. Low doses of these inhibitors may be beneficial, however larger doses resulted in a negative outcome (Grover *et al.*, 1998, 1999a,b). This phase III clinical trial, using L-NMMA as a treatment for patients with sepsis, had to be terminated early due to increased mortality as a result of an L-NMMA-induced fall in cardiac index in a number of patients (Grover *et al.*, 1998, 1999a,b). This was despite improving peripheral vascular tone. The mechanisms involved are unknown but are probably due to direct effects on cardiac tissue.

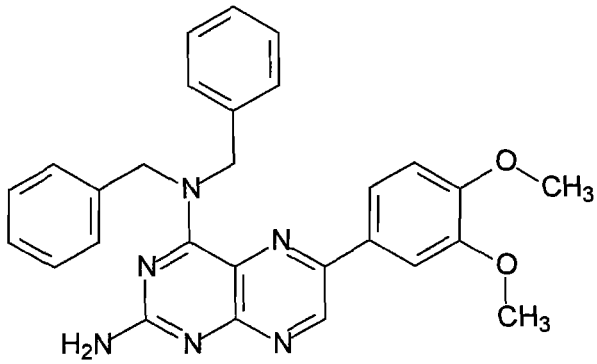

Aminopteridine

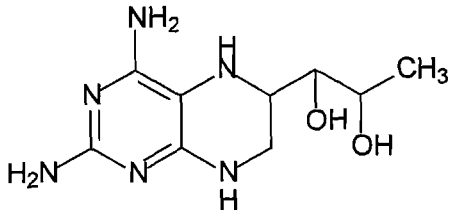

H_4aminopteridine

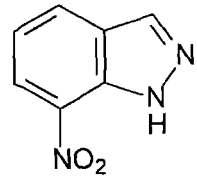

7-NI

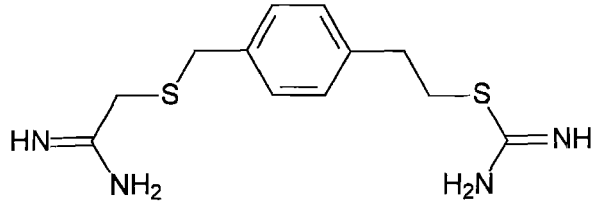

1,4-PBITU

Figure 2.9: Structures, co-factor inhibitors and isothioureas as NOS inhibitors.

In contrast, L-NMMA has been used to reduce UVB-induced skin inflammation, to treat headache and to block excess NO exhalation in asthma (Ashina *et al.*, 1999; Warren, 1994). However, Suda *et al.* (2002) found that prolonged treatment with L-NAME (N^G-nitro-L-arginine methyl ester) in eNOS knockout mice enhanced atherosclerosis suggesting that some NOS inhibitors have other harmful effects that are independent of their actions on NOS.

Table 2.3: NOS inhibitors: selectivity, potency and potential clinical applications

Compound	Clinical/model uses	Selectivity			IC_{50} (μM)		
		iNOS vs. eNOS	iNOS vs. nNOS	nNOS vs. eNOS	eNOS	iNOS	nNOS
L-NMMA	Unsuitable for sepsis, used for headache, reduces exhaled NO in asthmatics and UVB induced skin inflammation	0.5	0.7	0.7	3.5	6.6	4.9
L-NNA	Data unavailable	0.11	0.09	1.2	0.35	3.1	0.29
1400W	Not suitable for use in humans due to toxicity	>4000	32	>130	1000	0.23	7.3
L-NIL	L-NIL prodrug SC51 decreases exhaled NO in asthmatics	9	23	1.3	49	1.6	37
Vinyl L-NIO	Possible use to define the therapeutic potential for nNOS manipulation	5	0.002	120	12	60	0.1
7-NI	Attenuates lung injury in animal models and is involved in neuroprotection*	1.2	0.9	1.4	11.8	9.7	8.3
ARL 17477	Protective in animal model of cerebral ischemia	5	0.2	23	1.6	0.33	0.07
AR-C102222	Effective reduction of inflammation in models	>1000	50	>50	2	0.04	>100
GW273629	Reduces experimental postoperative ileus, beneficial in models of gastric damage	>125	>1.6	8	333	3.2	1.4

GW274150	Reduces experimental postoperative ileus, beneficial in models of gastric damage	78	1000	630	104	466	145
Aminoguanidine	Beneficial in models of stroke, reduces tissue	11	5.5	1.9	330	31	170
PBTIU	Use limited in humans due to toxic effects involving Na^+K^+ ATPase	190	N/A	N/A	9	0.047	N/A
FR038251	Different potencies and selectivities for NOS isoforms; possible iNOS inhibitor unknown effects in humans	8	13	3	25	3	6.3
FR038470	Different potencies and selectivities for NOS isoforms; possible iNOS inhibitor unknown effects in humans	38	1.7	11	8.8	53	1.9
FR191863	Not available	5	65	>4	>100	16	100

L-NNA: N^G-nitro-L -arginine, L-NMMA: N^G-monomethyl-L-arginine, 7-NI: 7-nitroindazole, ARL 17477: N-[4-(2-{[(3-chlorophenyl)methyl]amino}-ethyl)phenyl]-2-thiophenecarboximide diHCl, L-NIL: N^6-iminoethyl-L-lysine. L-NIO: N^5-iminoethyl-L-ornithine, 1400W: N-[3-(aminoethyl)benzyl]acetamidine, GW273629: S-[2-[(1-iminoethyl)-amino]ethyl]-4,4-dioxo-L-cysteine, GW274150: S-[2-[(1-iminoethyl)-amino]ethyl]-L-homocysteine, FR038251: 5-chloro-1,3-dihydro-2H-benzimidazol-2-one, FR038470: 1,3(2H,4H)-isoquinolinedione, FR191863: 5-chloro-2,4(1H,3H)-quinazolonedione, PBTIU: S,S0- 1,3-phenylene-bis(1,2-ethanediyl)bis-isothiourea. Addapted from Alderton *et al.* 2001; Hansen 1999; Kita *et al.* 2002; Pitzele 1999; Vallance & Leiper 2002.

The novel and highly selective iNOS inhibitor 1400W has been shown to reduce formation of oedema, neutrophil infiltration and macroscopic damage in experimentally induced acute colitis in the rat and supports the notion that selective iNOS inhibitors may be used in colitis treatment (Kankuri *et al.*, 2001). In addition, this compound has been shown to inhibit growth of solid cultured cancer cells (Thomsen *et al.*, 1997). However, the clinical use of 1400W in humans is doubtful due to its toxicity at high doses (Garvey *et al.*, 1997; Kankuri *et al.*, 2001; Thomsen *et al.*, 1997). Other compounds in this series include GW273629 and GW274150 and have been shown to reduce experimental postoperative ileus and may be beneficial in models of gastrointestinal damage.

Astra Zeneca developed a spiroquinazolone derivative denoted AR-C102222 which represents an alternative chemical approach for NOS inhibition. This compound has an IC_{50} of 0.04 μM, and is reported to be highly selective for iNOS. In *in vivo* studies, it was found to be effective in reducing inflammation in the standard carageenan paw oedema model and decreased adjuvant-induced arthritis in rats (Beaton *et al.*, 2001).

Structural modifications to one of the guanidine nitrogens of L-arginine led to the development of L-NNA (N^G-nitro-L-arginine), L-NAME and aminoguanidine, all of which are competitive inhibitors of NOS. Two recently developed compounds, based on aminoguanidine, PL-AG (pyridoxal aminoguanidine, fig. 2.10) and 8Q (8-quinolinecarboxylic acid hydrazide) have been shown by Pekiner *et al.* (2002) to selectively inhibit basal but not agonist stimulated NO production in the rat aorta.

L-NIO has been shown to be more selective for nNOS than iNOS or eNOS (table 2.3, Babu & Griffith, 1998a,b) and recent work by Hansel *et al.*, (2003) indicated that L-NIL (Fig. 2.8, table 2.3) inhibited iNOS activity. Furthermore, in a clinical trial using normal and asthmatic individuals it was shown that the prodrug of L-NIL, SC51 inhibits exhaled NO. This drug was well-tolerated and had no adverse effects on heart rate, blood pressure or forced expiratory volume. Whether such compounds or related versions will be of use therapeutically remains to be investigated.

Reducing harmful over-production of NO has vast therapeutic potential and inhibition of iNOS in particular has great use as an anti-inflammatory target in many diseases. Inhibition of nNOS has potential in CNS disorders involving neurodegeneration, neurotoxicity and pain (Low, 2005). Inhibition of NOS isoforms could however have detrimental consequences in addition to their beneficial effects. For example, if nNOS is

inhibited in the gastrointestinal and genitourinary systems it can cause spasm of the sphincters.

If iNOS is not selectively inhibited it could create a situation where under certain circumstances wound healing was inhibited and the risk of infection increased. In addition to permit prolonged use of NOS inhibitors, it is necessary to use isoform specific inhibitors with a greater degree of selectivity to eliminate the potential risk of unwanted inhibition of eNOS which could have the consequences of hypertension, increased activation of platelets and white blood cells and atherogenesis. For example, with isoform specific inhibitors, it might be preferable to inhibit NOS in specific cells or tissues. Birrell *et al.* (2003) have shown in models of allergic inflammation, and using 1400W to inhibit iNOS, that constitutive rather than inducible NOS isoforms are important and this has implications for the treatment of asthma where it might not be appropriate to use iNOS inhibitors as therapy.

In cancer (e.g. gliomas), another medicinal field of potential use is based upon the hypothesis that suppression of tumoural NOS has more of a therapeutic effect than an oncogenic effect. Some preliminary rodent studies using L-NAME in the C6 striatal implantation model showed inhibition of tumour growth and increased tumour necrosis (Swaroop *et al.*, 2000) and studies using iNOS knockout C6 cells suggested that iNOS was required for tumourogenicity (Yamaguchi *et al.*, 1999). Although both pharmacological and genetic engineering studies of various nonglial malignant cell lines *in vivo* have also suggested that NOS is important for tumourogenicity, other studies have shown that enhancement of iNOS activity leads to decreased tumourogenicity (Shinoda & Whittle, 2001). Further work on the biochemical and toxicological mechanisms of NO in gliomas will be required to clarify its potential for therapy.

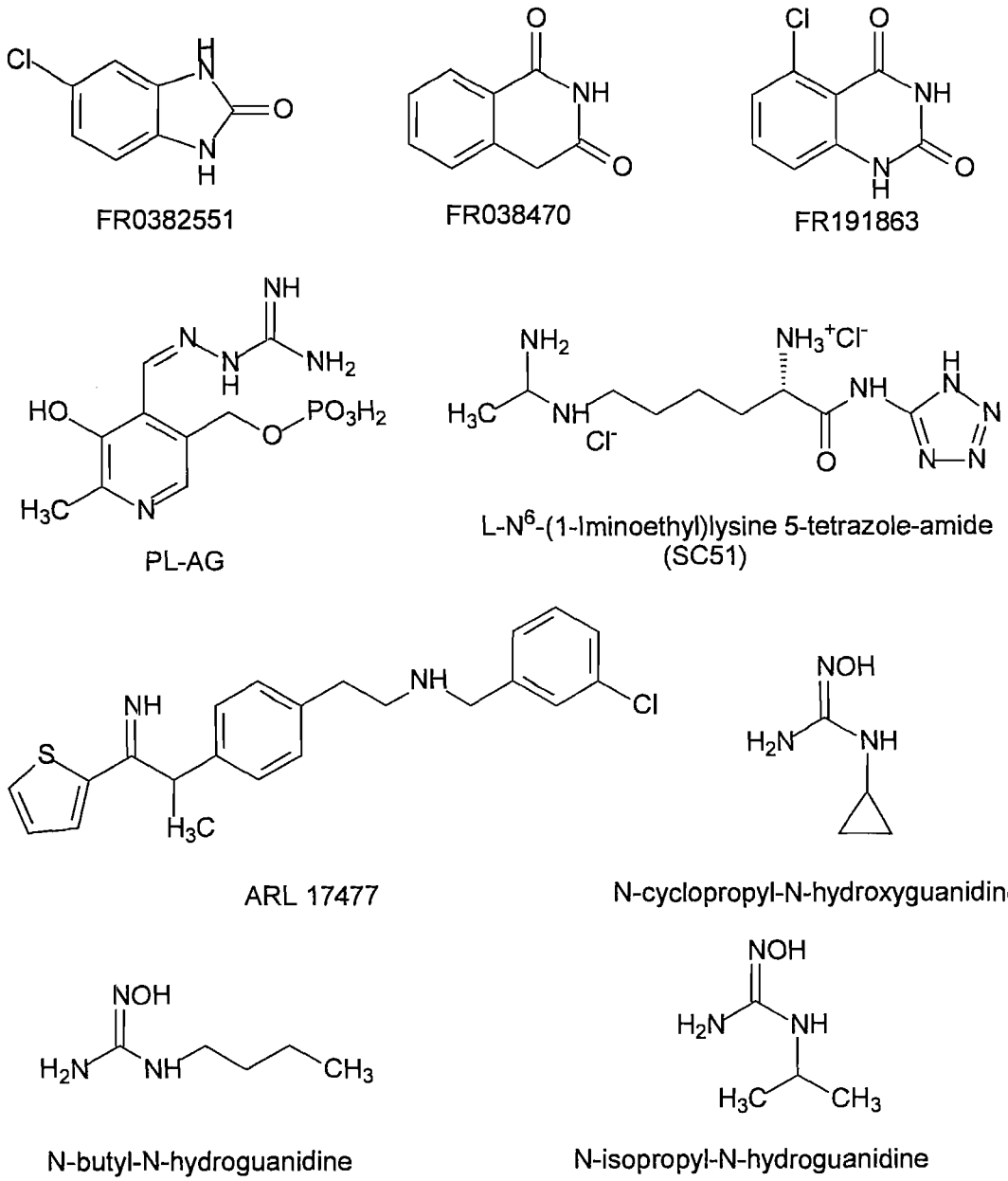

Figure 2.10: NOS inhibitors containing guanidine moieties.

2.5. Polycyclic amines and indole derivatives

Since the description of the antiviral properties of the adamantane amine, 1-amino-adamantane or amantadine (Davies *et al.*, 1964), significant interest into the chemistry of polycyclic amines has been shown. The pharmacological properties of the adamantane amine derivatives are well known and led to further investigation into the polycyclic cage amine derivatives.

Biological activity described for a class of polycyclic amine derivatives, the pentacycloundecylamines (fig. 2.11), suggests possible neuroprotective abilities for these compounds through modulation of voltage activated sodium, potassium and Ca^{2+} channels, as well as interaction with NMDA receptor operated channels. They show structural similarities to known NMDA antagonists, and their peripheral L-type calcium channel activities have also been described (Geldenhuys *et al.*, 2003a Van der Schyf *et al.*, 1986; Van der Walt *et al.*, 1988).

NMDA antagonists like amantadine and memantine have been clinically approved for the treatment of PD and AD (Lipton & Chen, 2004). In addition, memantine did not substantially affect normal synaptic activity and still prevented excessive NMDA receptor activation. Unlike other NMDA receptor antagonists, side effects are averted with memantine because of the preservation of physiological neurotransmission (Lipton & Chen, 2004).

Structural similarities and comparable activities between the pentacyclic cage compounds and adamantanamines indicate therapeutic potential for the former compounds (Oliver *et al.*, 1991a,b,c). These authors suggested that polycyclic amines may have potential as a new class of anti-parkinsonian agents due to their anticataleptic and anticholinergic activities. L-Type calcium channel antagonism has also been described for pentacycloundecylamines, in particular for the prototypical compound 8-benzyl-8,11-oxapentacyclo[5.4.0.$0^{2,6}$.$0^{3,10}$.$0^{5,9}$]-undecane (NGP1-01, fig. 2.11a, R=$NHCH_2Ph$) which was extensively studied in this regard (Malan *et al.*, 2000; Van der Schyf *et al.*, 1986).

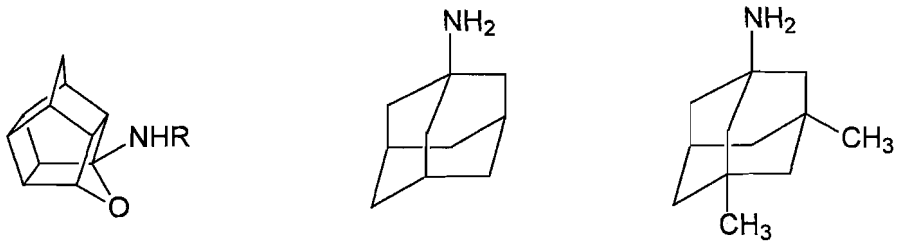

a) Pentacycloundecylamine derivative b) Amantadine c) Memantine

Figure 2.11: Structural similarities between the pentacycloundecane derivatives with amantadine and memantine.

The structural resemblance between the polycyclic cage structure of memantine and NGP1-01 prompted the evaluation of these compounds and their derivatives for possible neuroprotective activity (Geldenhuys *et al.*, 2003b). Putative protective activity was hypothesised to be initiated by a dual mechanism of action including attenuation of NMDA receptor activity and direct blocking of L-type Ca^{2+} channels, thereby preventing excessive influx of Ca^{2+} into neuronal cells.

Another benefit of the pentacycloundecylamines is their ability to enter the CNS. For drugs to exert meaningful effects in the CNS they have to cross the BBB and it was found that the pentacycloundecylamines penetrate the CNS in sufficient concentration to exert pharmacological effects (Zah *et al.*, 2003). It was proposed that the main mode of entry into the CNS was by means of passive diffusion across the BBB, due to the inherent hydrophobic nature of the polycyclic structure.

The polycyclic cage thus appears to be a useful scaffold to explore in order to design potential pharmacologically active compounds in the field of neurodegeneration.

2.6. Conclusion

Multiple synergistic pathways have been suggested to play crucial roles in the cell death cascade. Therefore, it would be an effective therapeutic strategy to employ a combination of compounds to affect multiple target sites in the cell-destruction pathway. Drugs such as budipine, an NMDA receptor antagonist; the dihydropyridine type of Ca^{2+} channel antagonists; *N*-nitro-L-arginine, an NO inhibitor; and iron chelators represent candidates for Parkinson's disease treatment. Perhaps the most effective mode of cell-protective therapy would be a combination of these compounds as opposed to monotherapy.

From the literature it is clear that 7-nitroindazole and melatonin have positive and promising effects in the treatment and prevention of neurodegenerative disorders. Melatonin treatment however, may be problematic due to its various physiological roles and multiple undesirable side effects. Experimental evidence also shows that melatonin influences aging and age-related processes and disease states. These effects are apparently related to its effectiveness as a free radical scavenger (Beyer *et al.*, 1998). Its possible mechanism of action include removal of O_2, scavenging of reactive oxygen species or their precursors, inhibiting ROS formation and binding metal ions needed for catalysis of ROS generation.

Melatonin and other indole derivatives might thus play a role in the treatment and prevention of neurodegenerative disorders caused by oxidative stress and reactive oxygen species.

Combining the structural features of the indole and the polycyclic cage structures, both with well documented pharmacological effects, could indeed provide the basis for novel structures with the potential to act via multiple modes of action, addressing the multi-component aspects of pathology of neurodegenerative diseases.

Molecular modelling

Chapter 3

3. Introduction

Medicinal chemists today are facing an ever increasing challenge to design new therapeutic agents for the treatment of human disease. For many years the main focus for discovering new drugs consisted of taking a lead structure and developing a chemical program for finding analogues exhibiting the desired pharmacodynamic properties.

These drug discovery methods are now being supplemented by more direct approaches made possible by the understanding of the molecular processes involved in the underlying disease. In this perspective, the initial point in drug design is the molecular target (receptor, enzyme) in the body instead of the existence of an already known lead structure (Cohen, 1996).

Computer aided molecular drug design and graphics (molecular modelling) has its origins in the 1980's and can be simply considered as a range of computational techniques that are based on theoretical chemistry methods and experimental data. It can be used either to analyse molecules and molecular systems or to predict molecular and pharmacodynamic properties.

These computational methods and molecular visualisation techniques currently available provide extensive insight into the precise molecular features that are responsible for the regulation of biological processes: molecular geometries, atomic and molecular electronic aspects and hydrophobic forces. All these structural characteristics are of great importance in the understanding of structure-activity relationships and in rational drug design (Cohen, 1996).

3.1. The substrate binding site of nNOS

Raman *et al.* (2001) described the crystal structure of 3-bromo-7-nitroindazole (3-Br-7-NI, 1OM5, fig. 3.1) complexed with the catalytic heme domain of nNOS. Both 7-nitroindazole (7-NI) (Babbedge *et al.*, 1993; Moore *et al.*, 1993; Wolff *et al.*, 1994) and 3-Br-7-NI (Bland-Ward & Moore, 1995) are potent inhibitors of all three NOS isoforms *in vitro*. Biochemical studies have shown that these compounds not only

compete with L-Arginine but also for the cofactor tetrahydrobiopterin (H_4B)-binding site (Alderton *et al.*, 1998; Mayer *et al.*, 1994; Wolff & Gribin, 1994). These inhibitors exhibit a high level of specificity for nNOS *in vivo* and expectedly fail to produce discernible changes in systemic blood pressure (Moore *et al.*, 1993; Handy & Moore, 1998).

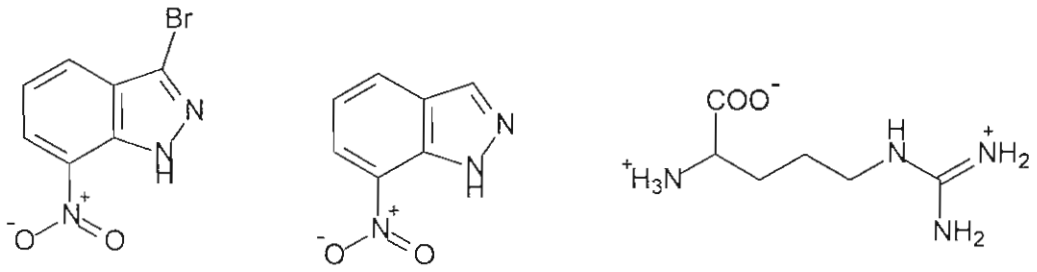

3-Br-7NI
3-bromo-7-nitroindazole

7-NI
7-nitroindazole

L-Arg
L-arginine

Figure 3.1: Structural formulas of the substrate and ligands used in the above crystallographic studies.

Although the exact mechanism for the specificity of these inhibitors to nNOS *in vivo* is poorly understood, it is thought that differences in uptake pathways of different cell types may play a role. More importantly, 7-NI and 3-Br-7-NI have been shown to be neuroprotective in animal models of stroke (Nanri *et al.*, 1998) and Parkinson's disease (Przedborski *et al.*, 1996; Zhang *et al.*, 2000). Therefore, understanding the molecular basis of 3-Br-7-NI recognition by NOS will aid in the development of new isoform-selective inhibitors that can be used in the treatment of neurodegenerative disorders involving NO-mediated neurotoxicity.

3.1.1. Molecular recognition of 3-Br-7-NI at the substrate binding

The active-site structure of nNOS is shown in fig. 3.2. The substrate, L-Arg, is positioned over the heme where H-bonds with Trp 587, Tyr 588, Glu 592, Gln 478 and Asp 597 help to orient the substrate for regioselective hydroxylation by, presumably, a Fe-linked O atom. The essential cofactor, H_4B, is bound at the intersubunit interface. Note that H_4B and the R-amino group of L-Arg both H-bond with the same heme propionate (Raman *et al.*, 2001).

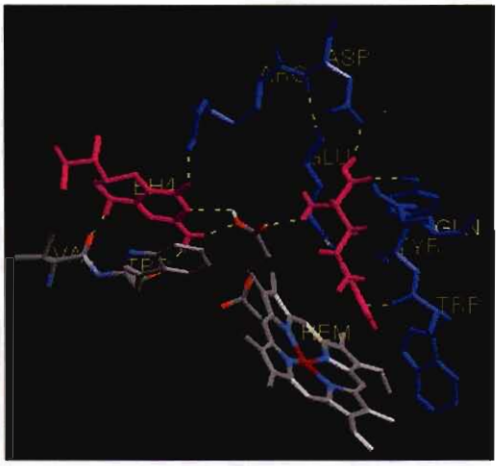

Figure 3.2: A molecular model of the nNOS active and H_4B binding sites (purple). Note that L-Arg (purple) and H_4B both H-bond with the same heme propionate.

Presumably, 3-Br-7-NI displaces L-Arg from the active site despite the fact that 3-Br-7-NI bears no structural similarity to L-Arg. To understand how 3-Br-7-NI binds to NOS, Li *et al*, 2003 solved the crystal structure of 3-Br-7-NI bound to the catalytic heme domain of nNOS at 2.30 Å resolution. 3-Br-7-NI occupies the site where L-Arg is normally bound (fig. 3.3). The orientation of the inhibitor is unambiguous due to the bulky density of the bromine atom used as a guide in positioning the inhibitor in the substrate cavity. When compared with L-Arg, 3-Br-7-NI is relatively planar and stacks parallel within van der Waals contact distance to the heme plane (fig. 3.3), and hydrogen-bonds with Met 589 and Heme.

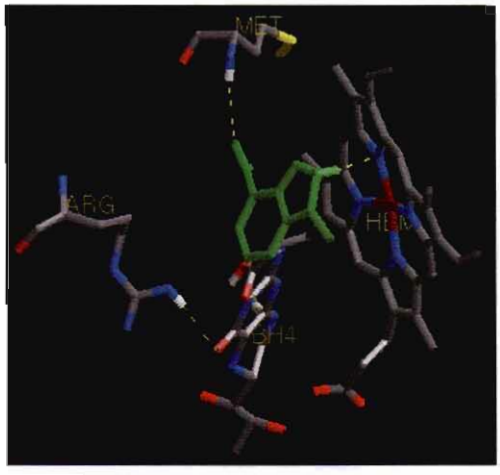

Figure 3.3: Molecular model where 3-Br-7-NI (green) displaces L-Arg from the active site.

3-Br-7-NI, being an aromatic heterocycle, albeit π-deficient at carbon atoms due to the number of ring N atoms, probably derives some of its binding energy from the π-π stacking interactions with the heme and many nonbonded contacts it entertains with the protein. Thus, the 3-Br-7-NI ring mimics the L-Arg guanidinium in both electrostatic stabilisation and π-stacking with the heme ring.

3.1.2. Implications of the binding site of NOS for drug design

There are many instances in which a protein differentiates between nearly identical inhibitors. NOS for instance can recognise the different arginine-based inhibitors by utilising the same set of contacts that are made to L-Arg alongside new interactions made with the substituent. Important to this interaction is the H-bonding potential of the Glu-592 side chain that participates in type I or type II interactions (Ippolito *et al.*, 1990; Singh *et al.*, 1987) and whether amidino (Li *et al.*, 2001), guanidino or ureido (Li *et al.*, 2000) groups are present in the inhibitor.

In the case of 3-Br-7-NI, it completely removes Glu-592 from engaging in direct H-bonded contact with the inhibitor. Secondly, it competes for both the substrate and cofactor binding sites at the same time. Due to this, 3-Br-7-NI is able to occupy one site and subsequently alter the specificity of a second site. From a study conducted by Raman *et al.* (2001) it was stated that an inhibitor which avoids H-bonded contact with one of the heme propionates, can serve as a potential template for designing drugs for isoform specificity. This phenomenon also has important implications for structure-based drug design. The target protein is usually treated as a binding surface template from which novel compounds with complementary shape and chemistry arise. In the conventional setting, a rigid geometry is assumed for the binding site, and this would not have predicted the binding of 3-Br-7-NI to NOS. The fact that Glu-592 adopts a new conformation in the 3-Br-7-NI complex has provided a structural basis for introducing knowledge-based dynamics information into drug-design strategies for NOS. It also emphasise the importance of dynamics, however small, in making a substantial contribution to the information content regarding how a target recognises a ligand. The authors have demonstrated that, although 3-Br-7-NI targets the substrate and cofactor-binding sites of NOS, its high specificity is garnered by adapting to a unique and altered protein conformation. The ability of 3-Br-7-NI to exploit this characteristic phenomenon provides a significant insight for the further development of therapeutically important isoform-specific NOS inhibitors (Raman *et al.*, 2001).

3.2. Methodology

The ligandfit module of Cerius$^{2®}$ (2002) is a molecular modelling program capable of determining possible sites for ligand binding. The PDB file of 1OM5, containing the coordinates for the neuronal NOS enzyme co-crystallised with the inhibitor, 3-Br-7-NI, was downloaded from RCSB Protein Data Bank (Li *et al.*, 2003). The structure of the protein and docked ligand was used to generate an active site model (fig. 3.4) for the neuronal NOS enzyme utilising the Ligandfit® module of Cerius$^{2®}$ (2002). The DREIDING2.21 force field and Gasteiger charges were used throughout the experiment and all other values were set to default unless otherwise specified.

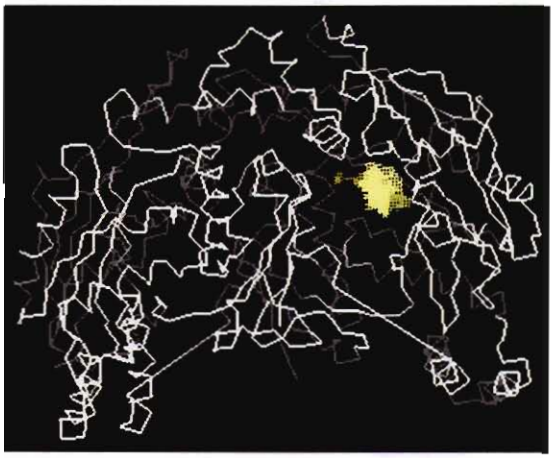

Figure 3.4: 1OM5 with the active site of nNOS (yellow) as determined by site search in trace rendering as calculated with Ligandfit®.

This active site model was used to investigate a series of polycyclic structures. The different conformations of the compounds selected for synthesis (fig. 3.5, compound **1-19**) generated by Catalyst 4.9® were exported to Cerius$^{2®}$ as a SD (structural data) file in order to facilitate docking of these conformations into the determined active site of the enzyme.

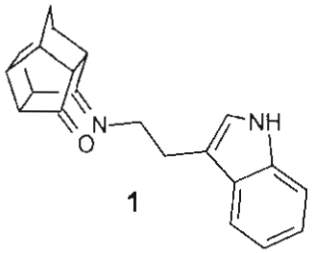

1

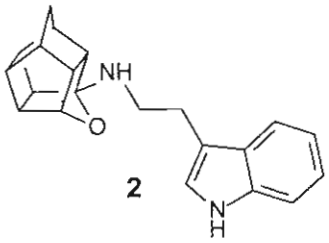

2

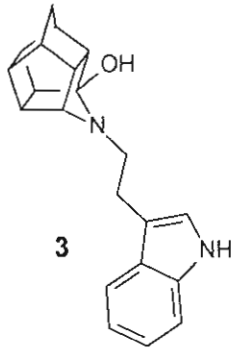

3

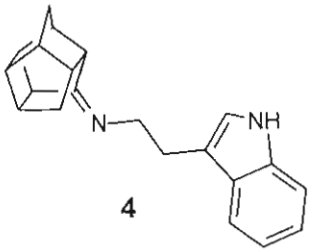

4

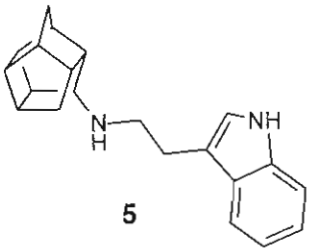

5

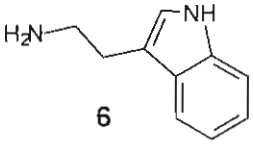

6

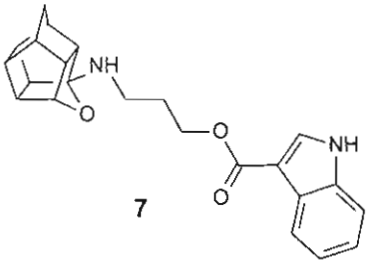

7

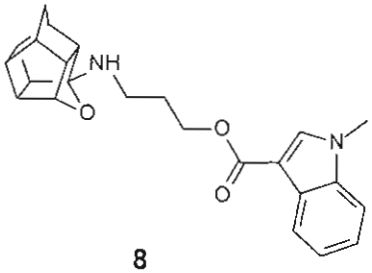

8

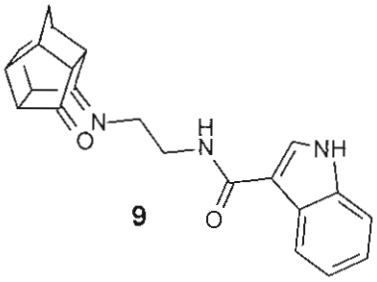

9

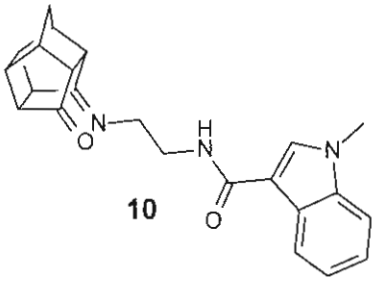

10

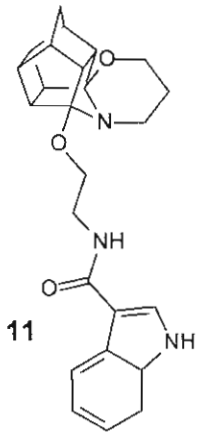

11

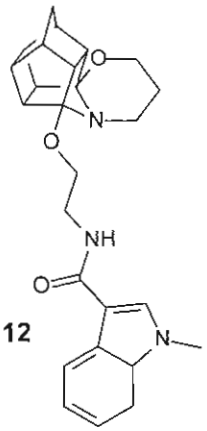

12

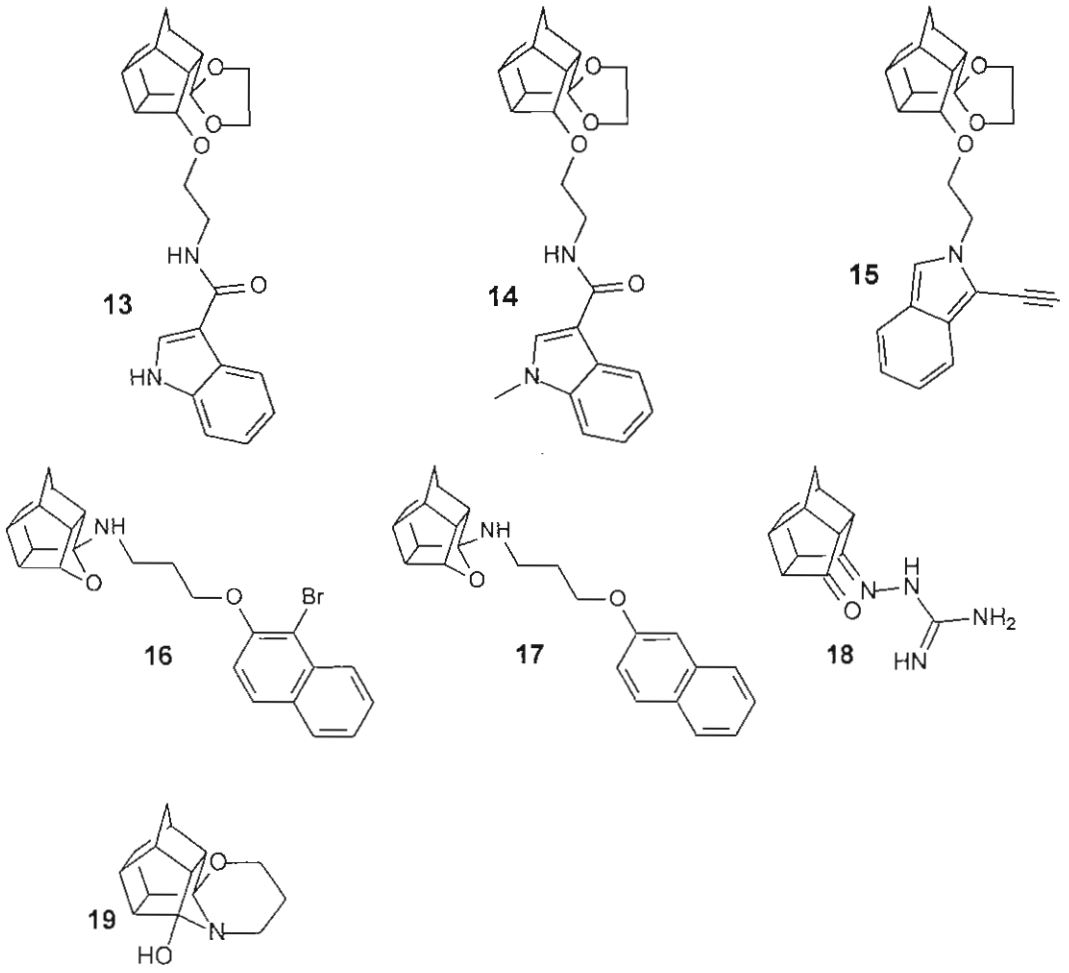

Figure 3.5: Proposed structures for *in vitro* evaluation for NOS activity

Before the docking was performed, the Monte Carlo parameters were set to 1000 to limit the amount of additional conformers generated and evaluated to a maximum of 1000. The default parameters were used in all other cases. The results of the fits were included into a study table and the compounds were sorted in order of the consensus score, Ligscore1 and Ludi score accordingly. The highest scores of the 5 best conformers of each compound, and thus best overall fit in the active site, were selected and evaluated for theoretical interaction with the NOS enzyme. The different drug conformations were fitted into the site to obtain orientation and hydrogen-bonds interactions (fig 3.6).

Figure 3.6: Possible interactions in the active site of all planned compounds for synthesis. Ligands were kept in default colours and adjacent amino acids are highlighted in either red or blue and hydrogen-bonds are indicated in yellow.

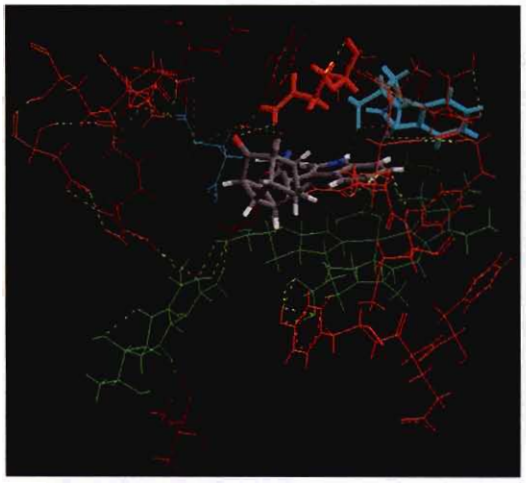

Compound **1**

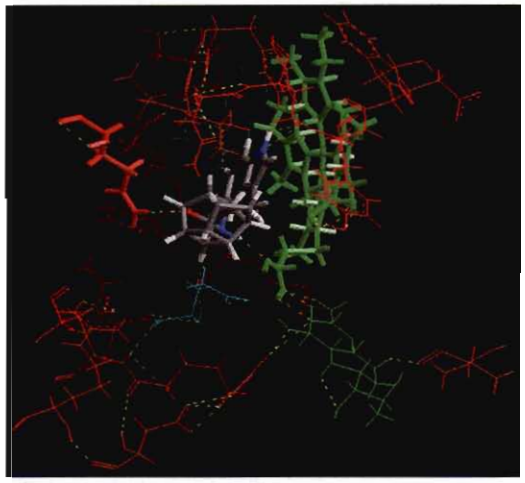

Compound **2**

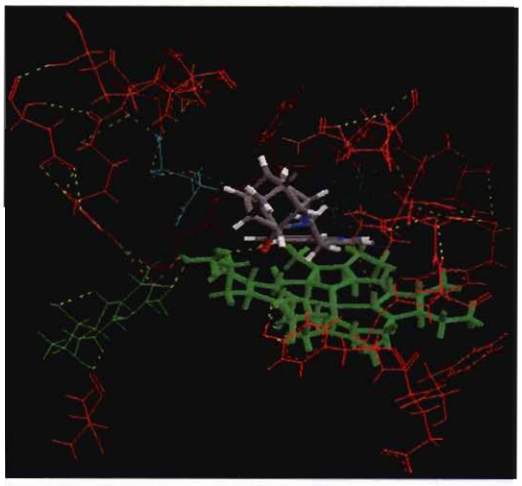

Compound **3**

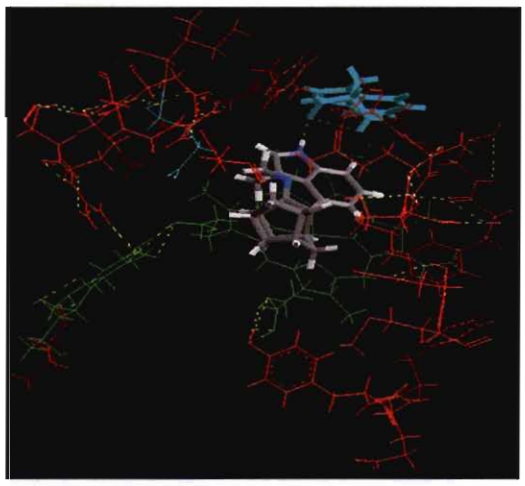

Compound **4**

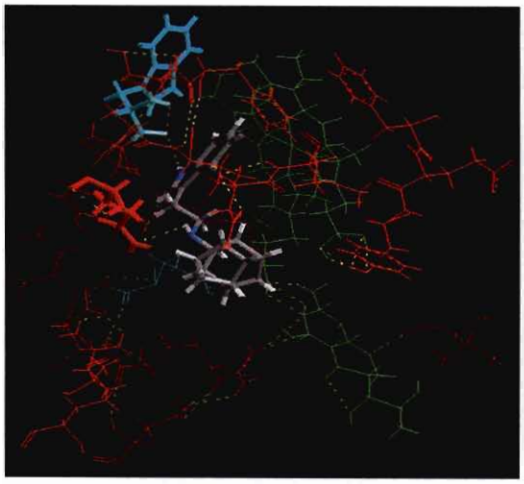

Compound **5**

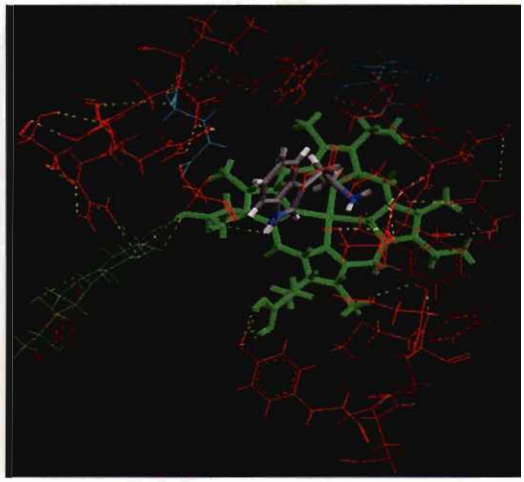

Compound **6**

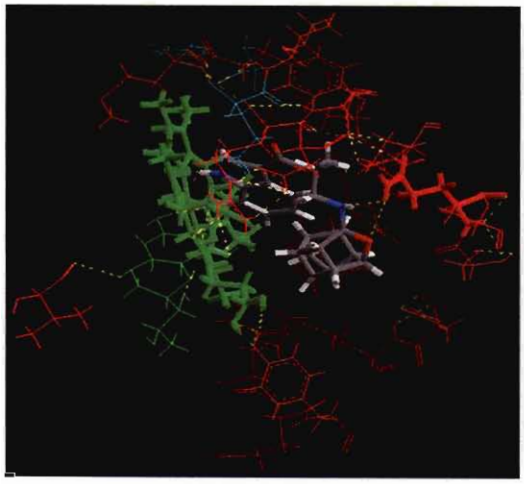

Compound **7**

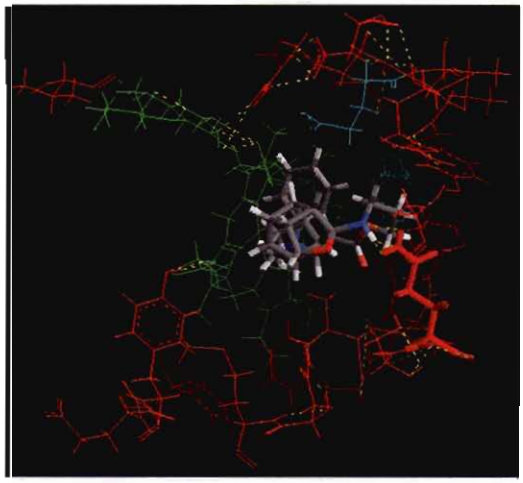

Compound **8**

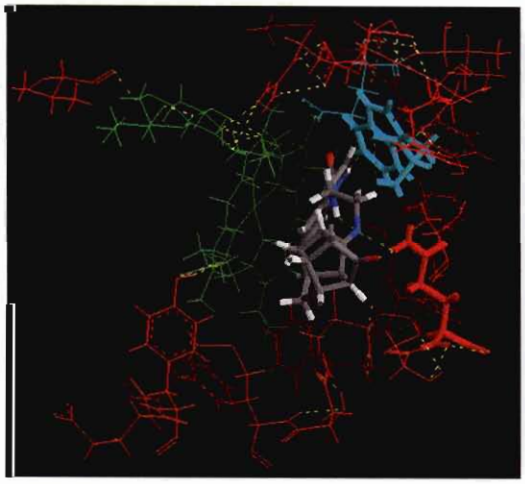

Compound **9**

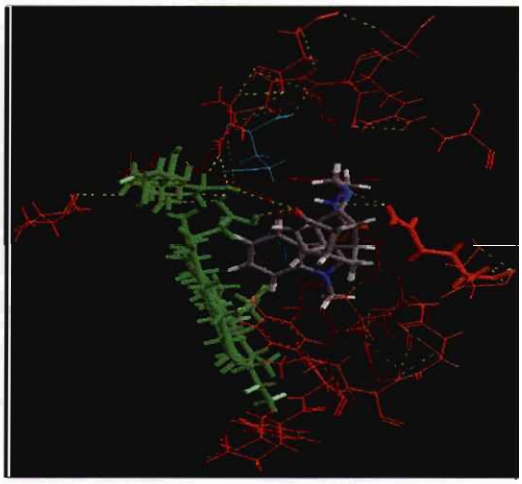

Compound **10**

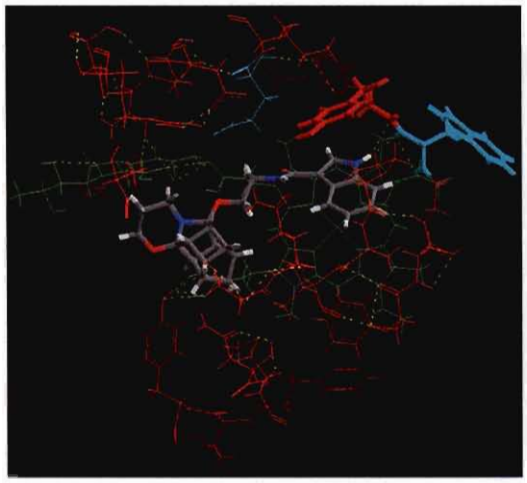

Compound **11**

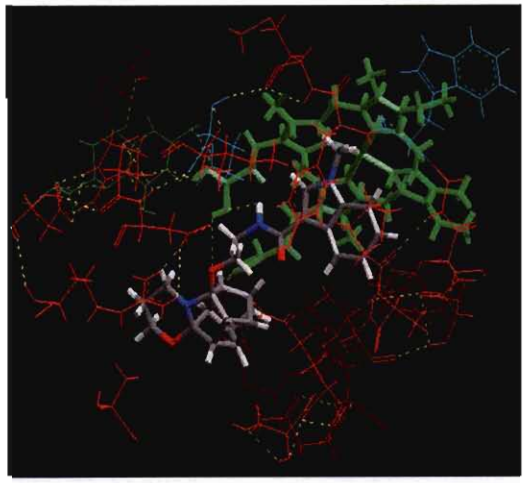

Compound **12**

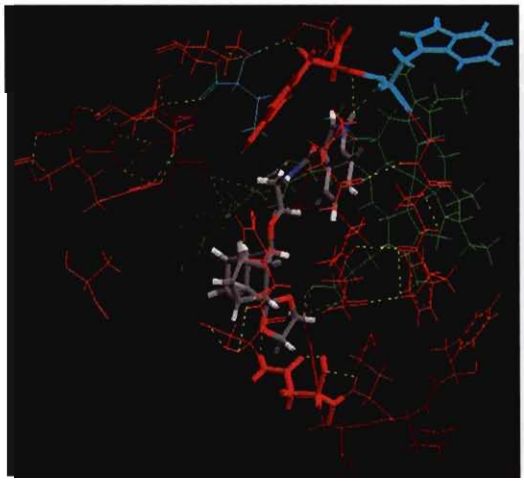

Compound **13**

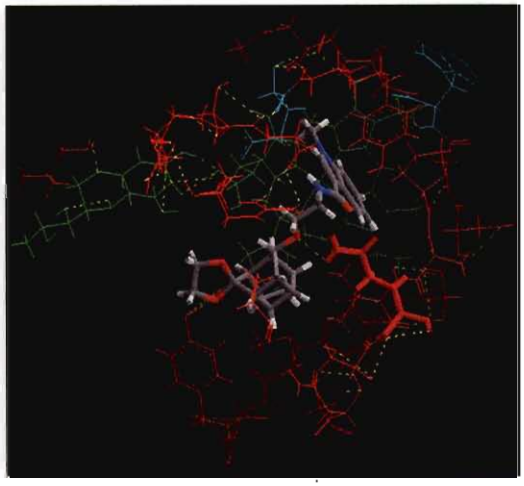

Compound **14**

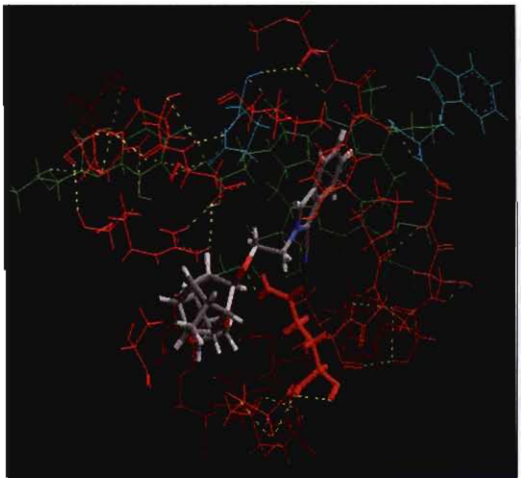

Compound **15**

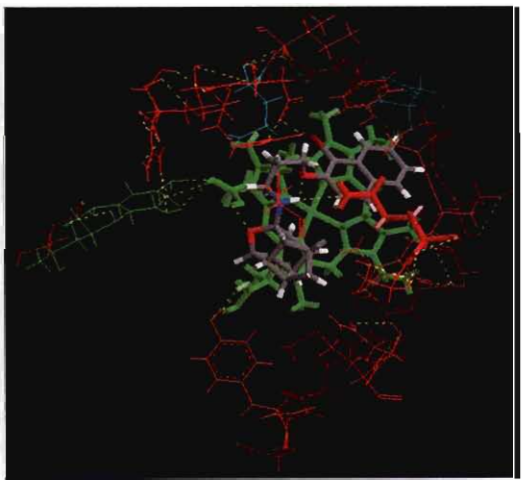

Compound **16**

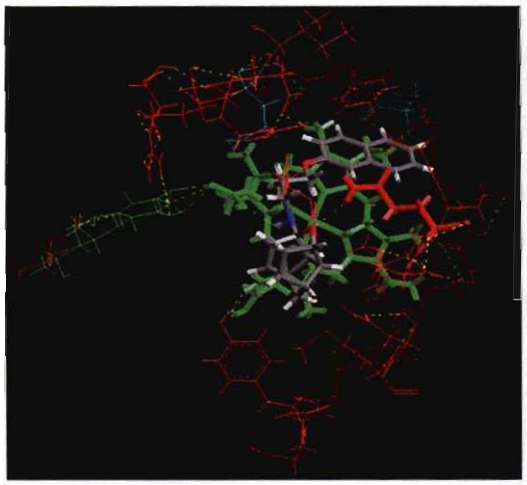

Compound **17**

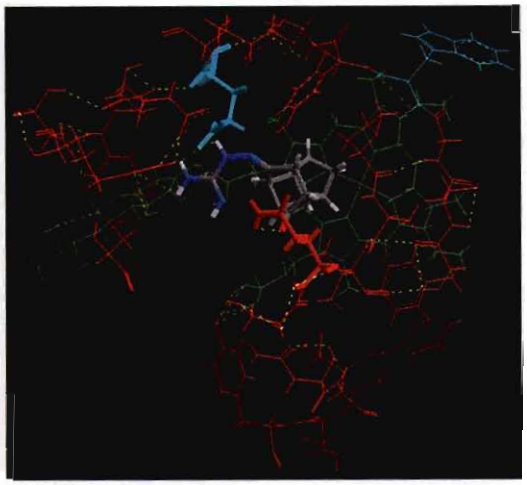

Compound **18**

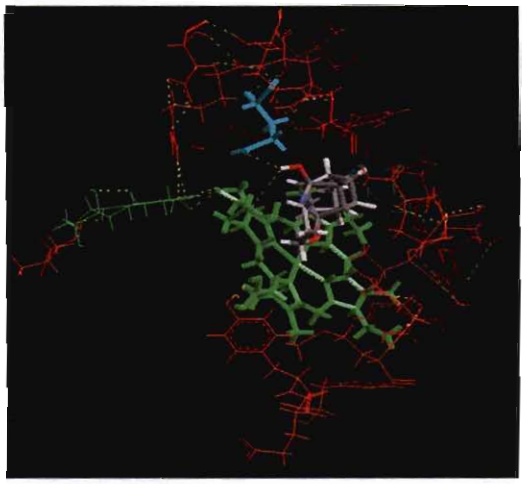

Compound **19**

3.3. Results and Discussion

Substrates (L-Arg or L-NHA) bind to the active site via an extensive hydrogen bond network involving both guanidinium and amino acid moieties to the surrounding enzyme residues. N^{ω}-Hydroxy-L-arginine (L-NHA) binds to the nNOS active site in a similar way to that of L-Arg (Li *et al.*, 2002). The protein-ligand interactions can be divided into two sites. One is the amino acid binding pocket where one of the carboxylate oxygen atoms of L-NHA accepts H-bonds from Tyr588 and Gln478 and the other carboxylate oxygen is within H-bonding distance of Asp597. The R-amino nitrogen forms H-bonds forming a bridge between the Glu592 side chain and one of the heme propionates.

The second site is right above the heme plane where the guanidine group maintains three hydrogen bonds via its bridging nitrogen and its unsubstituted terminal nitrogen (NH2) to the Glu592 side chain and the Trp587 carbonyl oxygen. The hydroxyl group of L-NHA does not coordinate to the heme iron but instead points away from it towards the backbone amide of Gly586 to form a weak H-bond or nonbonded contact. The L-NHA binding mode in nNOS is essentially identical to what has been reported for human eNOS (Fischmann *et al.*, 1999) and murine iNOS (Crane *et al.*, 2000).

Table 3.2: Summary of observed H-bond interactions between the best conformers of the compounds and adjacent amino acids.

Compound name	H-bond interaction	Compound name	H-bond interaction
Compound **1**	Gln478, Trp587	Compound **11**	Tyr588, Trp587
Compound **2**	Gln478	Compound **12**	Heme
Compound **3**	Heme	Compound **13**	Asn569, Trp587, Tyr588
Compound **4**	Trp587	Compound **14**	Gln478
Compound **5**	Trp587, Gln478	Compound **15**	Gln478
Compound **6**	Heme	Compound **16**	Heme, Gln478
Compound **7**	Heme, Gln478	Compound **17**	Heme, Gln478
Compound **8**	Gln478	Compound **18**	Glu592, Gln478
Compound **9**	Gln478, Trp587	Compound **19**	Heme, Glu592
Compound **10**	Gln478, Tyr588		

In all cases the indole ring was oriented either parallel or towards the heme in the binding cavity, with the cage structure located near the entrance cavity. A few of the test compounds formed hydrogen bonds with the amino acids necessary for activity, Tpr587, Glu592 and heme, and it was hypothesised that these compounds might show NOS inhibitory activity. Compounds that formed hydrogen-bonds with Tyr 588, Gln 478 and Asp 597 could also be active since these amino acids play only a role in the stabilisation and orientation of ligands in the cavity. From the docking studies it is clear that all the test compounds formed one or more H-bonds with heme, amino acids necessary for activity or stabilising amino acids.

3.4. Conclusion

From the docking study, it is clear that H-bonds are necessary for NOS activity. Since 3-Br-7-NI is capable of altering the conformation of the binding amino acids within the active site, the novel compounds may exhibit the same phenomenon.

The compounds that exhibited the best inhibition activity towards NOS *in silico* were compounds **1, 4, 5, 9, 11, 18, 19,** since they formed hydrogen bonds with the amino acids necessary for activity. However *in vitro* studies need to be conducted to determine the validity of the assumption and potential of these compounds for neuroprotection.

Synthetic procedures

Chapter 4

4. Instrumentation

Mass spectrometry (MS): An analytical VG 70-70E mass spectrophotometer with electron ionisation (EI) at 70 eV was used for MS and high resolusion mass spectrometry (HRMS). Relevant spectra are included in annexure 1.

Infrared (IR) absorption spectrophotometry: IR spectra were recorded on a Nicolet 470 FT-IR spectrophotometer, incorporating the samples in KBr pellets. Relevant spectra are included in annexure 1.

Melting point (mp): Melting points were measured using a Gallenkamp melting point apparatus and capillary tubes.

Nuclear magnetic resonance spectrometry (NMR): A Varian VXR300 spectrometer was used to obtain ^{1}H and ^{13}C spectra. ^{1}H spectra were recorded at a frequency of 300.075 MHz and ^{13}C spectra at 75.462 MHz, in a 7 Tesla magnetic field with tetramethylsilane (TMS) as internal standard and a bandwidth of 100 Hz at 24 KG applied for ^{1}H and ^{13}C decoupling. All chemical shifts are reported in parts per million (ppm) relative to TMS (δ = 0). The following abbreviations are used to indicate multiplicities of signals: s – singulet, bs – broad singulet, d – doublet, t – triplet and m – multiplet. Spectra of selected compounds are included in annexure 1.

4.1. Chromatographic methods

Mobile phases used were prepared on a volume-to-volume basis (v/v). Mobile phases containing chloroform, ethanol and ethylacetate were mostly used and when necessary new combinations were made using the Prism model of Nyiredy *et al.* (1985). Ultraviolet light (UV 254 nm and UV 366 nm), 2% ninhydrine solution and iodine vapours were used for visualisation on thin layer chromatography.

Thin layer chromatography: TLC was used to monitor all chemical reaction.

Column chromatography: Seperation and purification of product mixtures were done using flash chromatography (Still *et al.*, 1978) on glass columns filled with silica gel Merck® (0.063-0.200 mm).

4.2. Selection of compounds

From the general SAR of the polycyclic and indole derivatives and the results obtained from molecular modelling, the structures included in table 4.1 were selected for synthesis and evaluation

Table 3.1: Compounds evaluated and synthesised in this study.

Compound	Name	Structure
1	8-[3-(2-aminoethyl)indole]-pentacyclo[5.4.0.0^{2,6}.0^{3,10}.0^{5,9}]undecane-11-one	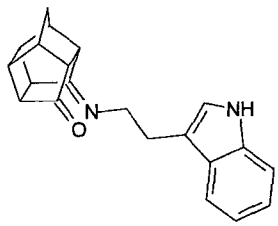
2	8-[3-(2-aminoethyl)indole]-8,11-oxapentacyclo[5.4.0.0^{2,6}.0^{3,10}.0^{5,9}] undecane	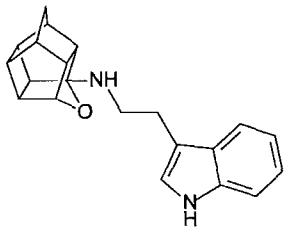
3	3-hydroxy-4-[3-(2-aminoethyl)indole]-azahexacyclo[5.4.1.0^{2,6}.0^{3,10}.0^{5,9}.0^{8,11}] dodecane	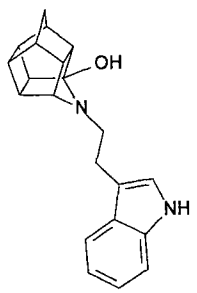
4	8-[3-(2-aminoethyl)indole]-pentacyclo[5.4.0^{2,6}.0^{3,10}.0^{5,9}]undecane	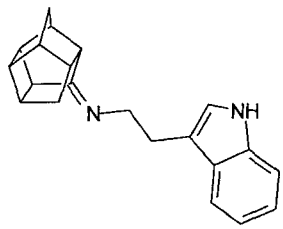

5	8-[3-(2-aminoethyl)indole]-pentacyclo[5.4.$0^{2,6}$.$0^{3,10}$.$0^{5,9}$]undecane	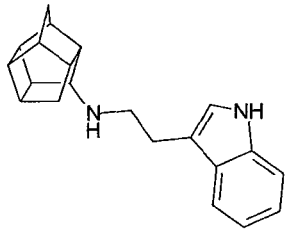
6	3-hydroxy-4,5-(1,3-oxazinane)-4-azahexacyclo[5.4.1.$0^{2,6}$.$0^{3,10}$.$0^{5,9}$.$0^{8,11}$] dodecane	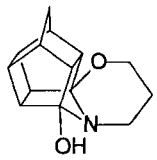
7	8-Ethoxy-8-ethylamino-pentacyclo[5.4.$0^{2,6}$.$0^{3,10}$.$0^{5,9}$]undecane-11-one	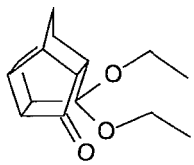

4.3. General synthetic route

The well-described Cookson's diketone, pentacyclo[5.4.0.$0^{2,6}$.$0^{3,10}$.$0^{5,9}$]undecane-8,11-dione (**A**, fig. 3.3), served as initial basis in all further synthetic preparations and were prepared in bulk according to literature (Cookson *et al.*, 1958, 1964). This reaction involved Diels-Alder adduct formation and subsequent photocyclisation to yield the polycyclic cage structure. The respective primary amine bases were then conjugated to this diketone by means of reductive amination (nucleophilic addition) to form the corresponding carbinolamine (**B**), followed by Dean-Stark dehydration. The intermediate imine (**C**) was then reduced with $NaBH_4$ and $NaBH_3CN$ in anhydrous methanol-THF to the final oxa-amine (**D**) and aza-amine (**E**) respectively.

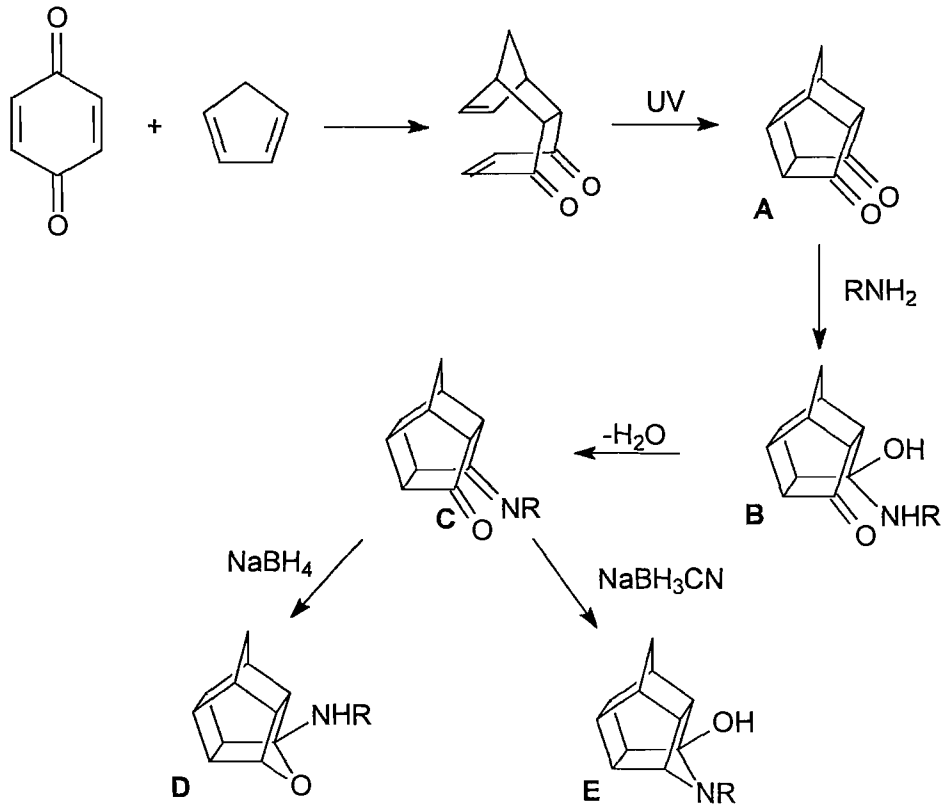

Figure 3.3: General route of synthesis for polycyclic indole derivatives.

4.3.1. Pentacyclo[5.4.0.$0^{2,6}$.$0^{3,10}$.$0^{5,9}$]undecane-8,11-dione (A)

p-Benzoquinone (10 g (0.0925 mole) purchased form Sigma-Aldrich was dissolved in dried benzene (100 ml) and protected from light by means of aluminium foil. The mixture was placed in an ice bath and allowed to cool down to 0-5°C.

Freshly monomerised cyclopentadiene (12.453 ml, 0.0925 mole) was added stoichiometrically in 1 ml aliquots to the reaction mixture while the temperature remained at approximately 0°C. This was done to prevent the formation of the diadduct. After the addition of the cyclopentadiene the reaction mixture was removed from the ice bath, protected from light and stirred for another hour while the reaction was monitored by means of thin layer chromatography (TLC). After confirmation that all the p-Benzoquinone was fully converted to the Diels-Alder adduct, the mixture was treated with activated charcoal and filtered through celite. The excess solvent was removed *in vacuo* to 10 ml and the rest was allowed to evaporate in a dark fume cupboard to afford the Diels-Alder adduct as light yellow crystals. The crystals were dissolved in ethyl acetate (4 g in 100 ml) and irradiated in a photochemical reactor with UV light for

approximately six hours. Decolouration of the solution indicated that cyclisation had occurred and the solvent was removed *in vacuo*. Evaporation of this solution afforded a light yellow residue that was purified by using Soxhlet extraction with cyclohexane to yield the diketone as fine, white powder. (Yield: 12.9 g, 80.05 %).

Spectral data were identical to the corresponding data reported previously (Cookson *et al.*, 1958).

4.3.2. Pentacyclo[5.4.0.$0^{2,6}$.$0^{3,10}$.$0^{5,9}$]undecane-8-one (J)

A mixture of pentacyclo[5.4.0.$0^{2,6}$.$0^{3,10}$.$0^{5,9}$]undecane-8,11-dione (**A**; 3 g, 17.22 mmole), ethylene glycol (1.2 g) and *p*-toluenesulfonic acid (20 mg, 0.01 mmole) in benzene (30 ml) was stirred under reflux for 5 hours (fig. 3.4). The reaction mixture was cooled and treated with activated charcoal which was subsequently removed by filtration. *In vacuo* removal of benzene yielded the monoethylene-acetal (**F**) as colourless crystals. A suspension of the acetal (**F**) was made in dry ether (10 ml) and over a period of 30 minutes gradually added to a suspension of lithium aluminium hydride (LAH; 300 mg) in dry ether (6 ml). The reaction mixture was refluxed for 2 hours and then cooled to 0°C. After reduction, excess LAH was deactivated with aqueous ammonium chloride and the organic phase concentrated *in vacuo* to afford clear homogenous oil (**G**). Hydrolysis of the acetal was done by stirring the oil in 6% hydrochloric acid (50 ml) for 2 hours at room temperature. Loss of the initial blue colour indicated complete hydrolysis upon which the reaction mixture was diluted with water (50 ml) and extracted with dichloromethane (5 x 20 ml). *In vacuo* removal of the organic solvent gave the hydroxy-ketone (**H**). A mixture of the hydroxy-ketone and hydrazine hydrate (5 ml) in diethylene glycol (60 ml) was stirred at 120°C for 1.5 hours. Potassium hydroxide (2 g) was added and the excess hydrazine and water distilled until the temperature reached 190°C, at which point the reaction mixture was refluxed for a further 3 hours. Dichloromethane extraction of the distillate yielded the pure alcohol (**I**) which was dissolved in 94% acetic acid (60 ml) and added to a mixture of chromium trioxide (4 g) in water (6 ml). The mixture was stirred at 90°C for 4 hours, cooled, diluted with water (300 ml) and extracted with dichloromethane (4 x 40 ml). After successive washes with water (3 x 100 ml), the organic phase was removed *in vacuo* to afford the desired monoketone (**J**).

Spectral data were identical to the corresponding data reported previously (Dekker & Oliver, 1978).

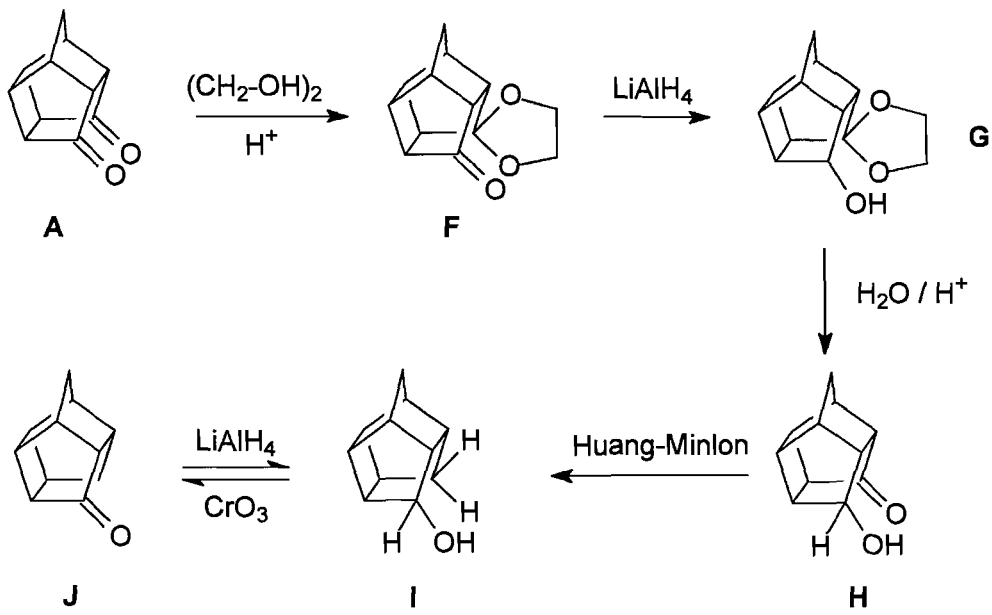

Figure 3.4: Synthesis of the monoketone (**J**) via the modified Huang-Minlon reduction of the hydroxy-ketone (**H**).

4.3.3. 8-[3-(2-aminoethyl)indole]-pentacyclo[5.4.0.0^{2,6}.0^{3,10}.0^{5,9}]undecane-11-one

Pentacyclo[5.4.0.0^{2,6}.0^{3,10}.0^{5,9}]undecane-8,11-dione (3 g, 17.22 mmole) was dissolved in tetrahydrofurane (THF; 20 ml) and cooled on an ice bath. 3-(2-aminoethyl)indole, 3.31g; 20.664 mmole) was dissolved in 40 ml tetrahydrofurane (THF) and slowly added to the reaction mixture while it was constantly stirred for 24 hours at room temperature. The THF was concentrated *in vacuo* to afford the hydroxylamine as a yellow oil. Dean-Stark dehydration in anhydrous benzene afforded the Schiff-base (8-[3-(2-aminoethyl)indole]-pentacyclo[5.4.0^{2,6}.0^{3,10}.0^{5,9}]undecane-11-one as a yellow oil. Purification by consecutive flash columns (silica gel stationary phase, 7:3 THF:EtOAc as eluent and silica gel stationary phase, 1:1:1 EtOAc:DCM:PE as eluent) afforded a pure yellow powder. (2.112 g, 38.8 %).

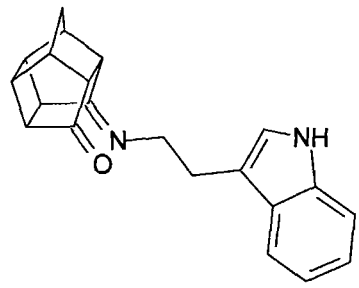

Physical Data: $C_{21}H_{20}N_2O$; **MS** m/z (Spectrum 1) = 316(M^+), 234, 221, 205, 186, 174, 145, 143, 130, 117, 103, 91, 81, 77, 66, 51, 44, 39, 28; **^{1}H NMR** (Spectrum 2, DMSO) δ = 1.35-1.80 (2 x m, 2H), 1.93-2.48 (m, 2H), 2.50-3.61 (4 x m, 9H), 6.89-7.58 (m, 4H); **^{13}C NMR** (Spectrum 3, DMSO) δ = 25.06 (CH), 26.28 (CH), 30.36 (CH), 38.15 (CH), 39.90 (CH_2), 43.39 (CH), 44.19 (CH), 54.38 (CH), 66.95 (CH_2), 136.20 (C), 212.89 (C).

4.3.4. 8-[3-(2-aminoethyl)indole]-8,11-oxapentacyclo[5.4.0.0^{2,6}.0^{3,10}.0^{5,9}]undecane

8-[3-(2-aminoethyl)indole]-pentacyclo[5.4.0^{2,6}.0^{3,10}.0^{5,9}]undecane-11-one (700 mg, 2.215 mmole) was dissolved in anhydrous methanol (5 ml) and tetrahydrofurane (THF; 21ml). To the resulting solution was added sodium borohydride (210 mg; 5.55 mmol) portionwise and it was stirred overnight at room temperature for effective reduction. The reaction mixture was concentrated *in vacuo* and water was added to the residue (100 ml). The mixture was extracted with dichloromethane (4 x 50 ml) and the combined fractions were washed with water (3 x 100 ml), dried over anhydrous magnesium sulphate, filtered and concentrated *in vacuo* to obtain a yellow powder. (496 mg, 70.3 %).

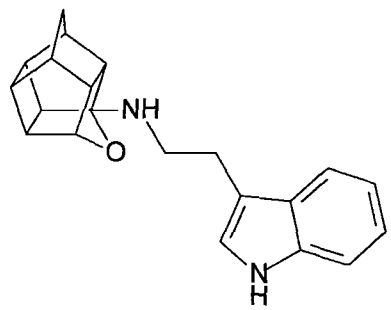

Physical Data: $C_{21}H_{22}N_2O$; **^{1}H NMR** (Spectrum 4, DMSO) δ = 0.964 (d, 1H, *J* = 10.41 Hz), 1.35 (s, 1H), 1.54 (d, 1H, *J* = 10.47 Hz), 2.07-2.23 (m, 4H), 2.49 (s, 5H), 2.81-2.86 (m, 2H), 3.32-3.39 (m, 2H), 3.61 (s, 2H), 6.28 (s, 2H), 6.95-7.54 (3 x m, 3H); **^{13}C NMR** (Spectrum 5, DMSO) δ = 30.37 (CH), 34.08 (CH_2), 38.11 (CH), 42.32 (CH), 42.35 (CH), 45.22 (CH), 70.47 (CH), 71.50 (CH), 118.12 (C).

4.3.5. 3-hydroxy-4-[3-(2-aminoethyl)indole]-azahexacyclo[5.4.1.0^{2,6}.0^{3,10}.0^{5,9}.0^{8,11}] dodecane

8-[3-(2-aminoethyl)indole]-pentacyclo[5.4.0^{2,6}.0^{3,10}.0^{5,9}]undecane-11-one (700 mg, 2.215 mmole) was dissolved in anhydrous methanol (35 ml) and acetic acid (2.1 ml). To the resulting solution was added sodium cyanoborohydride (280 mg; 4.46 mmole)

portionwise and it was stirred for 6 hours at room temperature for effective reduction. The reaction mixture was concentrated *in vacuo* and water was added to the residue (100ml). The resulting suspension was stirred, and an excess solid sodium bicarbonate was added portionwise until evolution of carbon dioxide ceased. The mixture was extracted with dichloromethane (4 x 50 ml) and the combined fractions were washed with water (3 x 100 ml), dried over anhydrous magnesium sulphate, filtered and concentrated *in vacuo* to obtain a yellow powder. (237 mg; 33.6 %).

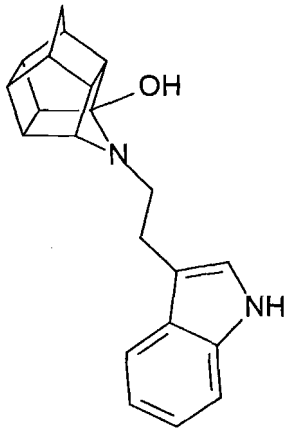

Physical Data: $C_{21}H_{22}N_2O$; **MS** m/z (Spectrum 6) = 318(M^+), 256, 236, 188, 149, 130, 117, 111, 97, 83, 81, 69, 57, 43, 28; **^{1}H NMR** (Spectrum 7, $CDCl_3$) δ = 1.67-1.85 (m, 1H), 2.07-2.88 (3 x m, 12H), 6.99-7.50 (3 x m, 3H); **^{13}C NMR** (Spectrum 8, $CDCl_3$) δ = 30.37 (CH), 36.09 (CH), 37.78 (CH_2), 38.67 (CH), 41.09 (CH), 41.24 (CH), 42.32 (CH), 43.04 (CH_2), 43.80 (CH), 44.03 (CH), 44.52 (CH), 45.15 (CH), 49.15 (CH), 53.15 (CH), 54.24 (CH), 55.56 (CH), 70.46 (CH), 79.98 (CH), 111.30 (CH), 118.16 (C), 214.79 (C).

4.3.6. 8-[3-(2-aminoethyl)indole]-pentacyclo[5.4.0^{2,6}.0^{3,10}.0^{5,9}]undecane

The monoketone (**J**, 975 mg, 6.085 mmole) was dissolved in tetrahydrofurane (THF; 30 ml) and cooled on an ice bath. 3-(2-aminoethyl)indole, 1.95 g; 12.171 mmole) was dissolved in 30 ml tetrahydrofurane (THF) and slowly added to the reaction mixture while it was constantly stirred for 24 hours at 0°C. After 24 hours the reaction mixture was removed from the ice bath and refluxed for 84 hours. The THF was concentrated *in vacuo* to afford the hydroxylamine as a yellow oil. Dean-Stark dehydration in anhydrous benzene afforded the Schiff-base (8-[3-(2-aminoethyl)indole]-pentacyclo[5.4.0^{2,6}.0^{3,10}.0^{5,9}]undecane as a yellow oil. Purification by flash chromatography (silica gel stationary phase, 5:2:2 $CHCl_3$:EtOH:EtOAc as eluent)

afforded a pure yellow oil. A pure yellow precipitate was obtained after drying in a vacuum oven. (1.625 g, 88.3 %).

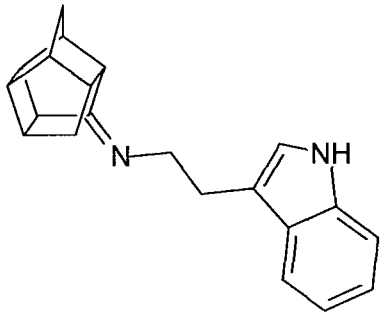

Physical Data: $C_{21}H_{22}N_2$; **IR** ν_{max} (Spectrum 9) = 3407, 2948, 2859, 1684, 1454, 1354, 1231, 1105, 734 cm^{-1}; **MS** m/z (Spectrum 10) = 302 (M^+), 172, 160, 144, 130, 117, 115, 106, 94, 79, 65, 53, 41, 28; **^{1}H NMR** (Spectrum 11, $CDCl_3$) δ = 1.21 (s, 2H), 1.35 (m, 1H), 1.71 (m, 1H), 2.16- 2.36 (m, 3H), 2.47-2.77 (m, 4H), 2.81-2.90 (m, 1H), 2.30-3.10 (m, 2H), 3.55 (t, 1H, *J* = 7.42 Hz), 3.60-3.74 (m, 1H), 6.94-7.63 (4 x m, 5H), 8.51 (bs, 1H); A mixture of two isomers were obtained and the signals of the second isomer is indicated in brackets.**^{13}C NMR** (Spectrum 12, $CDCl_3$) δ = 27.12 (27.27); (CH_2), 30.42 (30.69); (CH_2), 35.15 (no duplicate signal); (CH), 36.16 (36.59); (CH_2), 38.40 (38.47); (CH), 39.18 (39.69); (CH), 42.65 (43.20); (CH), 43.24 (43.45); (CH), 44.00 (no duplicate signal); (CH), 45.02 (no duplicate signal); (CH), 46.02 (no duplicate signal); (CH), 47.03 (no duplicate signal); (CH), 47.42 (47.51); (CH), 51.52 (no duplicate signal); (CH), 53.20 (53.29); (CH_2), 111.03 (111.06); (CH), 114.16 (114.24); (CH), 118.81 (118.97); (CH), 121.91 (121.96); (CH), 127.51 (127.53); (C), 136.40 (136.43); (C), 181.54 (181.78); (C); **HRMS** calcd. 302.1783, found 302.1776.

4.3.7. 8-[3-(2-aminoethyl)indole]-pentacyclo[5.4.0^{2,6}.0^{3,10}.0^{5,9}]undecane

8-[3-(2-aminoethyl)indole]-pentacyclo[5.4.0^{2,6}.0^{3,10}.0^{5,9}]undecane (777 mg, 2.57 mmole) was dissolved in anhydrous methanol (5 ml) and tetrahydrofurane (THF; 21ml). To the resulting solution was added sodium borohydride (110 mg; 2.9 mmol) portionwise and it was stirred overnight at room temperature for effective reduction. The reaction mixture was concentrated *in vacuo* and water was added to the residue (100 ml). The mixture was extracted with dichloromethane (4 x 50 ml) and the combined fractions were washed with water (2 x 100 ml), dried over anhydrous magnesium sulphate, filtered and concentrated *in vacuo* to obtain a yellow oil. Purification by consecutive flash columns

(silica gel stationary phase, 5:2:2 $CHCl_3$:EtOAc:EtOH as eluent and silica gel stationary phase, 7:3 EtOH:EtOAc as eluent) afforded a pure white powder. (592 mg, 75.6 %).

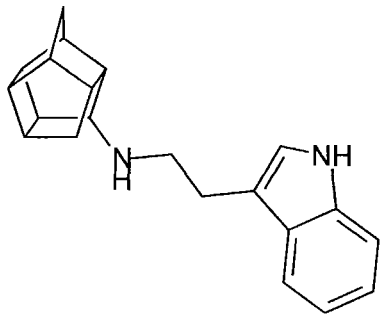

Physical Data: $C_{21}H_{24}N_2$; **IR** ν_{max} (Spectrum 13) = 3407, 2955, 2863, 1613,1446, 1346, 1227, 1109, 737 cm^{-1}; **MS** m/z (Spectrum 14) = 304(M^+), 174, 145, 131, 117, 115, 79, 67; **^{1}H NMR** (Spectrum 15, $CDCl_3$): δ 0.94 (m, 1H), 1.15 (d, 1H, *J* = 10.24 Hz), 1.42 (bs, 1H), 1.66 (d, 1H, *J* = 9.84 Hz), 2.13 (d, 1H, *J* = 11.95), 2.22 (m, 4H), 2.53 (m, 4H), 2.76 (t, 1H, *J* = 3.4 Hz), 2.96 (m, 4H), 7.11 (d, 1H, *J* = 1.13 Hz), 7.10 (m, 1H), 7.13 (m, 1H), 7.33 (d, 1H, *J* = 7.83 Hz), 7.63 (d, 1H, *J* = 7.77 Hz), 8.22 (bs, 1H); **^{13}C NMR** (Spectrum 16, $CDCl_3$): δ = 26.22 (CH_2), 28.69 (CH_2), 34.67 (CH_2), 36.20 (CH), 37.70 (CH), 40.73 (CH), 41.77 (CH), 41.92 (CH), 44.10 (CH), 44.62 (CH), 47.23 (CH), 49.24 (CH_2), 61.67 (CH), 111.04 (CH), 114.31 (C), 118.92 (CH), 119.11 (CH), 121.77 (CH), 121.86 (CH), 127.53 (C), 136.40 (C); **HRMS** calcd. 304.1939, found 304.1948.

4.3.8. Additional cage structures

As indoles with an aliphatic amine group could not be obtain from chemical suppliers, we planned to conjugate the known cage structure with aminopropanol, as linker, and then with selected indole carboxylic acids to obtain polycyclic indole esters. This however did not realise as expected, but novel rearranged cage structures were obtained.

4.3.8.1. 3-hydroxy-4,5-(1,3-oxazinane)azahexacyclo[5.4.1.$0^{2,6}$.$0^{3,10}$.$0^{5,9}$.$0^{8,11}$] dodecane

Pentacyclo[5.4.0.$0^{2,6}$.$0^{3,10}$.$0^{5,9}$]undecane-8,11-dione (3 g, 17.22 mmole) was dissolved in tetrahydrofurane (THF; 30 ml) and cooled on an ice bath. 3-Aminopropanol (1.31 ml; 17.22 mmole) was dissolved in 6 ml tetrahydrofurane (THF) and slowly added to the reaction mixture while it was constantly stirred for 2 hours at 0°C. After 2 hours the carbinolamine precipitated. The THF was removed *in vacuo* and the product was dehydrated by Dean-Stark in anhydrous benzene. The benzene was concentrated *in*

vacuo to 10 ml and the unexpected 3-hydroxy-4,5-(1,3-oxazinane) azahexacyclo[5.4.1.$0^{2,6}$.$0^{3,10}$.$0^{5,9}$.$0^{8,11}$] dodecane crystallised from it (2.49 g, 62.5 %).

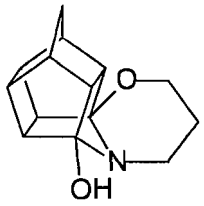

Physical Data: $C_{14}H_{17}NO_2$; **mp.** 168-172 °C; **IR** ν_{max} (Spectrum 17) = 3437, 3088, 2962, 2844, 1628, 1483, 1424, 1316, 1161, 1120, 1064, 949, 864, 663, 585; **MS** m/z (Spectrum 18) = 231(M^+), 214, 202, 187, 174, 151, 136, 117, 99, 91, 69, 55, 41, 28; **^{1}H NMR** (Spectrum 19, $CDCl_3$) δ = 1.51 (d, 1H, *J* = 10.57), 1.55-1.75 (m, 2H), 1.79 (d, 1H, *J* = 10.54), 2.52-3.01 (3 x m, 9H), 3.67-3.85 (2 x m, 2H), 4.71 (bs, 1H); **^{13}C NMR** (Spectrum 20, $CDCl_3$) δ = 24.25 (CH_2), 41.09 (CH_2), 41.55 (CH), 41.63 (CH), 42.42 (CH_2), 42.98 (CH), 44.04 (CH), 44.59 (CH), 45.81 (CH), 53.08 (CH), 55.04 (CH), 62.69 (CH_2), 101.63 (C); **HRMS** calcd. 231.1259, found 231.1250.

4.3.8.2. Proposed mechanism for rearrangement

The proposed rearrangement is similar one described for the acid-catalysed acetal formation by reaction of a ketone with an alcohol described in McMurray (1999). Hydronium ions are formed during the reaction and activate the imine nitrogen and thus the imine carbon through electron delocalisation. Once the carbonyl carbon is activated, the hydroxyl group of the 3-aminopropanol is folded back towards the cage structure to launch a nucleophilic attack. After ring closure, the free electron pair on the nitrogen is in close proximity of the adjacent carbonyl carbon and thus available for a further nucleophilic attack to afford the aza compound fig. 3.5.

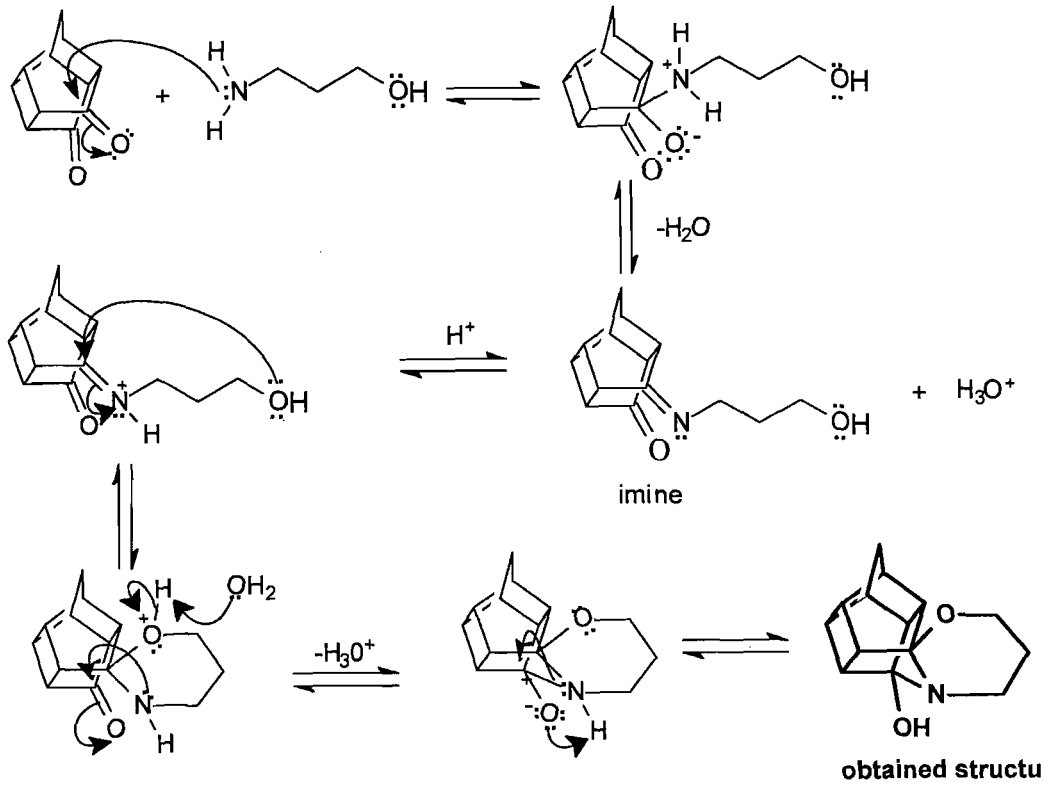

Figure 3.5: Proposed rearrangement mechanism to form 3-hydroxy-4,5-(1,3-oxazinane)-4-azahexacyclo[5.4.1.$0^{2,6}$.$0^{3,10}$.$0^{5,9}$.$0^{8,11}$]dodecane.

4.3.8.3. X-ray crystallography

The aim of x-ray crystallography is to obtain a three dimensional molecular structure from a crystal. A purified sample at high concentrations is crystallised and the crystals are exposed to an x-ray beam. The resulting diffraction patterns can then be processed, initially to yield information about the crystal packing symmetry and the size of the repeating unit that forms the crystal. This is obtained from the pattern of the diffraction paterns. The intensities of the paterns can be used to determine the structure parameters from which a map of the electron density can be calculated. Various methods can be used to improve the quality of this map until it is of sufficient clarity to permit the building of the molecular structure. The resulting structure is then refined to fit the map more accurately and to adopt a thermodynamically favoured conformation. (Smyth & Martin, 2000).

3-Hydroxy-4,5-(1,3-oxazinane)-4-azahexacyclo[5.4.1.$0^{2,6}$.$0^{3,10}$.$0^{5,9}$.$0^{8,11}$]-dodecane was crystallised from benzene at 4°C in a dark walk-in fridge. A single crystal of size 0.07 x 0.11 x 0.14 mm was used and cooled in a stream of nitrogen vapor to 113 K. Space

group Pbca, a = 12.3763 (7), b = 11.6597 (6), c = 15.0539 (8) Å, α = 90°, β = 90°, γ = 90° with Z = 8 formula units of $C_{14}H_{17}NO_2$; D_c = 1.414 g/cm^3 was used. Intensity data were collected on an Enraf Nonius Kappa CCD diffractometer with graphite-monochromated Mo K_α radiation (λ = 0.71073 Å), μ = 0.094 mm^{-1}). Refinement on F^2 converged to a weighted R value (wR_2) of 0.1689 for all reflections. The conventional R factor was 0.054 for 2048 reflections with I > 2.0σ (I). A summary of the crystal data, data-collection and refinement parameters is included in (table 3.2)

An interesting aspect of the molecular structure is that the six-membered ring adopts a chair conformation. The packing is determined by two intramolecular hydrogen bonds between O12 and N17 of two enantiomers packed against each other (fig 4.6).

Table 3.2: Summary of x-ray diffraction data.

Empirical formula	$C_{14}H_{17}NO_2$
Formula weight	231.29
Crystal system	Orthorhombic
Space group	*Pbca*
a (Å)	12.3763 (7) A alpha = 90 deg
b (Å)	11.6597 (6) A beta = 90 deg
c (Å)	15.0539 (8) A gamma = 90 deg
V (Å^3)	2172.3 (2)
Z	8
μ (mm^{-1})	0.094 (MoK_α)
F (000)	992
Reflections with I > 2.0σ (I)	1225
Calculated density (g/cm^3)	1.414
Crystal dimensions (mm)	0.07 x 0.11 x 0.14
Temperature (K)	113
Theta Min-Max (Deg)	3.2, 25.7
R_1	0.0573
wR_2	0.1689
S	1.02

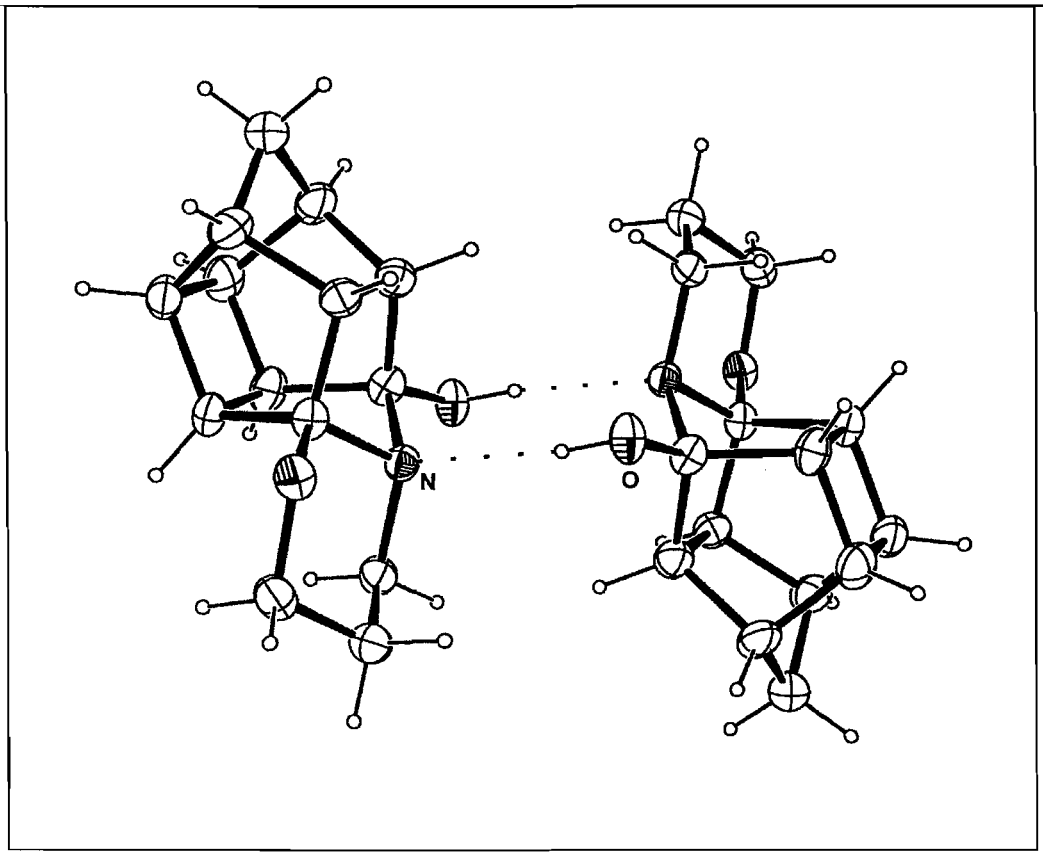

Figure 3.6: Structure of $C_{14}H_{17}NO_2$ as determined by x-ray crystallography, showing intermolecular hydrogen bonds between the two enantiomers.

4.3.9. 8-Ethoxy-8-ethylamino-pentacyclo[5.4.$0^{2,6}$.$0^{3,10}$.$0^{5,9}$]undecane-11-one

Pentacyclo[5.4.0.$0^{2,6}$.$0^{3,10}$.$0^{5,9}$]undecane-8,11-dione (5 g, 28.70 mmole) was dissolved in ethanol (EtOH; 50 ml) and cooled on an ice bath. 2-Bromoethylamine hydrobromide (5.88 g; 28.70 mmole) was dissolved in 50 ml ethanol (EtOH) and slowly added to the reaction mixture while it was constantly stirred at 0°C. After 4 hours the reaction mixture was removed from the ice bath and refluxed for another 24 hours. The EtOH was removed *in vacuo*, followed by Dean-Stark dehydration in anhydrous benzene. After removal of benzene *in vacuo*, the compound was purified by recrystalisation in EtOH:ETOAc:PE (7:3:1) to afford the unexpected 8-Ethoxy-8-ethylamino-pentacyclo [5.4.$0^{2,6}$.$0^{3,10}$.$0^{5,9}$]undecane -11-one. (1.504 g, 21.13 %)

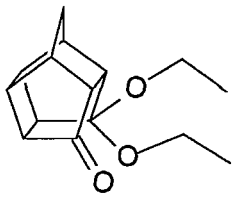

Physical Data: $C_{15}H_{20}O_3$; **mp.** 104 °C; **IR** ν_{max} (Spectrum 21) = 3444, 2962, 2881, 1729, 1472, 1443, 1394, 1324, 1227, 1164, 1060, 960, 938, 745, 537cm^{-1}; **MS** m/z (Spectrum 22) = 248(M^+), 219, 203, 175, 145, 122, 117, 109, 91, 81, 66, 55, 41, 29; **^{1}H NMR** (Spectrum 23, $CDCl_3$) δ = 1.08 (t, 3H, *J* = 7.07), 1.12 (t, 3H, *J* = 7.08 Hz), 1.49 (d, 1H, *J* = 10.99), 1.79 (d, 1H, *J* = 10.88), 2.30-2.92 (5 x m, 8H), 3.29-3.48 (2 x m, 4H) **^{13}C NMR** (Spectrum 24, $CDCl_3$) δ = 14.65 (CH_3), 15.59 (CH_3), 36.21, 38.20 (CH_2), 40.90, 41.83, 42.21, 42.77, 45.68, 49.81, 52.16, 56.52 (CH_2), 59.29 (CH_2), 107.04 (C), 214.25 (C); **HRMS** calcd. 248.1412, found 248.1388.

4.4. Conclusion and Discussion:

The synthesis of all compounds resulted in yields ranging between 21.13 % and 88.3 % and the lower yields could be attributed to the formation of various unidentified impurities. Various linkers were applied to obtain amides, esters or ethers, but rearrangement reactions to form novel polycyclic structures however predominated.

Varying success has thus been achieved with the synthesis of these compounds and its purification. Solubility and multiple reactions taking place made it difficult to obtain the compounds in pure form for characterisation and optimisation of these reactions for further use are thus essential.

The aim of this study was to design and synthesise a series of polycyclic indole derivatives and to evaluate these compounds for neuroprotective activity. A decrease in the production of free radicals, due to the inhibition of NOS, was indicative of neuroprotective activity.

It is hypothesised that the test compounds with an indole moiety may have the ability to be NOS inhibitors as well as free radical scavengers. Two assay procedures were carried out to evaluate these compounds for their possible neuroprotective potential. The first assay procedure to be employed was the oxyhemoglobin assay for the detection of NOS inhibition and the second was the NBT assay for lipid peroxidation.

5. Nitric oxide synthase determination

5.1. Introduction

Nitric oxide synthase (NOS) enzymes catalyses the NADPH- and O_2-dependent conversion of L-Arginine (L-Arg) to L-citrulline and nitric oxide (NO). The most frequently applied assay for the detection of nitric oxide (NO) under aerobic conditions is the oxyHb assay. This method is based on the reaction of NO with oxyHb which leads to the formation of metHb and nitrate (equation 5.1), a reaction that also largely accounts for the inhibitory effect of hemoglobin on the biological effects of NO (Feelisch *et al.*, 1996). The conversion of oxyHb to metHb is an indication of NOS activity by monitoring the absorbance difference between these two hemoglobin species.

The applicability of this method is primarily based on its sensitivity and specificity for NO under aerobic conditions, inexpensiveness, ease of implementation and for the rather modest technical requirements (Feelisch *et al.*, 1996).

$$\text{oxyHb} + \text{NO} \longrightarrow \text{metHb} + NO_3^- \qquad 5.1$$

In a aqueous solution under aerobic conditions, NO is highly unstable and susceptible to rapid reactions with oxygen (O_2), superoxide anions (O_2^-), thiols (RSH) and a variety of metal containing proteins (Feelisch *et al.*,1996). As is true for any method of NO quantification, the reaction of NO with the detection molecule should be more rapid than

that of the other competing species. In the oxyHb assay, this requirement is met by the high reaction rate between NO and oxyHb, which has been estimated to be 26 times faster than the auto oxidation of NO in aqueous solution (Hoshino *et al.*, 1993). The quenching or scavenging effect of superoxides may be limited by the addition of superoxide dismutase (SOD), both to increase the trapping efficiency of oxyHb for NO and to prevent the potential oxidation of oxyHb to metHb (Sutton *et al.*, 1976). Thiols will also not interfere with NO measurement since the reaction rate of NO/oxyHb is much faster than that of the reaction rate of NO/O_2 (Wink *et al.*, 1994). The rapid reaction between NO and oxyHb has the advantage of almost stoichiometrically trapping NO under most experimental conditions. Therefore, the oxyHb assay is somewhat unique among methods for NO determination in that it is less subjected to constraints imposed by competing reactions with oxygen, superoxide or thiols.

The absolute UV spectra of oxyHb is characterised by an intense absorption Soret- or γ-band with a maximum at 415 nm and two weaker β- and α-bands with absorption maxima at 542 nm and 577 nm (Feelisch *et al.*, 1996). Methemoglobin's γ-band has an absorption maximum at 405 nm and the α- and β-bands are only detectable under alkaline conditions at 575 and 540 nm, respectively. At certain wavelengths the absorption of metHb is thus more intense than that of oxyHb and vice versa. The differences between metHb's and oxyHb's spectral characteristics become evident when the spectra are superimposed (fig. 5.1).

The absorbance intensities of both species are only equal at a few discrete wavelengths equal. Such spectral points of identical absorbance intensity are the so-called *isosbestic* points and they do not change during the conversion of oxyHb to metHb. The absorbance difference at a given *isosbestic* point will stay zero throughout the entire reaction.

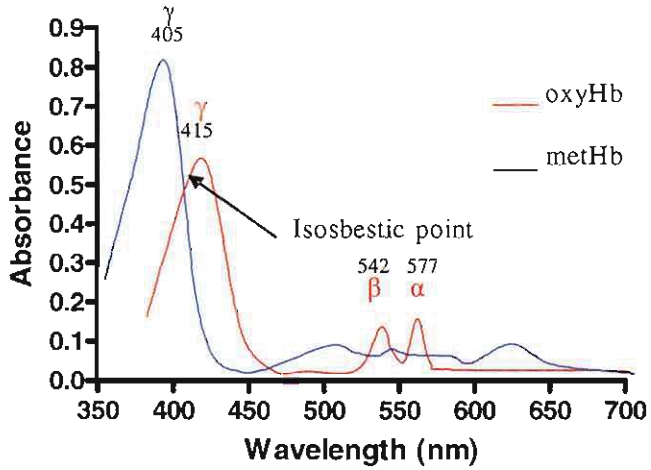

Figure 5.1: Superimposed absolute absorption spectra of oxyhemoglobin (oxyHb) and methemoglobin (metHb). Intersection points represent the *isosbestic* wavelengths at which the absolute absorbances of both species are identical (Feelisch *et al.*, 1996).

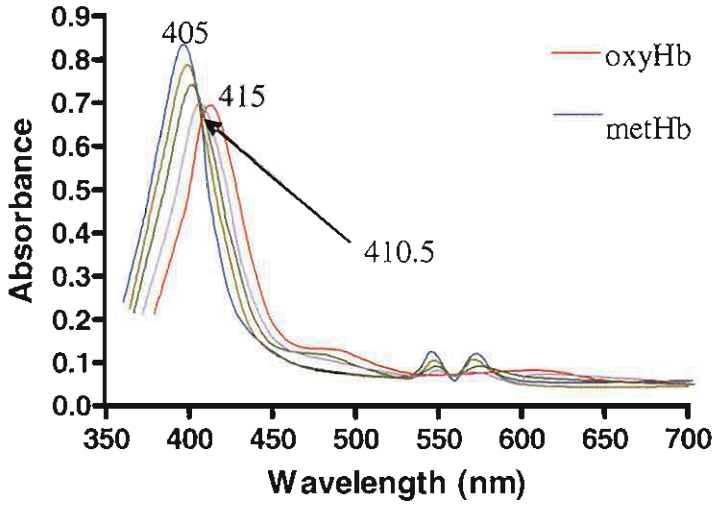

Figure 5.2: An example of the changes in the absolute spectrum of an oxyHb containing solution upon NO-mediated conversion to metHb. Although the total concentration of hemoglobin remains constant, the spectroscopic features change as oxyHb is converted to metHb (Feelisch *et al.*, 1996).

During this procedure, an absolute spectrum (fig. 5.1) is recorded with the sample and reference cuvettes containing oxyHb and vehicle, respectively. After the reaction is started, NO reacts with oxyHb to form metHb. The new spectra recorded over time will present the absolute spectra of varying mixtures of oxyHb and metHb (fig. 5.2).

The disadvantage of this procedure however, is that the actual concentrations of the individual hemoglobin derivatives can only be read from the absolute absorbance when complete conversion of oxyHb to metHb has occurred (Feelisch *et al.*, 1996). In order to obtain information about the extent of conversion and thus the amount of NO generated, the vehicle is no longer used as a reference, but only the oxyHb containing solution is employed. Instead of using the contents of a second cuvette, the absorbance of the same cuvette at a second wavelength is chosen as a reference. If the light absorption properties of the sample at a specific wavelength are recorded against the reference wavelength (difference spectra) in a repetitive manner, the changes in absorbance will reflect the loss of oxyHb and the simultaneous formation of metHb (fig. 5.3). In addition to the *isosbestic* points, there are certain regions corresponding to the formation of metHb where the absorbance increases (between 370 nm and 410.5 nm with a maximum at 401 nm) and regions corresponding to the loss of oxyHb where absorbance decreases (e.g. between 410.5 nm and 472 nm with a minimum at 421 nm). From the difference spectra, the wavelength at which maximum change in absorbance occurs and a nearby *isosbestic* wavelength is usually subtracted from each other to determine metHb formation.

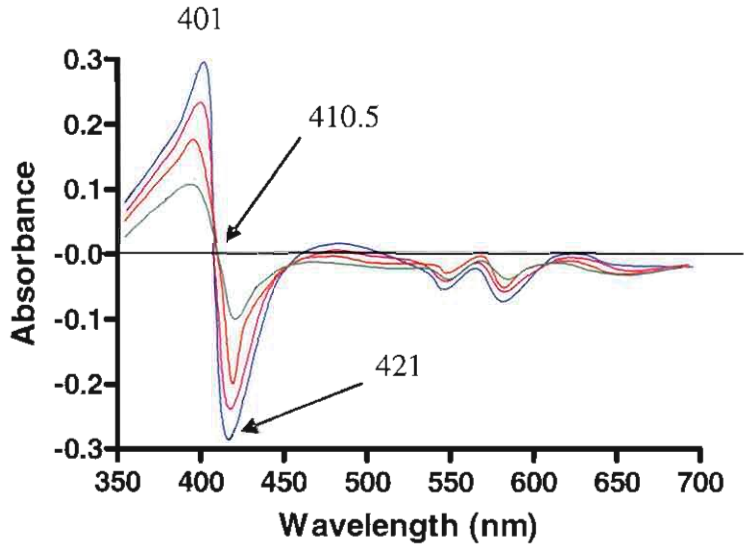

Figure 5.3: Repetitive scans of difference spectra. Spectra were recorded during conversion by NO of oxyHb to metHb illustrating maximum absorbance differences and *isosbestic* points (Feelisch *et al.*, 1996).

The more NO is generated the larger the absorbance difference (ΔA) will be. This linear relationship between the absorbance difference (ΔA) and the amount of metHb formed is used to calculate the change in metHb concentration. In order to calculate the time dependent increase of metHb concentration, the absorbance difference between a wavelength of maximal absorbance change (e.g. 401 nm) and an internal reference wavelength (e.g. 410.5 nm or 421 nm) are measured as a function of time. The slope of the resulting curve is a measure of the increase in metHb concentration and thus NO formation or enzyme activity (fig. 5.4).

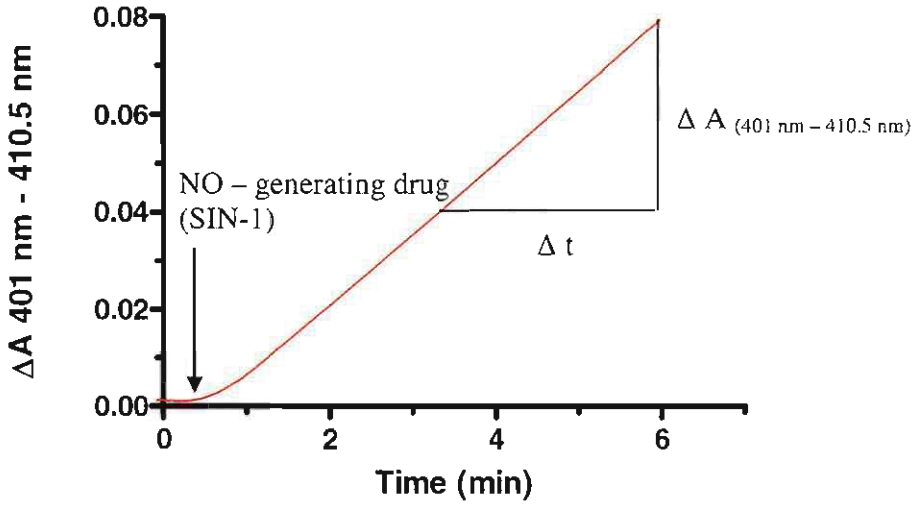

Figure 5.4: A typical recording of NO formation. Morpholinosydnonimine (SIN-1) was employed as a NO-generating drug and continuous time-dependent recording of the absorbance difference between 401 nm – 410.5 nm were preformed (Feelisch *et al.*, 1996).

5.2. Experimental procedures

The study protocol was approved by the Ethics Committee for Research on Experimental Animals of the North-West University (Potchefstroom campus). Male Sprague-Dawley rats were sacrificed by decapitation and the brain tissue was removed and preserved for homogenation. After homogenation, the aliquoted brain homogenate was stored at -70˚C. An adapted method described by Salter & Knowles (1998) was employed for the determination of NOS activity by measuring the conversion of oxyHb to metHb. All materials were purchased from Sigma-Aldrich (UK) and Merck (St. Louis, MO, USA). Continuous scans of spectra were recorded using a Varian Cary-50 UV-Visible spectrophotometer. The slope values were calculated at specific wavelengths, utilising the software package, Cary Win-UV (version 3.00) and the IC_{50} values were calculated from these inhibition data. All data analysis, calculation and graphs were done using Prism 4.02 (GraphPad, Sorrento Valley, CA).

5.2.1. Materials

The hemoglobin (0.144 mM) that mainly consists of metHb was firstly converted to its oxygenated form (Feelish *et al.*, 1996). This was achieved by gently dissolving the crystallised hemoglobin (20 mg) in distilled water (1.5 ml) and subsequent reduction with

sodium dithionate (2-3 fold molar excess). The solution immediately changed from brownish red (mixture of oxyHb and metHb) to a dark red (deoxyhemoglobin) colour after the reductant was added. Oxygenation was carried out by blowing 100% oxygen over the surface while the solution was gently swirled. The gradual colour change from dark red to bright red was indicative of the oxygenation of hemoglobin. Purification and desalting was performed by passing the resulting oxyHb solution through a Sephadex G-25 column. The oxyhemoglobin is eluted as a single bright-red band. The front and back edges of the band were discarded.

The concentration of the oxyHb was calculated by the method described by Feelish *et al.*, 1996). 10 µl of the oxyHb stock solution was added to 2990 µl of HEPES buffer in a cuvette and the absolute absorbance at 415 nm was determined against a buffer blank. The concentration of oxyHb (c_{oxyHb}) was calculated according to eq. 5.2 from the mean absorbance ($A_{m415\ nm}$) of three seperate determinations using a molar extinction coefficient $E_{415(oxyHb)}$ of 131.0 $mM^{-1}\ cm^{-1}$ (Van Assendelft, 1970).

$$c_{oxyHb} = \frac{A_{m415nm} \times 300\ (\text{dilution factor})}{E_{415(oxyHb)}} \qquad 5.2$$

Using the above equation, the final calculated oxyHb concentration of the stock solution was found to be 0.8 mM. The stock solution was then aliquoted in 200 µl units and stored at -70˚C.

Potassium phosphate buffer (100 mM) was prepared at room temperature by mixing both the monobasic (KH_2PO_4, 300 ml; 100 mM) and the dibasic (K_2HPO_4, 1347 ml; 100 mM) solutions and adjusting the pH to 7.4 by adding either KH_2PO_4 or K_2HPO_4.

Calcium chloride solution ($CaCl_2$; 12.5 mM) was prepared in the potassium phosphate buffer and L-arginine (1 mM) and NADPH (5 mM) in water (Salter & Knowles, 1998).

The test compounds were dissolved in potassium phosphate buffer or methanol (MeOH; final incubation concentration 5 %) to give a series of final incubation concentrations ranging from 10 µM to 10 mM. 7-Nitroindazole was dissolved in MeOH and used as the positive control in final concentrations ranging from 10 µM to 10 mM.

The extraction buffer was prepared by dissolving sucrose (320 mM), HEPES (20 mM) and ethylenediaminetetra-acetic acid (EDTA; 1 mM) in distilled water and adjusting the pH to 7.2 at room temperature by adding 10 % $HCl_{(aq)}$ (Salter & Knowles, 1998). The

following constituents were then added to the final concentrations indicated: D/L-dithiothretiol (DTT; 1 mM), leupeptin (10 µg/ml), soybean-trypsin inhibitor (10 µg/ml) and aprotinin (2 µg/ml). The extraction buffer was then made up to its final volume with distilled water and 50 ml aliquots were stored at -20°C until required.

Phenylmethylsulphonyl fluoride (PMSF; 10 mg/ml) was prepared as a separate solution in absolute ethanol and stored at -20°C. Because PMSF is unstable in aqueous solution, it is not included in the buffer at this stage, but only added to the extraction buffer during the extraction procedure.

5.2.2. Methods

5.2.2.1. Sample preparation

Extraction and storage of tissue samples prior to the assay were carried out at 0°C - 4°C to avoid loss of enzyme activity. Fresh rat brain was weighed in 50 ml pre-cooled Falcon tubes and placed on ice. After rinsing with ice cold extraction buffer, a measured volume of extraction buffer (5 ml/g tissue) was added to the tissue. The sample was then homogenised with a mechanical homogeniser while the temperature was maintained at 4°C. After 10 seconds of homogenisation the PMSF (10 µM/ml of extraction buffer) was added to the mixture and homogenised for a further 30 seconds. The homogenate was then centrifuged at 12000 x g for 10 minutes to minimise turbidity. Once the supernatant was collected, it was divided into 2 ml aliquots which were assayed immediately or rapidly frozen and stored at -70°C.

5.2.2.2. Assay procedure

Oxyhemoglobin, $CaCl_2$ and L-arginine were diluted in the potassium phosphate buffer to give final concentrations of 1.44 µM, 250 µM and 1 mM respectively and to make up at least 80% of the final reaction mixture volume. The reaction mixture was prewarmed for three minutes to the required assay temperature of 37°C. After adding NADPH to a final concentration of 100 µM along with the test compound or control, the reaction was started by the addition of tissue extract (100 µl).

After establishing the baseline, continuous scans with a scan rate of 600 nm/min every 12 seconds were recorded between 390 nm and 430 nm. The conversion of oxyHb to metHb was monitored over a period of 5 minutes (fig. 5.5).

5.2.3. Results and Discussion

From the continuous spectrophotometric scans, the slope value of the difference spectra between 401 nm and 421 nm were calculated and used as an index to determine NOS activity. Two of the recorded spectra of compound **4** are depicted in fig. 5.5 and fig. 5.6 and represents the control and 1 mM incubations respectively. Comparison of the two spectra revealed a marked change in absorbance at 401 nm, while the absorbance at 421 remained constant. The change in absorbance at 401 nm was used as an indication of the NOS inhibitory effect of compound **4**.

A decrease in absorbance at 401 nm is indicative of a decrease in metHb formation and thus a decrease in enzyme activity. Enzyme activity is expressed as the rate at which NO (or metHb) is generated. The resulting slope value of the change in absorbance between two specific wavelengths (e.g. 401 nm and 421 nm) over time is representative of this conversion rate (fig. 5.4). Although there was no change in absorbance at 421 nm, the slope value was still deducted from the slope value at 401 nm to take other variables into consideration such as pH, temperature and concentration.

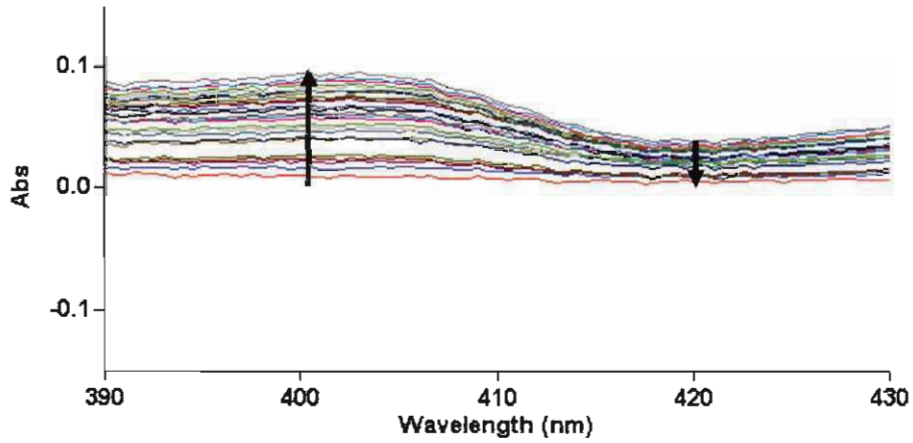

Figure 5.5: Spectrophotometric recordings of the control incubation (0 mM inhibitor). Recordings were monitored over a period of 5 minutes between 390 nm and 430 nm. Arrow at 401 nm and 421 nm indicate the change in absorbance (ΔA) over time.

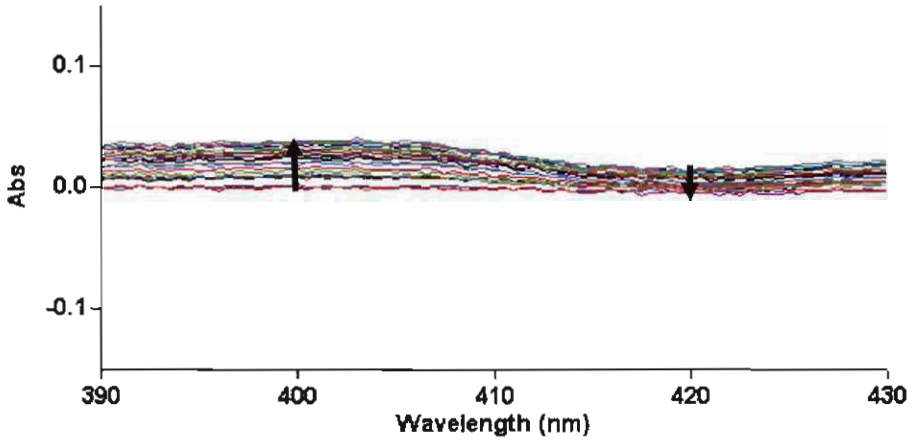

Figure 5.6: Spectrophotometric recordings of NOS activity at a 1 mM concentration of compound **4**. When compared to the spectra at 0 mM inhibitor (fig. 5.5), a marked change in absorbance can be seen. Arrow at 401 nm and 421 nm indicate the change in absorbance (ΔA) over time.

From the spectra depicted in fig. 5.5 and 5.6, the difference in the change of absorbance (ΔA) between 401 nm and 421 nm versus time was calculated by plotting the ΔA of the respective wavelengths against time (fig. 5.7 and 5.8). The resulting curves' slope values ($m_{\Delta A(401\ nm)}$ - $m_{\Delta A(421\ nm)}$) are indicative of the extent of oxyHb's conversion to metHb and is directly proportional to the amount of NO generated and enzyme activity.

A decrease in enzyme activity is observed when the slope value of the control was compared to that of the 1 mM inhibitor concentration (table 5.1). The slope values of the curves are linear over the first four minutes and can also be used as an indication of NO formation (fig. 5.7 and 5.8).

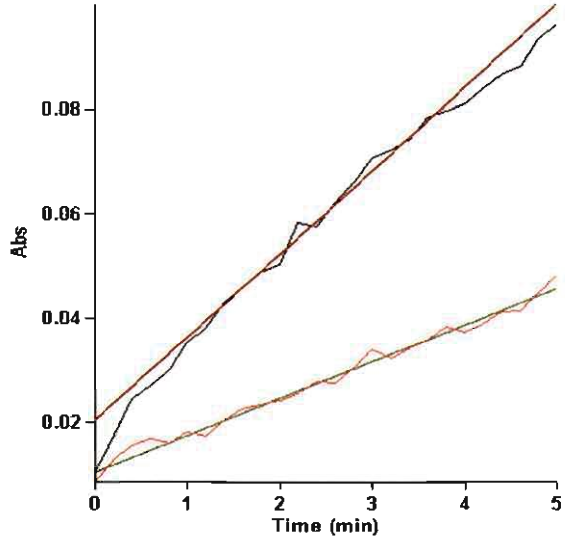

Figure 5.7: Determination of the change in absorbance of the control incubation. (0 mM inhibitor; fig. 5.5). The change in absorbance at 401 nm and 421 nm versus time was calculated and the difference of the respective slope values ($m_{\Delta A(401\ nm)}$ - $m_{\Delta A(421\ nm)}$) gives an indication of enzyme activity.

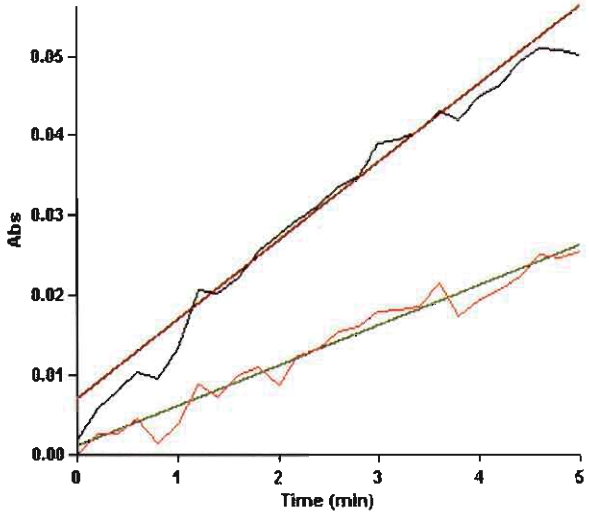

Figure 5.8: Determination of the change in absorbance with compound **4**. (1 mM inhibitor; fig. 5.6). The difference in slope values ($m_{\Delta A(401\ nm)}$ - $m_{\Delta A(421\ nm)}$) is respresentative of enzyme activity and in comparison with the control (fig. 5.7), indicates a decrease in enzyme activity with the addition of the novel inhibitor.

Table 5.1: Comparison of the resulting slope values of the control and 1 mM inhibitor incubation during the initial linear phase indicating a decrease in enzyme activity.

Incubation	Slope (m) values (Abs/min)			% NOS activity
	$m_{401\ nm}$	$m_{421\ nm}$	$m_{(401\ nm - 421\ nm)}$	
Control 1*	0.0110	0.0026	0.0084	~98.82
Control 2*	0.0157	0.0057	0.0100	~99.01
Control 3*	0.0159	0.0082	0.0077	~98.718
1 mM inhibitor 1*	0.0091	0.0053	0.0038	~44.47
1 mM inhibitor 2*	0.0099	0.0050	0.0049	~48.51
1 mM inhibitor 3*	0.0043	0.0010	0.0033	~42.31

* All incubations were done in triplicate and the data of control 1 and the incubation containing 1 mM inhibitor are depicted in fig. 5.7 and fig. 5.8.

During the initial linear phase (first four minutes), the enzyme activity of all test compound incubations were calculated as a percentage value of the control (incubations containing 0 mM inhibitor represents ~100 % activity). The corresponding dose response curves were obtained by plotting the inhibition data of enzyme activity against a series of logarithmic concentrations of the test compounds. The dose response curves of each experiment were calculated by dividing the resulting slope value through the slope value of the control and each experiment was conducted in triplicate. Data points are expressed as mean values with standard error of the mean.

The inhibition curves of selected compounds were superimposed on a single graph (fig. 5.12) and the calculated IC_{50} value were compared (table 5.2). From the calculated IC_{50} value; compounds **1, 3, 4, 5** revealed promising results as possible NOS inhibitors.

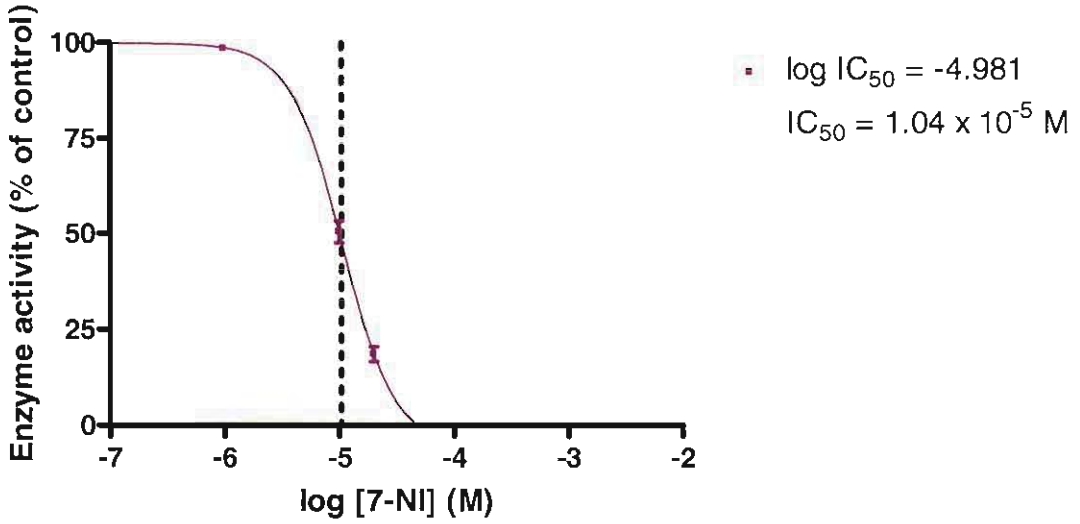

Figure 5.16: Inhibition curve of **7-NI** on NOS activity. L-arginine (100 mM) was used as substrate. Log (IC_{50}): -4.981; IC_{50}: 1.04 x 10^{-5} M as indicated by the dotted line.

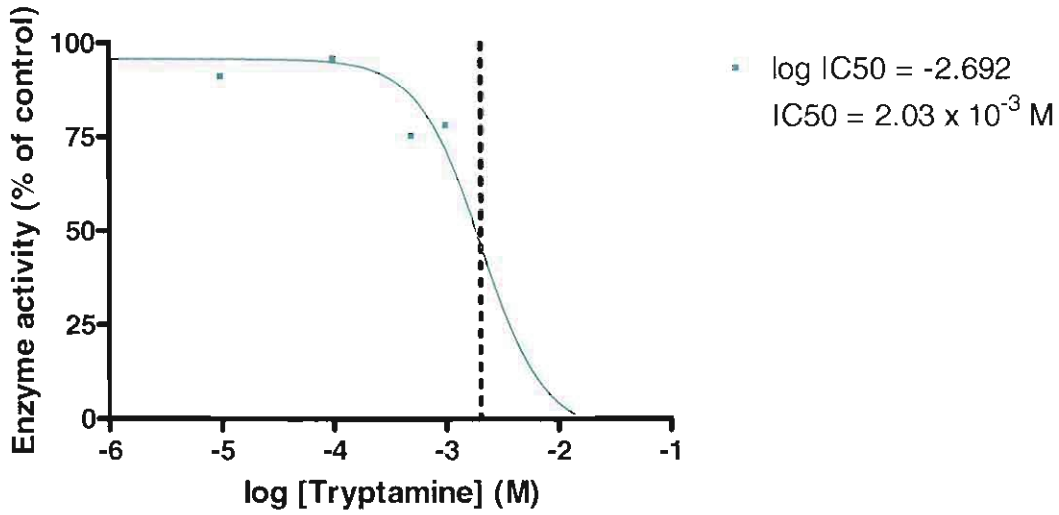

Figure 5.16: Inhibition curve of **3-(2-aminoethyl)indole** on NOS activity. L-arginine (100 mM) was used as substrate. Log (IC_{50}): -2.692; IC_{50}: 2.03 x 10^{-3} M as indicated by the dotted line.

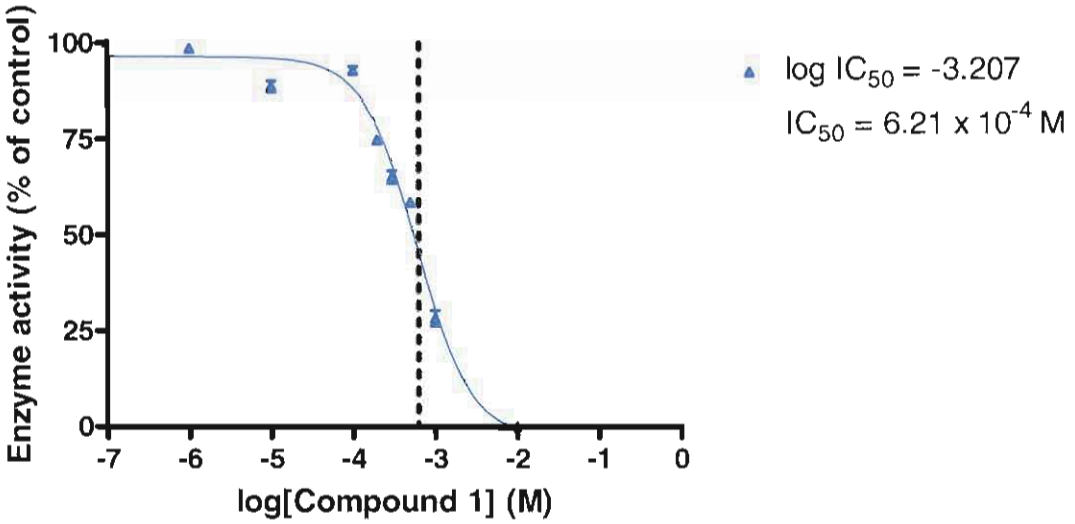

Figure 5.12: Inhibition curve of compound **1** on NOS activity. L-arginine (100 mM) was used as substrate. Log (IC_{50}): -3.207; IC_{50}: 6.21 x 10^{-4} M as indicated by the dotted line.

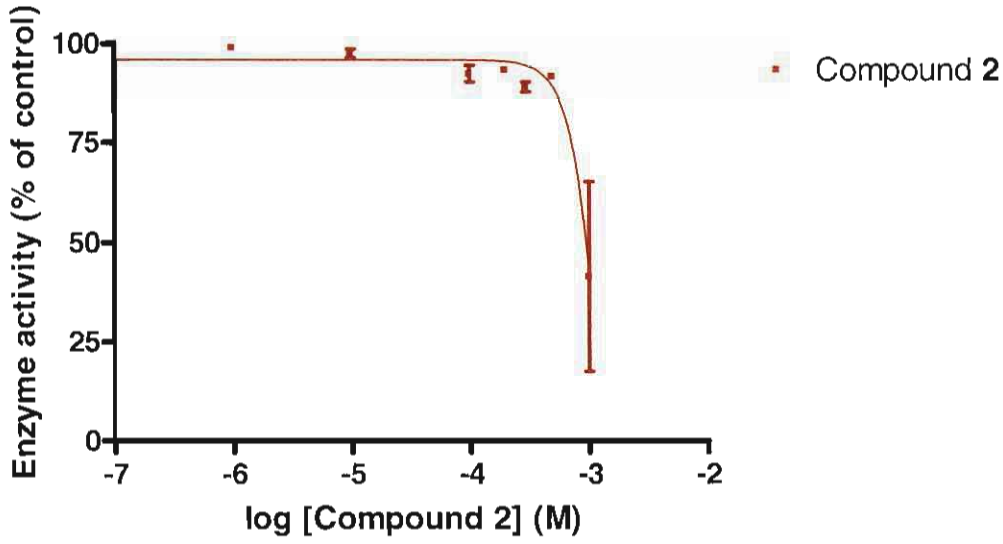

Figure 5.14: Inhibition curve of compound **2** on NOS activity. L-arginine (100 mM) was used as substrate. No IC_{50} value could be calculated due to solubility problems at 1 mM inhibitor concentration.

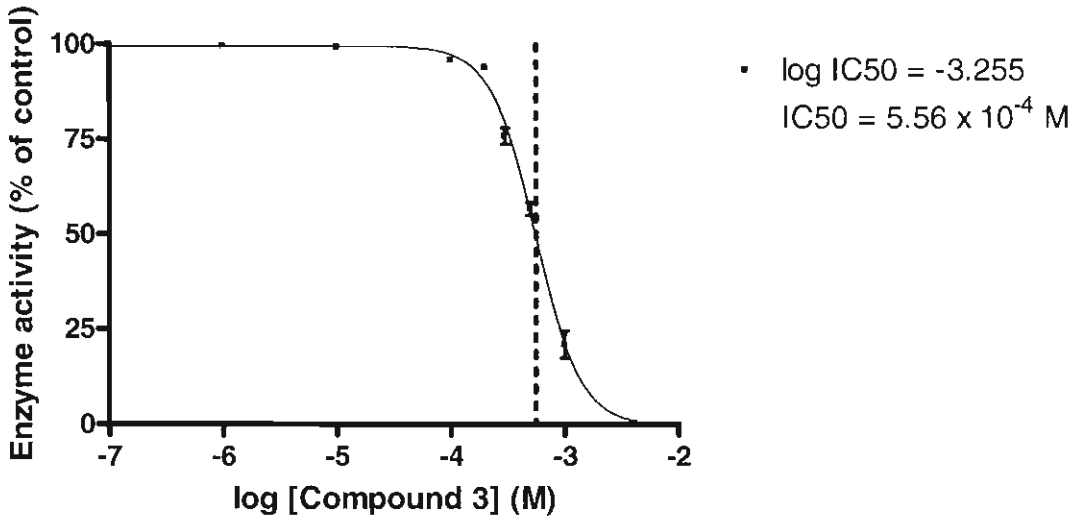

Figure 5.15: Inhibition curve of compound **3** on NOS activity. L-arginine (100 mM) was used as substrate. Log (IC_{50}): -3.255; IC_{50}: 5.56 x 10^{-4} M as indicated by the dotted line.

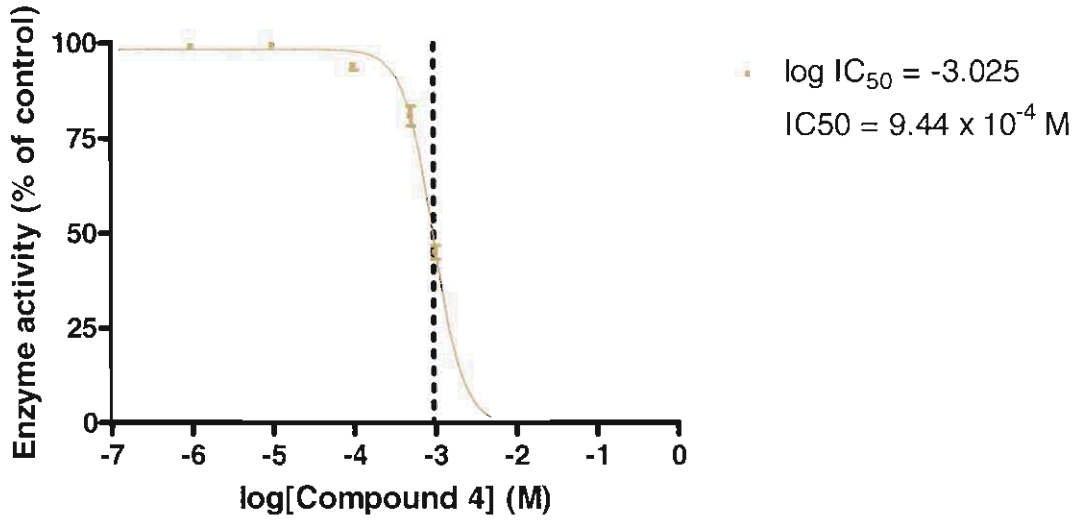

Figure 5.9: Inhibition curve of compound **4** on NOS activity. L-arginine (100 mM) was used as substrate. Log (IC_{50}): -3.025; IC_{50}: 9.44 x 10^{-4} M as indicated by the dotted line.

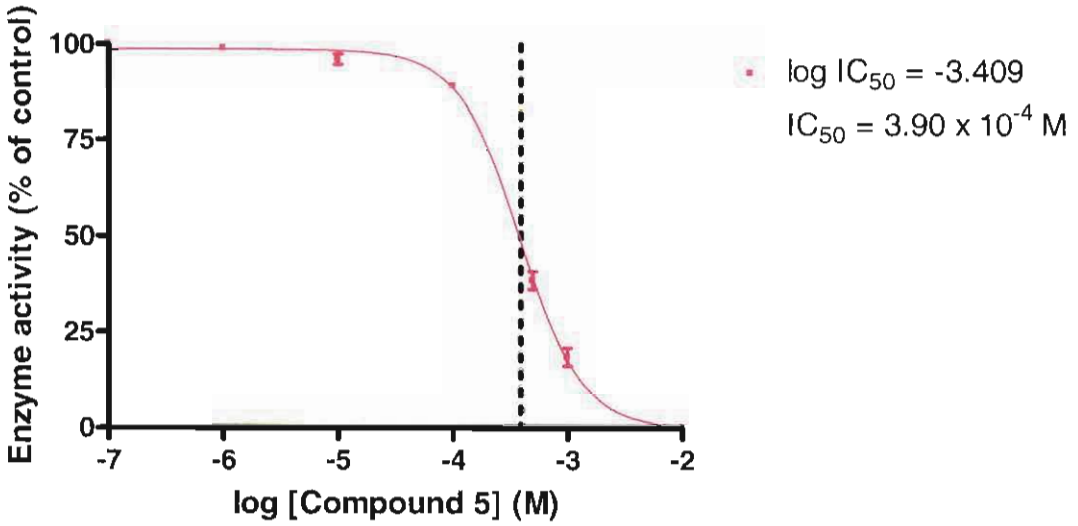

Figure 5.13: Inhibition curve of compound **5** on NOS activity. L-arginine (100 mM) was used as substrate. Log (IC_{50}): -3.409; IC_{50}: 3.9 x 10^{-4} M as indicated by the dotted line.

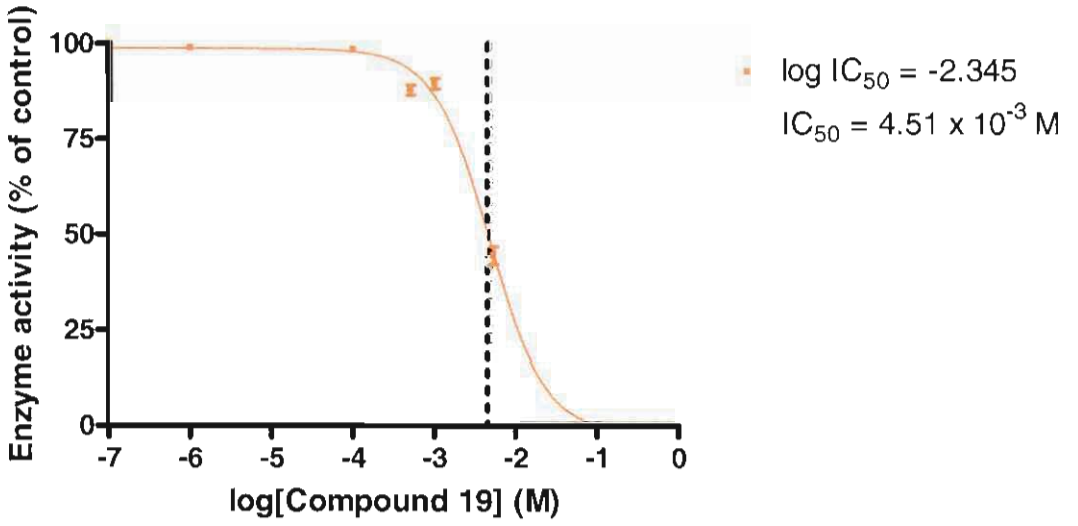

Figure 5.10: Inhibition curve of compound **19** on NOS activity. L-arginine (100 mM) was used as substrate. Log (IC_{50}): -2.345; IC_{50}: 4.51 x 10^{-3} M as indicated by the dotted line.

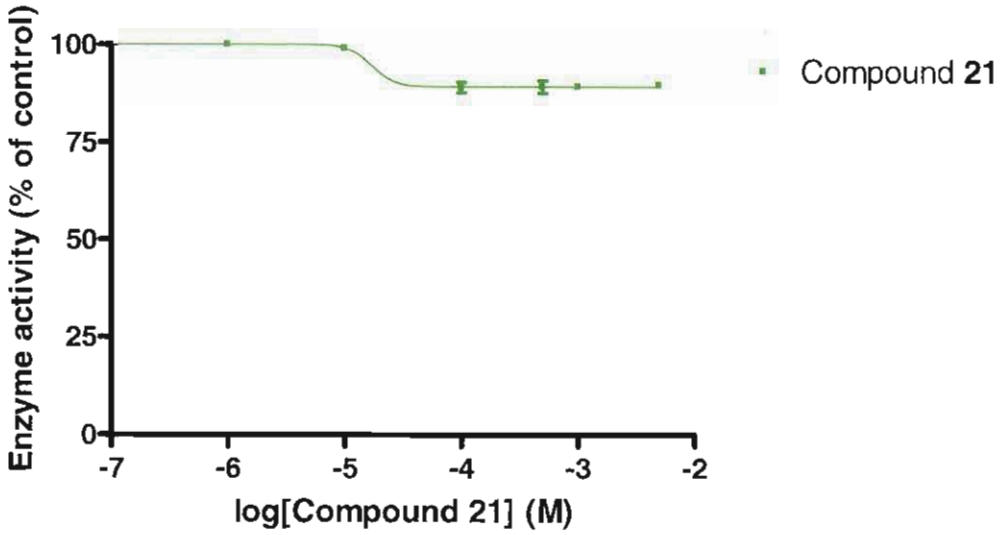

Figure 5.11: Inhibition curve of compound **21** on NOS activity. L-arginine (100 mM) was used as substrate. Only a 10 % inhibition was observed and no IC_{50} value could be calculated.

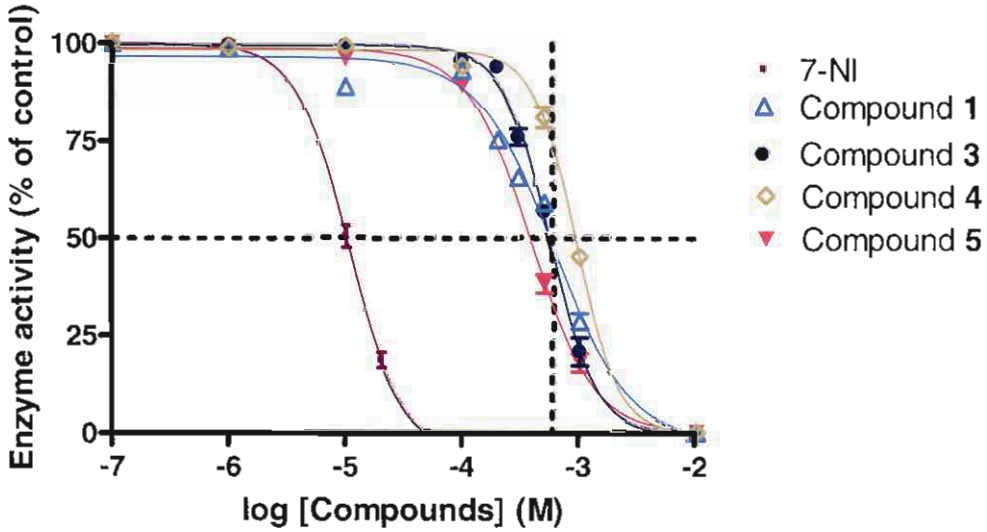

Figure 5.17: Superimposed inhibitory curves of test compounds with meaningfull IC_{50} values. At 125 µM compound **1** and **5** already showed a 15 % inhibition, but compound **3** and **4** only showed the same amount of inhibition at 250µM and 400µM, respectively.

Table 5.2: Summary of the test compounds with their corresponding IC_{50} values.

Compound	Structure	Log(IC_{50})	IC_{50}(M)
1	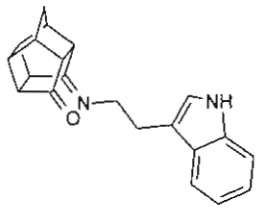	-3.207	6.21 X 10^{-4}
2	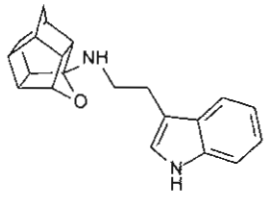	Solubility problems	
3	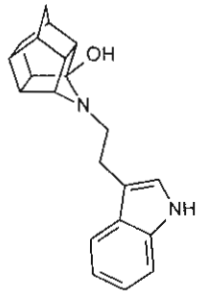	-3.255	5.56 X 10^{-4}
4	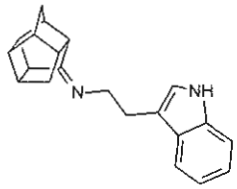	-3.025	9.44 X 10^{-4}
5	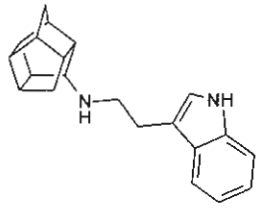	-3.409	3.9 X 10^{-4}

19	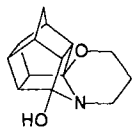	-2.345	4.51 X 10^{-3}
21	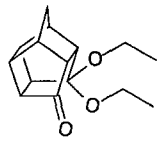	Only 10 % inhibition observed	
7-NI	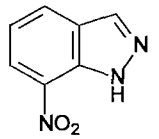	-4.981	1.04 X 10^{-5}
3-(2-amino-ethyl)indole	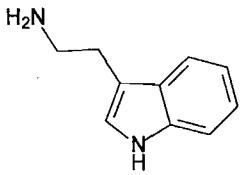	-2.692	2.03 X 10^{-3}

From the results it is clear that in the series of compounds evaluated, only the compounds containing an indole moiety, **1, 2, 3, 4** and **5** show promising NOS inhibition. Comparison of the IC_{50} values of the test compounds and 7-NI revealed that although the novel compounds are less potent than 7-NI, it showed promising results as NOS inhibitors with sub millimolar potency.

5.3. Lipid peroxidation

5.3.1. Introduction

Reactive oxygen species (ROS) are produced in the course of normal metabolism and these serve important physiological functions. When high levels of ROS exceeds the normal needs of the cell, it may indiscriminately damage the latter's structural and functional integrity either by directly modifying cellular DNA, proteins, and lipids or by initiating chain reactions that can bring about extensive oxidative damage to these critical molecules (Cui *et al.*, 2004). Although the human body possess endogenous antioxidants such as α-tocopherol and melatonin against ROS, it can sometimes be

inadequate, leading to oxidative stress where the production of ROS exceeds the antioxidant defences of the organism.

Although cells possess an intricate network of defence mechanisms to neutralise excess ROS and reduce oxidative stress, some tissues, especially the brain, are much more vulnerable to oxidative stress because of their elevated consumption of oxygen and the consequent generation of large amounts of ROS. For the same reason, the mitochondrial DNA (mtDNA) of brain cells is highly susceptible to structural alterations resulting in mitochondrial dysfunction. Several lines of evidence strongly suggest that these effects of ROS may be etiologically related to a number of neurodegenerative disorders (Cui *et al.*, 2004).

ROS is a collective term that includes all reactive forms of oxygen, including both the radical and nonradical species that participate in the initiation or propagation of radical chain reactions. Singlet oxygen is a very reactive ROS and induces various effects through its action on polyunsaturated fatty acids (PUFAs) and DNA. When molecular oxygen is reduced to water in the electron transport chain, there is a stepwise addition of four electrons, resulting in the formation of several hydrogen-containing ROS, such as hydroperoxyl radical, superoxide radical, hydrogen peroxide, and the hydroxyl radical (Table 5.3; Cui *et al.*, 2004).

Table 5.3: Formation of ROS by reduction of molecular oxygen in the electron transport chain.

(i) $O_2 + e + H^+ \longrightarrow HO_2$ (hydroperoxyl radical)
(ii) $HO_2 \longrightarrow H^+ + O_2^-$ (superoxide radical)
(iii) $O_2^- + 2H^+ + e \longrightarrow H_2O_2$ (hydrogen peroxide)
(iv) $H_2O_2 + e \longrightarrow OH^- + OH$(hydroxyl radical)
(v) $OH + e + H^+ \longrightarrow H_2O$
(vi) $O_2^- + H_2O_2 \longrightarrow OH^- + OH + O_2$ (Haber - Weiss reaction)
(vii) $Fe^{2+} + H_2O_2 \longrightarrow OH^- + OH + Fe^{3+}$ (Fenton reaction)

There are several observations suggesting that the brain may be particularly vulnerable to these ROS (Reiter, 1995; Olanow, 1993; Muller, 1997; Halliwell, 2001). Some of the most important of these are summarised below:

- The brain consumes a fifth of the total oxygen inspired and carries out the turnover of large quantities of ATP at a high rate. Since approximately 5% of oxygen consumed by cells is estimated to be reduced to ROS, relatively higher amounts of ROS may be generated in the brain as compared to other tissues that use less oxygen.
- Brain is rich in PUFAs, which are particularly susceptible to ROS damage.
- The release of excitatory neurotransmitters, such as glutamate, induces a cascade of reactions in the postsynaptic neuron, resulting in the formation of ROS. Depending on the density of such neurons, this could cause localised lesions in the nervous system.
- The liberation of ROS during the oxidation of dopamine by monoamine oxidase in the nerve terminals of dopaminergic neurons may produce increased oxidative stress in brain regions, such as substantia nigra. This is suggested to have a causative role in the etiology of PD.
- The brain contains almost no catalase and less glutathione peroxidase and vitamin E, when compared to liver.
- An endogenous antioxidant produced in the pineal gland, called melatonin, is found to be a good scavenger of ROS, but its concentration decreases markedly with age.

5.3.2. Experimental procedures

A study protocol was approved by the Ethics Committee for Research on Experimental Animals of the North-West University (Potchefstroom campus). Male Sprague-Dawley rats were sacrificed by decapitation and the brain tissue was removed and preserved for homogenation. All materials were purchased from Sigma-Aldrich (UK) and Merck (St. Louis, MO, USA). A modified version of the thiobarbituric acid (TBA) assay of Ottino & Duncan (1996) was used to screen test compounds at a concentration of 1 mM for lipid peroxidation. Detection of lipid peroxidation relies on the on the bases of the complex formation between malondialdehyde (MDA) and TBA (fig. 5.18), generating a pink coloured complex that was spectrophotometrically measured at 532 nm.

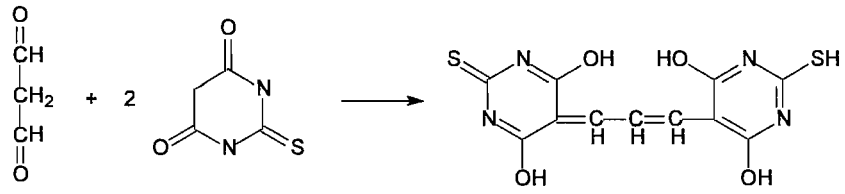

Figure 5.18: Reaction between MDA and TBA.

The formed MDA is used as an estimation of the degree of lipid peroxidation in the assay.

5.3.3. Assay procedure

Sprague-Dawley rats (± 250 g) were sacrificed by decapitation and the brain tissue was removed and preserved for homogenation. Excessive blood was removed by rinsing the tissue with phosphate-buffered saline (PBS), that consisted of 137 mM NaCl, 2.7 mM KCl, 10 mM K_2HPO_4 and 2 mM KH_2PO_4 at pH 7.4. The brain tissue, weighing between 1.6 and 2 g were homogenised in phosphate-buffered saline to give a final homogenate solution of 10 %. Homogenate preparation was carried out on ice. All the samples were prepared by adding 800 µl of the 10 % homogenate in test tubes and subsequently 200 µl PBS for the control and 100 µl PBS for all test compounds to give a final volume of 1 ml. 50 µl Hydrogen peroxide (5 mM) was used as a toxin to generate hydroxyl radicals and initiate lipid peroxidation in the rat brain hemogenates. 25 µl Iron(III)chloride (4,88 mM) and 25 µl ascorbic acid (1,4 mM) were used to increase the generation of hydroxyl radicals (Table 5.4).

Table: 5.4: Composition of test tubes prior spectrophotometric analysis.

Test tubes	Homogenate (10%)	PBS	H_2O_2 (5 mM)	$FeCl_3$ (4.88 mM)	Vit. C (1.4 mM)	Compound
	ml	ml	ml	ml	ml	ml
a) Control	0.8	0.2	-	-	-	-
b) **1**	0.8	0.1	0.05	0.025	0.025	0.1
c) **2**	0.8	0.1	0.05	0.025	0.025	0.1
d) **3**	0.8	0.1	0.05	0.025	0.025	0.1
e) **4**	0.8	0.1	0.05	0.025	0.025	0.1
f) **5**	0.8	0.1	0.05	0.025	0.025	0.1
g) **19**	0.8	0.1	0.05	0.025	0.025	0.1
h) **21**	0.8	0.1	0.05	0.025	0.025	0.1

All test compounds were dissolved in DMSO to give concentrations of 10 mM and futher diluted to a concentration of 1 mM for incubation. The test tubes were vortexed and kept on ice. After incubation at 37°C for 60 minutes in an ossilation water bath, the turbid solutions were centrifuged at 2000 x g for 20 minutes. The clear supernatant was transferred to clean test tubes. before 0.5 ml butylated hydroxytoluene (0.5 g/l; BHT), 1 ml trichloroacetic acid (10 %; TCA) and 0.5 ml 2-thiobarbituric acid (0.33 %; TBA) were added to the mixture. The newly prepared test tubes were vortexed again and incubated for another 60 minutes at 60°C. After cooling on ice, 2 ml butanol was added to each test tube before it was vortexed and centrifuged again for 10 minutes at 2000 x g. The organic phase was transferred to clean cuvettes and analysed with a Milton Roy sectronic 1201 spectrophotometer at 532 nm with butanol used as the blanco. Trolox (10 mM), a known antioxidant, was used as a standard. The values were expressed as nmol MDA equivalents per mg tissue.

5.3.4. Results and Discussion

The adopted method was tested by inducing free radical generation with a known free radical generator, hydrogen peroxide, in rat brain homogenate. Hydrogen peroxide produced a marked increase in lipid peroxidation (Table 5.5). Therefore, the modified method could be used to determine lipid peroxidation in biological samples, with satisfactory results.

Table 5.5: Concentration-dependent effect of hydrogen peroxide on lipid peroxidation in rat brain homogenate.

Hydrogen peroxide concentration (mM)	Malondialdehyde (nmol per mg tissue)
Control	0.0054
0.1	0.0243
0.5	0.0251
1	0.0274

As shown in table 5.5, exposure of rat brain homogenate to various concentrations (0 – 1 mM) of hydrogen peroxide (H_2O_2) increased lipid peroxidation in a concentration-

dependent manner. All test tubes were treated with 0.5 mM H_2O_2 to iniated lipid peroxidation.

Materials of animal origin usually contain large amounts of protein, to which malondialdehyde may be bound (Draper & Hadley 1990). It is therefore imperative to release the protein-bound malondialdehyde by adding trichloroacetic acid and subsequently heating the mixture.

It is also important to prevent adsorption of the thiobarbituric acid-malondialdehyde complex onto insoluble protein. This is facilitated by the removal of any solid material by centrifugation.

The malondialdehyde levels (nmol per mg tissue) were obtained from a calibration curve (fig. 5.19). Regression analysis showed that concentration and absorbance were linear with a regression value of 0.9997. Each point on the calibration curve was based on triplicate determinations.

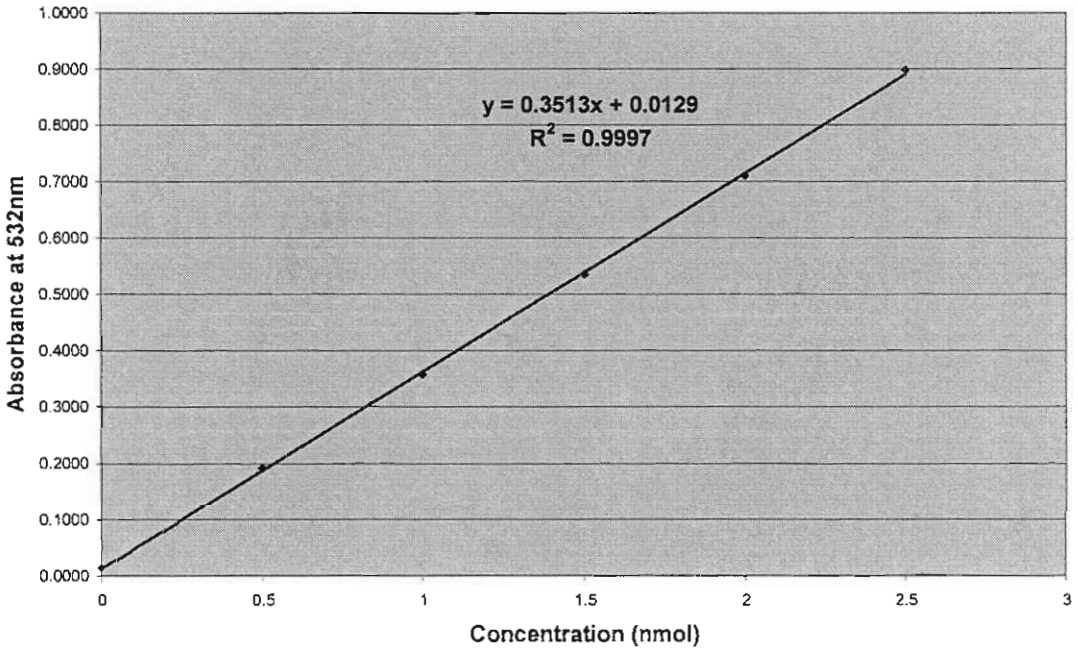

Figure 5.19: Calibration curve for the detection of lipid peroxidation.

The recorded absorbance values of the test compounds were substituted into the linear regression equation (eq. 5.2) obtained from the calibration data.

$$y = 0.3513x + 0.0129 \quad (5.2)$$

The recorded absorbance values were divided by 0.8 to determine the amount MDA per mg tissue. Comparison of these data with trolox can be expressed in nmol MDA per mg tissue (fig. 5.20). All the test compounds except compound 8, 21 revealed promising antioxidant activity when compared with trolox.

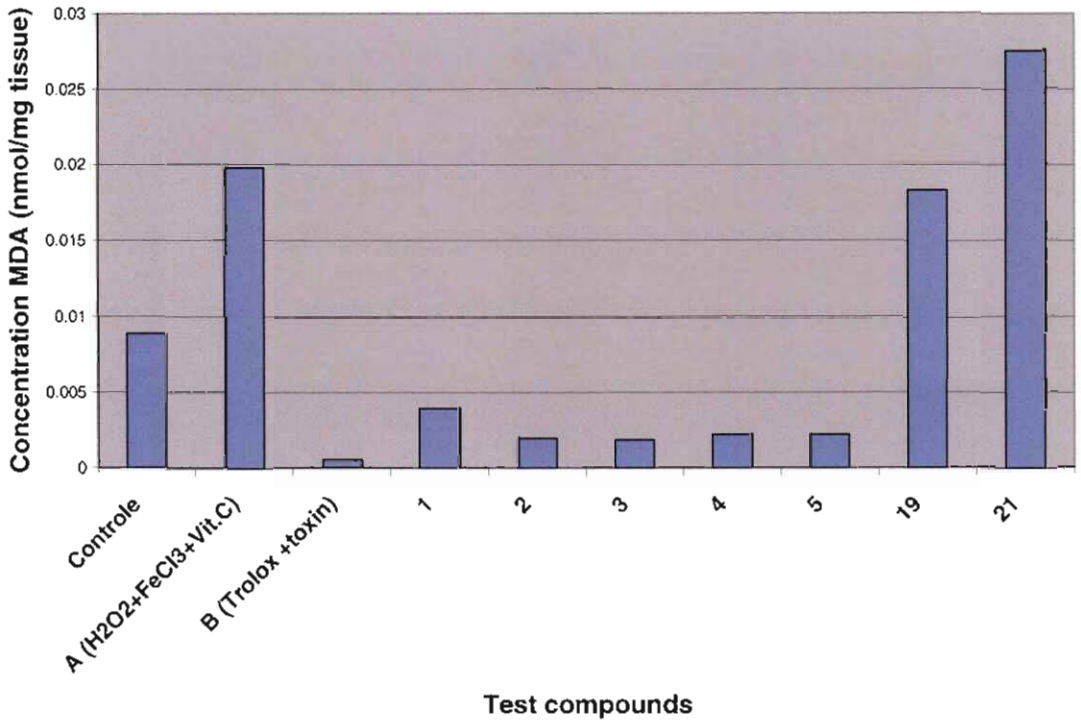

Figure 5.20: Antioxidant capacity of test compounds in comparison with trolox, a known antioxidant.

5.4. Conclusion

The series of compounds were evaluated for NOS and anti-oxidative activity. Compouds **1, 2, 3, 4** and **5** showed promising results as NOS inhibitors. Comparison of the IC_{50} values of the test compounds and 7-NI revealed that although they were less potent than 7-NI, it still showed promising results as NOS inhibitors. The novel compounds **1, 2, 3, 4** and **5** also had excellent anti-oxidative properties when compared to trolox. The polycyclic cage structure that was applied as carrier molecule, thus not only serve as pharmacokinetic enhancer but also to improve pharmacodynamics. With the cage

structures' described calcium channel activity and taking the above aspects into account, these novel compounds may find application as multipotent drugs in neuroprotection.

Summary, discussion and conclusion

Chapter 6

6. Introduction

Designing drugs with multifunctional modes of action has received much attention lately (Van der Schyf *et al.*, 2006). For this reason a compound that acts as calcium channel blocker, NOS inhibitor and free radical scavenger may be of value in the quest for neuroprotective drugs. We therefore decided to synthesise a series of pentacycloundecyl derivatives with known Ca^{2+} channel activity (Geldenhuys *et al.*, 2003a Van der Schyf *et al.*, 1986; Van der Walt *et al.*, 1988), incorporating an indole moiety (compounds **1, 2, 3, 4** and **5**) for which anti-oxidant and NOS activity has been described (Chang *et al.*, 2000).

Computer modelling, synthesis and biological evaluation of the novel compounds were performed to determine their potential as neuroprotective drugs.

6.1. Molecular modelling

Molecular modelling was performed on a series of polycyclic indole derivatives to identify potential drug candidates for nitric oxide synthase (NOS) as the target. A docking study utilising Catalyst 4.9® and the Ligandfit module of Cerius²® was performed to achieve this. A crystallised nNOS structure (1OM5) was retrieved from the RCSB Protein Data Bank, the active site was identified and the novel series of compounds was docked into the active site using Ligandfit®. The DREIDING2.21 force field and Gasteiger charges were used throughout the experiment and all other values were set to default. After completing the docking procedure, hydrogen bonds were calculated to identify possible conformations for favourable interactions.

In all the cases the indole ring was oriented towards the heme moiety and the cage structure located near the entrance cavity. Compounds **1, 3, 4, 5, 6, 7, 9, 11, 12, 13, 16, 17, 18, 19** formed hydrogen bonds with essential amino acid residues Tpr587, Glu592 and heme. Compounds **2, 8, 10, 14, 15** formed bonds to Tyr 588, Gln 478 and Asp 597, amino acids only play a role in the stabilisation and orientation of ligands in the cavity. The molecular modelling study clearly suggests that selected compounds will form hydrogen bond interactions with the amino acids and heme essential for substrate binding and thus have the potential to interact and inhibit the NOS enzyme.

6.2. Synthesis

High yields of the Cookson diketone (Cookson *et al.*, 1964) were obtained from ultraviolet irradiation of the *p*-benzoquinone-cyclopentadiene adduct. The monoketone was synthesised from diketone to restrict the reaction to only one ketone group. Both these pentacycloundecyl structures were used as intermediates in further amination reactions. A series of polycyclic indole derivatives were synthesised by reductive amination of the monoketone and diketone structures.

Various linkers were to be applied between the cage structures and the indole moiety, but due to multiple reactions and rearrangements of the cage structures, no amides, ethers or esters could be obtained. Five novel tryptamine compounds were synthesised with percentage yields varying between 33.6 % and 88.3 %. Flash column chromatography was mostly used in the purification of the compounds. Other methods applied included recrystallisation and acid-base extractions. Seven compounds were adequately purified and characterised for biological evaluation.

6.3. Biological evaluation

The selected compounds were tested for NOS activity and antioxidant capacity. An *in vitro* oxyhemoglobin (oxyHb) assay was employed to determine NOS activity of the novel compounds. This assay is based on the reaction between NO and oxyHb with the subsequent formation of methemoglobin (metHb). NO formation and thus NOS activity could be obtained by measuring the change in absorbance (ΔA) during the conversion of oxyHb to metHb.

Of the newly synthesised compounds, structures **1, 4, 3, 5** demonstrated meaningful NOS inhibition in the micromolar range. Solubility problems were observed during biological testing of compound **2** and no IC_{50} value could be calculated.

The indole moiety was compared with aminoguanidine (a known selective NOS inhibitor) to see if there is a resemblance. From this comparison a conclusion was drawn that the unsaturated amine moiety might be an important pharmacophoric entity for effective NOS inhibition (fig 6.1)

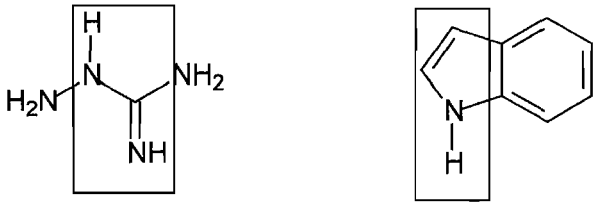

guanidine indole

Figure 6.1: Comparison of guanidine with an indole moiety.

The dose response curves of the individual compounds compared well with cage guanidine structures (Wilkes, 2005), although it proved to be less potent than 7-NI.

The test compounds were also screened for antioxidative properties. An adapted method of Ottino & Duncan (1996) was used for the detection of lipid peroxidation. This process is based on the formation of a complex between malondialdehyde (MDA) and thiobarbituric acid (TBA), resulting in a pink coloured complex that can be spectrophotometrically analysed at 532 nm.

Hydrogen peroxide was used as a free radical generator and trolox, a known antioxidant, was used as standard reference. Of the newly synthesised compounds, all the tryptamine compounds possessed excellent antioxidative properties when compared with trolox. The indole moiety probably plays an important role in this activity.

6.4. Conclusion

The urgent need of selective nNOS inhibitors are of great importance in the treatment of neurodegenerative disorders. Considering that NOS is primarily activated by the NMDA receptor, the combination of three properties (calcium channel blocking, selective NOS inhibition and antioxidative capacity) makes these novel compounds excellent drugs for possible treatment of neurodegenerative disorders.

The results obtained in this study clearly indicate the potential of these novel indole cage structures as NOS inhibitors and anti-oxidants. With the cage structures' described calcium channel activity and taking the above aspects into account, these novel compounds may find application as multipotent drugs in neuroprotection.

In conclusion, the aim of this study to design and evaluate a novel series of polycyclic indole derivatives for NOS and antioxidant activity was achieved and the results obtained gave some insights for future investigation. These should include further

optimisation of the indole and cage structures and their synthesis as well as NOS isoform selectivity studies.

7. Bibliography:

8. References:

ACUÑA-CASTROVIEJO, D., ESCAMES, G., MACÍAS, M., MUÑOZ HOYOS, A., MOLINA CARBALLO, A., ARAUZO, M., MONTES, R. & VIVES, F. 1995. Cell protective role of melatonin in the brain. *Journal of Pineal Research*, 19:57–63.

ACUÑA-CASTROVIEJO, D., ROMERO, H.E. & CARDINALI, D.P. 1986. Changes in gamma-aminobutyric acid high affinity binding to cerebral cortex membranes after pinealectomy or melatonin administrations to rats. *Neuroendocrinology*, 43:24–31.

ALDERSON, P. & ROBERTS, I. 2005. Corticosteroids for acute traumatic brain injury. *Cochrane Database Systematic Reviews*, 1:CD000196.

ALDERTON, W. K., BOYHAN, A., & LOWE, P. N. 1998. Nitroarginine and tetrahydrobiopterin binding to the haem domain of neuronal nitric oxide synthase using a scintillation proximity assay. *Biochemical. Journal*, 332:195-201.

ALDERTON, W.K., COOPER, C.E. & KNOWLES, R.G. 2001. Nitric oxide synthases: structure, function and inhibition. *Biochemical Journal*, 357:593–615.

ALEXI, T., HUGHES, P.E., FAULL, R.L.M. & WILLIAMS, C.E. 1998. 3-nitropropionic acid's lethal triplet: cooperative pathways of neurodegeneration. *Neuro Report*, 9:R57-R64.

ASHINA, M., LASSEN, L.H., BENDTSEN, L., JENSEN, R. & OLESEN, J. 1999. Effect of inhibition of nitric oxide synthase on chronic tension-type headache: a randomised crossover. *Lancet*, 353:287–289.

BABBEDGE, R. C., BLAND-WARD, P. A., HART, S. L. & MOORE, P. K. 1993. Inhibition of rat cerebellar nitric oxide synthase by 7-nitro indazole and related substituted indazoles. *British Journal of Pharmacology*, 110:225.

BABU, B.R. & GRIFFITH, O.W. 1998a. Design of the isoform-selective inhibitors of nitric oxide synthase. *Current Opinion in Chemical Biology*, 2:491–500.

BABU, B.R. & GRIFFITH, O.W. 1998b. N^5-(1-imino-3-butenyl)-L-ornithine. A neuronal isoform selective mechanism based inactivator of nitric oxide synthase. *Journal of Biological Chemistry*, 273:8882–8889.

BACH, A.W.J., LAN, N.C., JHONSON, D.L. ABELL, C.W., BEMKENEK, M.E. KWAN, S.W., SEEBURG, P.H. & SHIH, J.C. 1988. cDNA cloning of human liver monoamine oxidase A and B: molecular basis of differences in enzymatic properties. *Proceedings of the National Academy of Sciences of the United States of America*, 85:4934-4938.

BEATON, H., BOUGHTON-SMITH, N., HAMLEY, P., GHELANI, A., NICHOLLS, D.J., TINKER, A.C. & WALLACE, A.V. 2001. Thienopyridines: nitric oxide synthase inhibitors with potent *in vivo* activity. *Bioorganic and Medicinal Chemistry Letters*, 11:1027–1030.

BECK, C., WOLLMUTH, L.P., SEEBURG, P.H., SAKMANN, B. & KUNER, T. 1999. NMDAR channel segments forming the extracellular vestibule inferred from the accessibility of substituted cysteines. *Neuron*, 22:559–570.

BERRY, M.D., JUORIO, A.V. & PATERSON, I.A. 1994. The functional role of monoamine oxidases A and B in the mammalian central nervous system. *Progress in Neurobiology*, 42:375-391.

BEYER, C.E., STEKETEE, J.D. & SAPHIER, D. 1998. Antioxidant properties of melatonin—an emerging mystery. *Biochemical Pharmacology*, 56:1265-1272.

BIJKDAOUENE, L., ESCAMES, G., LEÓN, J., FERRER, J.M.R., KHALDY, H., VIVES, F. & ACUÑA-CASTROVIEJO, D. 2003. Changes in brain amino acids and nitric oxide after melatonin administration to pentylenetetrazole-induced seizures in rats. *Journal of Pineal Research*, 35:54–60.

BIRRELL, M.A., McCLUSKIE, K., HADDAD, E.B., BATTRAM, C.H., WEBBER, S.E., FOSTER, M.L., YACOUB, M.H. & BELVISI, M.G. 2003. Pharmacological assessment of the nitric oxide synthase isoform in eosinophilic inflammation in a rat model of sephadex-induced airway inflammation. *Journal of Pharmacology and Experimental Therapeutics*, 304:1285–1291.

BLAND-WARD, P. A., & MOORE, P. K. 1995. 7-Nitro indazole Derivatives are potent inhibitors of brain, endothelium and inducible isoforms of nitric oxide synthase. *Life Sciences*, 57:PL131- PL135.

BRORSON, J.R., SCHUMACKER, P.T. & ZHANG, H. 1999. Nitric oxide acutely inhibits neuronal energy production. *Journal of Neuroscience*, 19:147-158.

BRUSCO, L.I., MARQUEZ, M. & CARDINALI, D.P. 1998. Monozygotic twins with Alzheimer's disease treated with melatonin: case report. *Journal of Pineal Research*, 25:260–263.

CAJOCHEN, C., KRÄUCHI, K. & WIRZ-JUSTICE, A. 2003. Role of melatonin in the regulation of human circadian rhythms and sleep. *Journal of Neuroendocrinology*, 15:432–437.

CASSARINO, D.S. & BENNETT Jr, J.P. 1999. An evaluation of the role of mitochondria in neurodegenerative diseases: mitochondrial mutations and oxidative pathology, protective nuclear responses and cell death in neurodegeneration. *Brain Research Reviews*, 29:1-25.

CASTILHO, R.F., HANSSON, O., WARD, M.W., BUDD, S.L. & NICHOLLS, D.G. 1998. Mitochondrial control of acute glutamate excitotoxicity in cultured cerebellar granule cells. *Journal of Neuroscience*, 18:10277-10286.

CAWTHON, R.N., PINTAR, J.E., HASELTINE, F.P. & BREAKEFIELD, X.O. 1981. Differences in the structure of A and B forms of human monoamine oxidase. *Journal of Neurochemistry*, 37:363-372.

CHANG, H,M., LING, E.A., LUE, J.H., WEN, C.Y. & SHIEH, J.Y. 2000. Melatonin attenuates neuronal NADPH-d/NOS expression in the hypoglossal nucleus of adult rats following peripheral nerve injury. *Brain Research*, 873:243-251.

CHEN, H.V. & LIPTON, S.A. 2006. The chemical biology of clinically tolerated NMDA receptor antagonists. *Journal of Neurochemistry*, 97:1611-1626.

CHOI, D. 1995. Calcium still center-stage in hypoxic-ischemic neuronal death. *Trends in Neurosciences*, 18:58-60.

CHUNG, S.Y. & HAN, S.H. 2003. Melatonin attenuates kainic acid-induced hippocampal neurodegeneration and oxidative stress through microglial inhibition. *Journal of Pineal Research*, 34:95–102.

COHEN N.C. 1996. The molecular modelling perspective in drug design. (*In* Cohen, N.C., *eds.* Guidebook on molecular modelling in drug design. San Diego : Academic Press. p. 1-17).

COOKSON, R.C., GRUNDELL, E. & HUDEC, J. 1958. Synthesis of cage-like molecules by irradiation of Diels-Alder adducts. *Chemistry and Industry*, 1003-1004.

COOKSON, R.C., CRUNDWELL, E., HILL, R.R. & HUDEC, J. 1964. Photochemical cyclisation of Diels-Alder adducts. *Journal of the Chemical Society*, 3062-3075.

CRANE, B.R., ARVAI, A.S., GHOSH, S., GETZOFF, E.D., STUEHR, D.J. & TAINER, J.A. 2000. Structures of the N^{ω}-Hydroxy-L-Arginine complex of inducible nitric oxide synthase oxygenase dimer with active and inactive pterins. *Biochemistry*, 39:4608-4621.

CUI, K., LUO, X., XU, K. & VEN MURTHY, M.R. 2004. Role of oxidative stress in neurodegeneration: recent developments in assay methods for oxidative stress and nutraceutical antioxidants. *Progress in Neuro-Psychopharmacology and Biological Psychiatry*, 28:771-799.

DAFF, S. 2001. Control of electron transfer in neuronal NO synthase. *Biochemical Society Transactions*, 29:147–152.

DAFF, S. 2003. Calmodulin-dependent regulation of mammalian nitric oxide synthase. *Biochemical Society Transactions*, 31:502–505.

DANBOLT, N. C. 2001. Glutamate uptake. *Progress in Neurobiology*, 65:1-105.

DAVIES, W.L., GRUNERT, R.R., HAFF, R.F. McGAHEN, J.W., NEUMAYER, E.M., PAULSHOCK, M., WATTS, J.C., WOOD, T.R., HERMANN, E.D. & HOFFMANN, E.C. 1964. Antiviral activity of adamantamine. *Science*, 144:862-863.

DAWSON, V. L. & DAWSON, T. M. 1996. Nitric oxide actions in neurochemistry. *Neurochemistry International*, 29:97.

DAWSON, V.L., DAWSON, T.M., LONDON, E.D., BREDT, D.S. & SNYDER, S.H. 1991. Nitric oxide mediates glutamate neurotoxicity in primary cortical cultures. *Proceedings of the National Academy of Sciences of the United States of America*, 88:6368-6371.

DEKKER, T.G. & OLIVER, D.W. 1978. Synthesis of (D_3)-trishomocuban-4-ol via ion rearrangement of pentacyclo[5.4.0.$0^{2,6}$.$0^{3,10}$.$0^{5,9}$]undecane-8-ol. *South African Journal of Chemistry*, 32:45-48.

DEMPSEY, R.J. & RAGHAVENDRA, R.V. 2003. Cytidinediphosphocholine treatment to decrease traumatic brain injury-indiced hippocampal neuronal death, cortical contusion volume and neurological dysfunction in rats. *Journal Neurosurg*, 98:867-873.

DINGLEDINE, R., BORGES, K., BOWIE, D. & TRAYNELIS, S. F. 1999. The glutamate receptor ion channels. *Pharmacological Reviews*, 51:7-61.

DJEBAILI, M., GUO, Q. & PETTUS, E.H. 2005. The neurosteroids progesterone and allopregnanolone reduce cell death, gliosis and functional deficits after traumatic brain injury in rats. *Journal of Neurotrauma*, 22:106-118.

DRAGUNOW, M., MACGIBBON, G.A., LAWLOR, P., BUTTERWORTH, N., CONNOR, B., HENDERSON, C., WALTON, M., WOODGATE, A., HUGHES, P. & FAULL, R.L.M. 1998. Apoptosis, neurotrophic factors and neurodegeneration. *Reviews in Neurosciences*, 8:223-265.

DRAPER, H.H. & HADLEY, M. 1990. Malondialdehyde determination as an index of lipid peroxidation. (*In* Packer, L., Alexander, A. N., eds. Methods in Enzymology. 186. San Diego : Academic Press. p. 421-431.)

DRÖGE, W. 2002. Free radicals in the physiological control of cell function. *Physiological Reviews*, 82:47–95.

DUBOCOVICH, M.L., RIVERA-BERMUDEZ, M.A., GERDIN, M.J. & MASANA, M.I. 2003. Molecular pharmacology, regulation and function of mammalian melatonin receptors. *Front Biosci*, 8:1093–1108.

DUGAN, L.L. & CHOI, D.W. 1999. Hypoxic-ischemic brain injury and oxidative stress. (*In* Siegel, G.J., Agranoff, B.W., Albers, R.W., Fischer, S.K. & Uhler, M.D. eds. Basic Neurochemistry: Molecular, Cellular and Medical aspects. Philadelphia : Lippincott-Raven Publishers. p. 711-729.)

DYKENS, J.A. 1994. Isolated cerebral and cerebellar mitochondria produce free radicals when exposed to elevated Ca^{2+} and Na^{+}: implications for neurodegeneration. *Journal of Neurochemistry*, 63:584-591.

DWYER, M. A., BREDT, D. S. & SNYDER, S. H. 1991. Nitric oxide synthase: Irreversible inhibition by L-N^{G}-Nitroarginine in brain *in vitro* and *in vivo*. *Biochemical and Biophysical Research Communications*, 176:1136.

EL-SHERIF, Y., HOGAN, M.V., TESORIERO, J. & WIERASZO, A. 2002. Factors regulating the influence of melatonin on hippocampal evoked potentials: comparative studies on different strains of mice. *Brain Research*, 945:191–201.

EMBORG, M.E. & KORDOWER, J.H. 2000. Delivery of therapeutic molecules into the CNS. *Progress in Brain Research*, 128:323–32.

ENKHBAATAR, P., MURAKAMI, K., SHIMODA, K., MIZUTANI, A., MCGUIRE, R., SCHMALSTEIG, F., COX, F., HAWKINS, H., JODOIN, J., LEE, S., TRABER, L., HERNDON D. & TRABER, D.L. 2003. Inhibition of neuronal nitric oxide synthase (nNOS) by 7-nitroindazole attenuates acute lung injury in an ovine model. *American Journal of Physiology - Regulatory, Integrative and Comparative Physiology*, 285:R366–R372.

FEELISH, M., KUBITZEK, D. & WERRINGLOER, J. 1996. The oxyhemoglobin assay. (*In* Feelish, M. & Stamler, J.S., eds. Methods in nitric oxide research. London : Wiley & Sons Ltd. p. 455-478.)

FISCHMANN, T.O., HRUZA, A., NIU, X.D., FOSSETTA, J.D., LUNN, C.A., DOLPHIN, E., PRONGAY, A.J., REICHERT, P., LUNDELL, D.J., NARULA, S.K. & WEBER, P.C. 1999. Structural characterization of nitric oxide synthase isoforms reveals striking active-site conservation. *Natural Structural Biology*, 6:233- 242.

FOWLER, C.J., ORELAND, L., MARCUSSON, J. & WINBLAD, B. 1980. Titration of human brain monoamine oxidase-A and -B by clorgyline and L-deprenyl. *Naunyn-Schmiedeberg's Archives of Pharmacology*, 311:263-272.

GARVEY, E.P., OPLINGER, J.A., FURFINE, E.S., KIFF, R.J., LASZLO, F., WHITTLE, B.J.R. & KNOWLES, R.G. 1997. 1400W is a slow, tight binding and highly selective inhibitor of inducible nitric-oxide synthase *in vitro* and *in vivo*. *Journal of Biological Chemistry*, 272:4959–4963.

GELDENHUYS, W.J., MALAN, S.F., MURUGESAN, T., VAN DER SCHYF, C.J. & BLOOMQUIST, J.R. 2003a. Synthesis and biological evaluation of pentacyclo[5.4.$0^{2,6}$.$0^{3,10}$.$0^{5,9}$]undecane derivatives as potential tharapeutic agents in Parkinson's disease. *Bioorganic and Medicinal Chemistry*, 2:1799-1806.

GELDENHUYS, W.J., TERRE'BLANCHE, G., VAN DER SCHYF, C.J. & MALAN, S.F. 2003b. Screening of novel pentacyclo-undecylamines for neuroprotective activity. *European Journal of Pharmacology*, 458:73-79.

GERLACH, M., BLUM-DEGEN, D., LAN, J. & RIEDERER, P. 1999. Nitric oxide in the pathogenesis of Parkinson's disease. *Advances in Neurology*, 80:239-245.

GIUSTI, P., LIPARTITI, M., FRANCESCHINI, D., SCHIAVO, N., FLOREANI, M. & MANEV, H. 1996. Neuroprotection by melatonin from kainate-induced excitotoxicity in rats. *FASEB Journal*, 10:891–896.

GLOVER, V. & SANDLER, M. Clinical chemistry of monoamine oxidase. *Cell Biochemistry and Function*, 4:89-97.

GREENE, J.G. & GREENAMYRE, J.T. 1996a. Bioenergetics and glutamate excitotoxicity. *Progress in Neurobiology*, 48:613-634.

GREENE, J.G. & GREENAMYRE, J.T. 1996b. Manipulation of membrane potential modulates malonate-induced striatal excitotoxicity *in vivo*. *Journal of Neurochemistry*, 66:637-643.

GROVER, R., BAKKER, J., MCLUCKIE, A., ANDERSSON, J. & LEGALL, J.R. 1998. The nitric oxide synthase inhibitor 546C88 promotes the resolution of shock in patients with severe sepsis. *Critical Care Medicine*, 26:A29.

GROVER, R., LOPEZ, A., LORENTO, J., STEINGRUB, J., BAKKER, J., WILLATTS, S., MCLUCKIE, A. & TAKALA, J. 1999a. Multicenter, randomised, placebo-controlled, double bind study of the nitric oxide synthase inhibitor 546C88: effect on survival in patients with septic shock. *Critical Care Medicine*, 27:A33.

GROVER, R., ZACCARDELLI, D., COLICE, G., GUNTUPALLI, K., WATSON, D. & VINCENT, J.L. 1999b. An open-label dose escalation study of the nitric oxide synthase inhibitor, N^G-methyl-L-arginine hydrochloride (546C88), in patients with septic shock. *Critical Care Medicine*, 27:913–922.

GUNASEKAR, P.G., KANTHASAMY, A.G., BOROWITZ, J.L. & ISOM, G.E. 1995. NMDA receptor activation produces concurrent generation of nitric oxide and reactive oxygen species: implication from cell death. *Journal of Neurochemistry*, 65:2016–2021.

HALLIWELL, B. 2001. Role of free radicals in the neurodegenerative diseases: therapeutic implications for antioxidant treatment. *Drugs Aging*, 18:685-716.

HANDY, R.L.C., HARB, H.L., WALLACE, P., GAFFEN, Z., WHITEHEAD, K.J. & MOORE, P.K. 1996. Inhibition of nitric oxide synthase by 1-(2-trifluoromethylphenyl) imidazole (TRIM) in vitro : antinociceptive and cardiovascular effects. *British Journal of Pharmacology*, 119:423.

HANDY, R.L.C. & MOORE, P.K. 1998. 7-nitroindazole (7-NI) fails to increase blood pressure in animals: the 7-NI conundrum. *Trends in Pharmacological Sciences*, 19:350.

HANSEL, T.T., KHARITONOY, S.A., DONNELLY, L.E., ERIN, E.M., CURRIE, M.G., MOORE, W.M., MANNING, P.T., RECTER, D.P. & BARNES, P.J. 2003. A selective inhibitor of inducible nitric oxide synthase inhibits exhaled breath in healthy volunteers and asthmatics. *FASEB Journal*, 17:1298–1300.

HANSEN, D.W. 1999. Nitric oxide synthase inhibitors with cardiovascular therapeutic potential. *Expert Opinion on Therapeutic Patents*, 9:537–547.

HERRLING, P. L. 1994. Clinical implications of NMDA receptors. (*In* Colingridge, G.L., Watkins, J.C., eds. The NMDA receptor. Oxford : Oxford University Press, p. 376-394.

HEVEL, J.M., WHITE, K.A. & MARLETTA, M.A. 1991. Purification of the inducible murine macrophage nitric oxide synthase. Identification as a flavoprotein. *Journal of Biological Chemistry*, 266:22789-22791.

HOSHINO, M., OZAWA, K., SEKI, H. & FORD, P.C. 1993. Photochemistry of nitric oxide adducts of water-soluble iron(III) porphyrin and ferrihemoproteins studied by nanosecond laser photolysis. *Journal of the American Chemical Society*, 115:9568-9575.

HUGHES, P.E., ALEXI, T. & SCHREIBER, S.S. 1997. A role for the tumour suppressor gene p53 in regulating neuronal apoptosis. *Neuro Report*, 8:v-xii.

HUGHES, P.E., ALEXI, T., WALTON, M., WILLIAMS, C.E., DRAGUNOW, M., CLARK, R.G. & GLUCKMAN, P.D. 1999. Activity and injury-dependent expression of inducible transcription factors, growth factors, and apoptosis-related genes within the central nervous system. *Progress in Neurobiology*, 57:421-450.

HURLEY, S.D., OLSCHOWKA, J.A. & O'BANION, M.K. 2002. Cyclooxygenase inhibition as a strategy to ameliorate brain injury. *Journal of Neurotrauma*, 19:1-15.

IPPOLITO, J.A., ALEXANDER, R.A. & CHRISTIANSON, D.W. 1990. Hydrogen bond stereochemistry in protein structure and function. *Journal of Molecular Cell Biology*, 215:457-471.

KALARIA, R.N. & HARIK, S.I. 1987. Blood-brain barrier monoamine oxidase: enzyme characterization in cerebral microvessels in six mammilian species, including humans. *Journal of Neurochemistry*, 49:856-864.

KALARIA, R.N., MITCHELL, M.J. & HARIK, S.I. 1988. Momoamine oxidase of the human brain and liver. *Brain*, 111:1441-1451.

KANKURI, E., VAALI, K., KNOWLES, R.G., LÄHDE, M., KORPELA, R., VAPAATALO, H. & MOILANEN, E. 2001. Suppression of acute experimental colitis by a highly selective inducible nitric oxide synthase inhibitor, N-[3-(aminoethyl)benzyl]acetamidine. *Journal of Pharmacology and Experimental Therapeutics*, 298:1128–1132.

KEITH, C.T., BORISY, A.A. & STOCKWELL, B.R. 2005. Multicomponent therapeutics for networked systems. Nat Rev Discov, 4:71-78.

KEMP, J.A. & MCKERMAN, R.M. 2002. NMDA receptor pathways as drug targets. *Nature Neuroscience*, 5:1039–1042.

KERWIN, J.F., LANCASTER, J.R. & FELDMAN, P.L. 1995. Nitric Oxide: A new paradigm for secondmessengers. *Journal of Medicinal. Chemistry*, 38:4342-4362.

KHALDY, H., LEÓN, J., ESCAMES, G., BIJKDAOUENE, L. & ACUÑA-CASTROVIEJO, D. 2003. Synergistic effects of melatonin and deprenyl protect against MPTP-induced mitochondrial damage and DA depletion. *Neurobiology of Aging*, 24:491–500.

KHALDY, H., LEÓN, J., ESCAMES, G., MARTÍN, M., MACÍAS, M. & ACUÑA-CASTROVIEJO, D. 2002. Circadian rhythm of dopamine and their metabolites in mouse striatum: effects of pinealectomy and melatonin replacement. *Neuroendocrinology*, 75:201–208.

KITA, Y., MURAMOTO, M., FIJIKAWA, A., YAMAZAKI, T., NOTSU, Y. & NISHIMURA, S. 2002. Discovery of novel inhibitors of nitric oxide synthase. *Journal of Pharmacy and Pharmacology*, 54:1141–1145.

KNOWLES, R.G. PALACIOS, M. PALMER, M.R.J. & MONCADA, S. 1989. Formation of nitric oxide from L-Arginine in the central nervous system: A transduction mechanism for stimulation of the soluble guanylate cyclase. *Proceedings of the National Academy of Sciences of the United States of America*, 86:5159-5162.

KONRODI, C., KORNHUBER, J., FROELICH, L., FRITZE, J., HEINSEN, H., BECKMANN, H., SCHULZ, E. & RIEDERER, P. 1989. Demonstration of Monoamine oxidase-A and -B in the human brainstem by histochemical techniques. *Neurosciences*, 33:383- 400.

KORNHUBER, J. & WELLER, M. 1997. Psychotogenicity and N-methyl-D-aspartate receptor antagonism: implications for neuroprotective pharmacotherapy. *Biological Psychiatry*, 41:135-144.

KRUMAN, I., BRUCE-KELLER, A.J., BREDESEN, D., WAEG, G. & MATTSON, M.P. 1997. Evidence that 4-hydroxynonenal mediates oxidative stress-induced neuronal apoptosis. *Journal of Neuroscience*, 17:5089-5100.

LANGHAM, J., GOLDFRAD, C., TEASDALE, G., SHAW, D. & ROWAN,K. 2003. Calcium channel blockers for acute traumatic brain injury. *Cochrane Database of Systematic Reviews*, 4:CD000565.

LEIPER, J., SANTA MARIA, J., CHUBB, A., MACALLISTER, R.J., CHARLES, I.G., WHITLEY, G.S. & VALLANCE, P. 1999. Identification of two human dimethylarginine dimethylamino hydrolase with distinct tissue distributions and homology with microbial arginine deiminases. *Biochemical Journal*, 343:209–214.

LEIPER, J. & VALLANCE, P. 1999. Biological significance of endogenous methylarginines that inhibit nitric oxide synthases. *Cardiovascular Research*, 43:542–548.

LENZLINGER, P.M., MORGANTI-KOSSMANN, M., LAURER, H.L. & MCINTOSH, T.K. 2001. The duality of the inflammatory response to traumatic brain injury. *Molecular Neurobiology*, 24:169–181.

LEÓN, J., VIVES, F., CRESPO, E., CAMACHO, E., ESPINOSA, A., GALLO, M. A., ESCAMES, G. & ACUNA-CASTROVIEJO, D. 1998. Modification of nitric oxide synthase activity and neuronal response in rat striatum by melatonin and kynurenine derivates. *Journal of Neuroendocrinology*, 10:297-302.

LEWEN, A., MATZ, P. & CHAN, P.H. 2000. Free radical pathways in CNS injury. *Journal of Neurotrauma*, 17:871–890.

LEWINSOHN, R., GLOVER, V. & SANDLER, M. 1980. Development of benzylamine oxidase and monoamine oxidase A and B in man. *Biochemical Pharmacology*, 29:1221-1230.

LI, H., MARTASEK, P., MASTERS, B.S.S.,POULOS, T.L. & RAMAN, C.S. 2003. Structure of rat neuronal NOS heme domain with 3-Bromo-7-Nitroindazole bound.

LI, H., RAMAN, C.S., GLASER, C.B., BLASKO, E., YOUNG, T.A., PARKINSON, J.F., WHITLOW, M. & POULOS, T.L.J. 1999. Crystal structures of zinc-free and -bound heme domain of human inducible nitric-oxide synthase. Implications for dimer stability and comparison with endothelial nitric-oxide synthase. Biological Chemistry, 274:21276.

LI, H., RAMAN, C.S., MARTÁSEK, P., KRÁL, V., MASTERS, B.S.S. & POULOS, T.L. 2000. *Journal of Inorganic Biochemistry,*. 81:133-139.

LI, H., RAMAN, C.S., MARTÁSEK, P., MASTERS, B.S.S. & POULOS, T.L. 2001. Crystal structure of nitric oxide synthase bound to nitro indazole reveals a novel inactivation mechanism. *Biochemistry*, 40:5399-5406.

LI, H., SHIMIZU, H., FLINSPACH, M., JAMAL, J., YANG, W., XIAN, M., CAI, T., WEN, E.Z., JIA, Q., WANG, P.G. & POULOS, T.L. 2002. The novel mode of N-alkyl-N'-hydroxyguanidine to neuronal nitric oxide synthase provides mechanistic insights into NO biosynthesis. *Biochemistry*, 41:13868-13875.

LI H. & POULOS T.L. 2005. Structure-function studies on nitric oxide synthases. *Journal of Inorganic Biochemistry*, 99:293-305.

LIPTON, S.A., CHOI, Y.B., TAKAHASHI, H., ZHANG, D., LI, W., GODZIK, A. & BANKSTON, L.A. 2002. Cysteine regulation of protein function – as exemplified by NMDA-receptor modulation. *Trends in Neurosciences*, 25:474–480.

LIPTON, S.A. & CHEN, H.V. 2004. Paradigm shift in neuroprotective drug development: clinically tolerated NMDA receptor inhibition by memantine. *Cell death and Differentiation*, 11:18-20

LOW S.Y. 2005. Application of pharmaceuticals to nitric oxide. *Molecular aspects of Medicine*, 26:97-138.

MALAN, S.F., VAN DER WALT, J.J. & VAN DER SCHYF, C.J. 2000. Structure-activity relationships of polycyclic aromatic amines with calcium channel activity. *Archive der pharmzie*, 333(1):10-17.

MANEV, H., UZ, T., KHARLAMOV, A. & JOO, J.Y. 1996. Increased brain damage after stroke or excitotoxic seizures in melatonin-deficient rats. *FASEB Journal*, 10:1546–1551.

MARLETTA M.A. 1993. Nitric oxide synthase structure and mechanism. *Journal of Biological Chemistry*, 268:12231-12234.

MARKLUND, N. *et al.* 2004. Excitotoxicity and traumatic brain injury. Pathology, treatment approaches and controversies. (*In* Ferrarese, C. & Beal, M.F., eds. Excitotoxicity in Neurological Diseases. Kluwer Academic Publishers p. 254–271.)

MARKLUND, N. *et al.* 2005. Administration of monoclonal antibodies neutralising the inflammatory mediators tumor necrosis factor alpha and interleukin-6 does not attenuate acute behavioural deficits following experimental traumatic brain injury in the rat. *Restororative Neurology and Neuroscience*, 23:31-42.

MARKLUND, N., BAKSHI, A., CASTELBUONO, D.J., CONTE, V., MCINTOSH, T.K. 2006. Evaluation of Pharmacological Treatment Strategies in Traumatic Brain Injury. *Current Pharmaceutical Design*, 12:1645-1680.

MARTIN, L.J., AL-ABDULLA, N.A., BRAMBRINK, A.M., KIRSCH, J.R., SIEBER, F.E. & PORTERA-CAILLIAU, C. 1998. Neurodegeneration in excitotoxicity, a global cerebral ischemia, and target deprivation: a perspective on the contributions of apoptosis and necrosis. *Brain Research Bulletin*, 46:281-309.

MCCALL, T.B. BOUGHTON-SMITH, N.K. PALMER, R.M.J. WHITTLE, B.J.R. & MONCADA, S. 1989. Synthesis of nitric oxide from L-arginine by neutrophils: Release and interaction with superoxide anion. *Biochemical Journal*, 261:293-296.

MCMURRAY, J. 1999. Organic Chemistry. 5th ed. California : Brooks/Cole. 771 p.

MELDRUM, B. & GARTHWAITE, J. 1990. Excitatory amino acid neurotoxicity and neurodegenerative diseases. *Trends in Pharmacological Sciences*, 11:379-387.

MAYER, B., KLATT, P., WERNER, E. R., & SCHMIDT, K. 1994. Molecular mechanisms of inhibition of porcine brain nitric oxide synthase by the antinociceptive drug 7-nitro-indazole. *Neuropharmacology*, 33:1253-1259.

MENCHER, S.K. & WANG, L.G. 2005. Promiscuous drugs compared to delective drugs. *BioMed Central Clinical Pharmacology*, 5:3.

MIZUNO, Y., SUZUKI, K., SONE, N. & SAITOH, T. 1987. Inhibition of ATP synthesis by 1-methyl-4-phenylpyridinium ion (MPP^+) in isolated mitochondria from mouse brain. *Neuroscience Letters*, 81:204-208.

MONCADA, S. PALMER, R.M. J. & HIGGS, E.A. 1991. Nitric Oxide: Physiology, pathophysiology and pharmacology. *Pharmacological Reviews*, 43:109-142.

MONTGOMERY, Jr. E.B., KOLLER, W.C., LAMANTIA, T.J., NEWMAN, M.C., SWANSON-HYLAND, E., KASZNIAK, A.W. & LYONS, K. 2000a. Early detection of probable idiopathic Parkinson's disease. I. Development of a diagnostic test battery. *Mov Disord*, 15:467–73.

MONTGOMERY, Jr. E.B., LYONS, K. & KOLLER, W.C. 2000b. Early detection of probable idiopathic Parkinson's disease. II. A prospective application of a diagnostic test battery. *Mov Disord*,15:474–8.

MOORE, P.K., OLUYOMI, A.O., BABBEDGE, R.C., WALLACE, P., HART S.L. 1991. L-NG-nitro arginine methyl ester exhibits antinociceptive activity in the mouse. *British Journal of Pharmacology*, 102:198.

MOORE, P.K., WALLACE, P., GAFFEN, Z., HART, S.L., BABBEDGE, R.C. 1993. *Britsh Journal of Pharmacology*, 110:219.

MORALES, D.M., MORALES, D.M., MARKLUND, N., LEBOLD, D., THOMPSON, H. J., PITKANEN, A., MAXWELL, W.L., LONGHI, L., LAURER, H., MAEGELE, M., NEUGEBAUER, E., GRAHAM, D.I., STOCCHETTI, N., MCINTOSH, T.K. 2005. Experimental models of traumatic brain injury: do we really need to build a better mousetrap? *Neuroscience*, 136:971-989.

MOREL, P., TALLINEAU, C., PONTCHARRAUD, R., PIRIOU, A. & HUGHET, F. 1999. Effects of 4-hydroxynonenal, a lipid peroxidation product, on dopamine transport and Na^+/K^+-ATPase in rat striatal synaptosomes. *Neurochemistry International*, 33:531-540.

MULLER, D.P.R. 1997. Neurological disease. (*In*: Sies, H. ed. Antioxidants in disease mechanisms and therapy. New York : Academic Press. p. 557– 580.

MUÑOZ-HOYOS, A., SANCHEZ-FORTE, M., MOLINA-CARBALLO, A., ESCAMES, G., MARTIN-MEDINA, E., REITER, R.J., MOLINA-FONT, J.A. & ACUÑA-CASTROVIEJO, D. 1998. Melatonin's role as an anticonvulsant and neuronal protector. Experimental and clinical evidence. *Journal of Child Neurology*, 13:501–509.

MURRAY, R.K. 1996. The biochemical basis of some neuropsychiatric disorders. (*In* Murray, R.K., Granner, D.K., Mayes, P.A. & Rodwell, V.W. eds. Harper's Biochemistry. Stamford, Conn. : Appleton & Lange. p. 794-813.

NAKAO, N. & BRUNDIN, R. 1997. Effects of a-phenyl-tert-butyl nitrone on neuronal survival and motor function following intrastriatal injections of quinolinic acid or 3-nitropropionic acid. *Neuroscience*, 76:749-761.

NANRI, K., MONTECOT, C., SPRINGHETTI, V., SEYLAZ, J., & PINARD, E. 1998. The selective inhibitor of neuronal nitric oxide synthase, 7-nitroindazole, reduces the delayed neuronal damage due to forebrain ischemia in rats. *Stroke*, 29:1248-1254.

NYIREDY, S.Z., ERDELMEIER, C.A.J., MEIER, B. & STICHER, O. 1985. "Prisma": ein model zur optimierung der mobilen phase für die dünnschichtchromatographie, vorgestelt an hand vershiedener naturstofftrennungen. *Planta Medica*: 241-246.

OLANOW, C.W. 1993. A radical hypothesis for neurodegeneration. *Trends in Neurosciences*, 16:439–444.

OLIVER, D.W., DEKKER, T.G., SNYCKERS, F.O. & FOURIE, T.G. 1991a. Synthesis and biological activity of D_3-trishomocubyl-4-amines. *Journal of Medicinal Chemistry*, 34(2):851-854.

OLIVER, D.W., DEKKER, T.G. & SNYCKERS, F.O. 1991b. Antiviral properties of 4-amino-(D_3)-trishomocubanes. *Arzneimittel-forschung/drug research*, 41(1):549-552.

OLIVER, D.W., DEKKER, T.G. & SNYCKERS, F.O. 1991c. Pentacyclo[5.4.$0^{2,6}$.$0^{3,10}$.$0^{5,9}$]ndecylamines. Synthesis and pharmacology. *European Journal of Medicinal Chemistry*, 26:375-379.

OLNEY, J.W., HO, O.L. & RHEE, V. 1971. Cytotoxic effects of acidic and sulphur containing amino acids on the infant mouse central nervous system. *Experimental Brain Research*, 14:61-76.

OTTINO, P. & DUNCAN, J.R. Effects of α-tocopherol succinate on free radical and lipid peroxidation levels in BL6 melanoma cells. *Free Radical Biology and Medicine*, 7:1145-1151.

PEDERSEN, W.A., CASHMAN, N.R. & MATTSON, M.P. 1999. The lipid peroxidation product 4-hydroxynonenal impairs glutamate and glucose transport and choline acetyltransferase activity in NSC-19 motor neuron cells. *Expimental Neurology*, 155:1-10.

PEKINER, C., KELICEN, P., UMA, S. & MIWA, I. 2002. Two nitric oxide synthase inhibitors: pyridoxal aminoguanidine and 8-quinolinecarboxylic hydrazide selectively

inhibit basal but not agoniststimulated release of nitric oxide in rat aorta. *Pharmacological Research*, 46:317–320.

PENG, T.I., JOU, M.J., SHEU, S.S. & GREENAMYRE, J.T. 1998. Visualisation of NMDA receptor-induced mitochondrial calcium accumulation in striatal neurons. *Expimental Neurology*, 149:1-12.

PETROS, A., BENNETT, D. & VALLANCE, P. 1991. Effects of nitric oxide synthase inhibitors in hypotension in patients with septic shock. *Lancet*, 338:1557–1558.

PETROS, A., LAMB, G., LEONE, A., MONCADA, S., BENNETT, D. & VALLANCE, P. 1994. Effects of a nitric oxide synthase inhibitor in humans with septic shock. *Cardiovascular Research*, 28:34–39.

PETTMANN, B. & HENDERSON, C.E. 1998. Neuronal cell death. *Neuron*, 20:633-647.

PITKÄNEN, A., LONGHI, L., MARKLUND, N., MORALES, D.M. & MCINTOSH, T.K. 2005. Neurodegeneration and neuroprotective strategies after traumatic brain injury. *Drug Discovery Today: Disease Mechanisms*, 2:409-418.

PITZELE, B.S. 1999. The inhibition of isoforms of nitric oxide synthase: non-cardiovascular aspects. *Expert Opininion on Therapeutic Patents*, 9:549–566.

POLLOCK, J.S. FöRSTERMANN, U. MITCHEL, J.A. WARNER, T.D. SCHMIDT, H.H. NAKANE, M. & MURAD, F. 1991. Purification and characterization of particulate endothelium derived relaxing factor synthase from cultured and native bovine aortic endothelial cells. *Proceedings of the National Academy of Sciences of the United States of America*, 88:10480-10484.

PORTERA-CAILLIAU, C, PRICE, D.L. & MARTIN, L.J. 1997. Excitotoxic neuronal death in the immature brain is an apoptosis-necrosis morphological continuum. *Journal of Comparative Neurology*, 378:70-87.

POU S., POU W.S., BREDT D.S., SNYDER S.H. & ROSEN G.M. 1992. Generation of superoxide by purified brain nitric oxide synthase. *Journal of Biological Chemistry*, 267:24173–6.

POU S., KEATON L., SURICHAMORN W. & ROSEN G.M. 1999. Mechanism of superoxide generation by neuronal nitric-oxide synthase. *Journal of Biological Chemistry*, 274:9573–80.

PRESTA A., WEBER-MAIN A.M., STANKOVICH M.T. & STIEHR D.J. 1998. Comparative effects of substrates and pterin cofactor on the heme midpoint potential in inducible and neuronal nitric oxide synthases. *Journal of the American Chemical Society*, 120:9460–5.

PRZEDBORSKI, S., JACKSON-LEWIS, V., YOKOYAMA, R., SHIBATA, T., DAWSON, V. L., & DAWSON, T. M. 1996. Role of neuronal nitric oxide in 1-Methyl-4-Phenyl-1,2,3,6-Tetrahydropyridine (MPTP)-induced dopaminergic neurotoxicity. *Proceedings of the National Academy of Sciences of the United States of America*, 93:4565-4571.

RAGHUPATHI, R. 2004. Cell death mechanisms following traumatic brain injury. *Brain Pathology*, 14:215-222.

RAMAN, C.S., LI, H., MARTÁSEK, P., SOUTHAN, G., MASTERS, B.S.S. & POULOS, T.L. 2001. Crystal structure of nitric oxide synthase bound to nitro indazole reveals a novel inactivation mechanism. *Biochemistry*, 40:13448-13455.

REITER, R.J. 1995. Oxidative processes and antioxidative defense mechanisms in the aging brain. *FASEB Journal*, 9:26– 533.

REITER, R.J. 1998. Oxidative damage in the central nervous system: protection by melatonin. *Progress in Neurobiology*, 56:359–384.

ROBERTS, I. *et al.*, 2000. Aminosteroids for acute traumatic brain injury. *Cochrane Database Systematic Reviews*,. 4:CD001527.

ROSEN G.M., TSAI P. & POU S. 2002. Mechanism of free-radical generation by nitric oxide synthase. *Chemical Reviews*, 102:1191–200.

ROSEN G.M., TSAI P., WEAVER J., PORASUPHATANA S., ROMAN L.J. & STARKOV A.A. 2002. Role of tetrahydrobiopterin in the regulation of neuronal nitric-oxide synthase-generated superoxide. *Journal of Biological Chemistry*, 277:40275–80.

ROMAN L.J., MATTÁSEK P. & MASTERS B.S.S. 2002. Intrinsic and extrinsic modulation of nitric oxide synthase activity. *Chemical Reviews*, 102:1179–89.

SALTER, M. & KNOWLES, R.G. 1998. Assay of NOS activity by the measurement of conversion of oxyhemoglobin to methemoglobin by NO. (*In* Titheradge, M.A., ed. Methods in molecular biology, vol. 100. Nitric oxide protocols. Totowa, New Jersey : Humana press. p. 61-65.

SATTLER, R. & TYMIANSKI, M. 2000. Molecular mechanisms of calciumdependent excitotoxicity. *Journal of Molecular Medicine*, 78:3-13.

SHINODA, J. & WHITTLE, I.R. 2001. Nitric oxide and glioma: a target for novel therapy. *Br. J. Neurosurg*, 15:213–220.

SHOHAMI, E., YANNAI, E.B., HOROWIT, M. & KOHEN, R. 1997. Oxidative stress in closed head injury: brain antioxidant capacity as an indicator of functional outcome. *Journal of Cerebral Blood Flow Metabolism*, 17:1007–1019.

SIDDHANTA U., PREST A., FAN B., WOLAN D., ROUSSEAU D.L. & STUEHR D.J. 1998. Domain swapping in inducible nitric-oxide synthase. Electron transfer occurs between flavin and heme groups located on adjacent subunits in the dimer. *Journal of Biological Chemistry*, 273:18950–8.

SIMONIAN, N.A. & COYLE, J.T. 1996. Oxidative stress in neurodegenerative diseases. *Annual Review of Pharmacology and Toxicology*, 36:83-106.

SINGH, J., THORNTON, J.M., SNAREY, M. & CAMPBELL, S.F. 1987. The geometries of interacting arginine-carboxyls in proteins. *FEBS Letters*, 224:161-171.

SKET, D. & PAVLIN, R. 1985. Monoamine oxidase in single nerve cell bodies from locus coeruleus of the rat : A microgasometric study. *Biochemical Pharmacology*, 34:1025-1028.

STILL, W.C., KAHN, M. & MITRA, A. 1978. Rapid chromatographic technique for preparative separations with moderate resolusion. *Journal of Organic Chamistry*, 43:2923-2925.

SMYTH, M.S. & MARTIN, J.H.J. 2000. X-ray crystallography. *Journal of Clinical Pathology*, 53:8–14.

STOUT, A.K., RAPHAEL, H.M., KANTEREWICZ, B.I., KLANN, E. & REYNOLDS, I.J. 1998. Glutamate-induced neuron death requires mitochondrial calcium uptake. *Nature Neuroscience*, 1:366-373.

STUEHR, D. J., CHO, H. J., KWON, N. S. WEISE, M. F. & NATHAN, C.F. 1991. Purification and characterization of the cytokine-induced macrophage nitric oxide synthase: a FAD-Containing and FMN-Containing Flavoproteins. *Proceedings of the National Academy of Sciences of the United States of America*,. 88:7773-7777.

STUEHR D.J., KWON N.S., NATHAN C.F., GRIFFITH O.W., FELDMAN P.L. & WISEMAN J. 1991. N^{ω}-Hydroxy-L-arginine is an intermediate in the biosynthesis of nitric oxide from L-arginine. *Journal of Biological Chemistry*, 266:6263–95.

SUDA, O., TSUTSUI, M., MORISHITA, T., TANIMOTO, A., HORIUCHI, M., TASAKI, H., HUANG, P.L., SASAGURI, Y., YANAGIHARA, N. & NAKASHIMA, Y. 2002. Long-term treatment with Nx-nitro-L-arginine methyl ester (L-NAME) causes arteriosclerotic coronary lesions in endothelial nitric oxide synthase-deficient mice. *Circulation*, 106:1729–1735.

SUTTON, H.C., ROBERTS, P.B. & WINTERBOURN, C.C. 1976. The rate of reation of superoxide radical ion with oxyhaemoglobin and methaemoglobin. *Biochemical Journal*, 155:503-510.

SWAROOP, G.R., KELLY, P.A.T., BELL, H., YAMAGUCHI, S., SHINODA, J. & WHITTLE, I.R. 2000. The effects of chronic nitric oxide synthase expression on glioma pathophysiology. *British Journal of Neurosurgery*, 14:543–548.

SZABO, C., ZINGERELLI, B., O'CONNOR, M. & SALZMAN, A.L. 1996. DNA strand breakage, activation of poly, (ADP-ribose) synthetase, and cellular energy depletion are involved in the cytotoxicity of macrophages and smooth muscle cells exposed to peroxynitrite. *Proceedings of the National Academy of Sciences of the United States of America*, 93:1753-1758.

TATTON, W.G. & CHALMERS-REDMAN, R.M.E. 1998. Mitochondria in neurodegenerative apoptosis: an opportunity for therapy? *Annals of Neurology*, 44:S134-S141.

THOMSEN, L.L., SCOTT, J.M., TOPLEY, P., KNOWLES, R.G., KEERIE, A.J. & FREND, A.J. 1997. Selective inhibition of inducible nitric oxide synthase inhibits tumor growth *in vivo*: studies with 1400W, a novel inhibitor. *Cancer Research*, 57:3300–3304.

TIPTON, K.F. 1973. Biochemical aspects of monoamine oxidase. *British Medical. Bulletin*, 29:116-119.

VALLANCE, P. & LEIPER, J. 2002. Blocking NO synthesis: how, where and why?. *Nature Reviews Drug Discovery*, 1:939–950.

VALLANCE, P. 2003. Nitric oxide: therapeutic opportunities. Fundam. *Clinical. Pharmacology*, 17:1–10.

VAN ASSENDELFT, O.W. 1970. Light Absorption Spectra of Hemoglobin Derivatives. (*In* Spectrophotometry of haemoglobin derivatives. Assen: Royal VanGorcum Ltd. p. 47-73.

VAN DER SCHYF, C.J., SQUIER, G.J. & COETZEE, W.A. 1986. Characterisation of NGP0-1), an aromatic polycyclic amine, as calcium antagonist. *Pharmacological Research Communications*, 18:407.

VAN DER SCHYF, C.J., GELDENHUYS, W.J. & YOUDIM, M.B.H. 2006. Multifunctional drugs with different CNS targets for neuropsychiatric disorders. *Journal of Neurochemistry*, 99:1033-1048.

VAN DER WALT, J.J., VAN DER SCHYF, C.J., VAN ROOYEN, J.M., DE JAGER, J. & VAN AARDE, M.N. 1988. Calcium current blockade in the cardiac myocytes by NGP1-01, an aromatic polycyclic amine. *South African Journal of Chemistry*, 84:448-450.

VATASSERY, G.T. 1992. Vitamin E: neurochemistry and implication for Parkinson's disease. *Annals of the New York Academy of Sciences*, 669:92–110.

VORHERR, T., KNOPFE, L., HOFMANN, F., MOLLNER S., PFEUFFER, T. & CARAFOLI, E. 1993. The Calmodulin binding domain of nitric oxide synthase and adenylyl cyclase. *Biochemistry*, 32:6081–6088.

WARREN, J.B. 1994. Nitric oxide and human skin blood flow responses to acetylcholine and ultraviolet light. *FASEB Journal*, 8:247–251.

WESTLUND, K.N., DENNEY, R.M., ROSE, R.M. & ABELL, C.W. 1988. Localization of distinct monoamine oxidase a and monoamine oxidase b cell populations in human brainstem. *Neuroscience*, 25:439-456.

WILKES, D.K. 2005. Polycyclic aminoguanidines: novel entities for neuroprotection. North-West University. (Dissertation – M.Sc.) 82p.

WINK, D.A., NIMS, R.W., DARBYSHIRE, J.F., CHRISTODOULOU, D., HANBAUER, I., COX, G.W., LAVAL, F., COOK, J.A., KRISHNA, M.C. DeGRAFF, W.G. & MITCHELL, J.B. 1994. Reaction kinetics for nitrosation of cysteine and glutathione in aerobic nitric oxide solutions at neutral intermediates generated in the NO/O_2 reaction pH. Insights into the fate and physiological effects of intermediates generated in the NO/O_2 reaction. *Chemical Research in Toxicology*, 7:519-525.

WOLFF, D. J., & GRIBIN, B. J. 1994. *Archives of Biochemistry and Biophysics*, 311:300-306.

WOLFF, D. J., LUBESKIE, A., & UMANSKY, S. 1994. *Archives of Biochemistry and Biophysics*, 314:360-366.

WOLIN M.S. 2000. Interactions of oxidants with vascular signal systems. *Arteriosclerosis, Thrombosis, and Vascular Biology*, 20:1430–42.

WOLLMUTH, L.P. & SOBOLEVSKY, A.I. 2004. Structure and gating of the glutamate receptor ion channel. *Trends in Neurosciences*, 27:321–328.

WONG, E.H. & KEMP, J.A. 1991. Sites for antagonism on the N-methyl-D-aspartate receptor channel complex. *Annual Review of Pharmacology and Toxicology*, 31:401–425.

YAMAGUCHI, S., SHINODA, J., HOLMES, M.C. & WHITTLE, J.R. 1999. Is tumourogenicity dependent on glioma expression of iNOS? Studies using antisense knockout of iNOS expression C6 glioma cell line. *Neurooncology*, 1:S103.

YAMAMOTO, H. & TANG,H. 1998. Effects of 2-amino-7-phosphonoheptanoic acid, melatonin or N-nitro-L-arginine on cyanide or N-methyl-D-aspartate-induced neurotoxicity in rat cortical cells. *Toxicology Letters*, 94:13–18.

YOUNG, B. *et al.* 1996. Effects of pegorgotein on neurologic outcome of patients with severe head injury. A multicenter, randomised controlled trial. *JAMA*, 276: 538-543.

ZAH, J., TERRE'BLANCHE, G., ERASMUS, E. & MALAN, S.F. 2003. Physiological prediction of a brain-blood distribution profile in polycyclic amines. Bioorganic and Medicinal Chemistry, 11(17):3569-3578.

ZEEVALK, G.D. & NICKLAS, W.J. 1990. Chemically induced hypoglycemia and anoxia: relationship to glutamate receptor-mediated toxicity in retina. *Journal of Pharmacology and Experimental Therapeutics*, 253:1285-1292.

ZHANG, Y., DAWSON, V.L., & DAWSON, T.M. 2000. *Neurobiology of Disease*, 7:240-250.

ZHANG, J., DAWSON, V.L., DAWSON, T.M. & SNYDER, S.H. 1994. Nitric oxide activation of poly(ADP-ribose) synthetase in neurotoxicity. *Science*, 263:687-689.

- Infrared spectroscopy
- Mass spectrometry
- ^{1}H nuclear magnetic resonance spectrometry
- ^{13}C magnetic resonance spectrometry

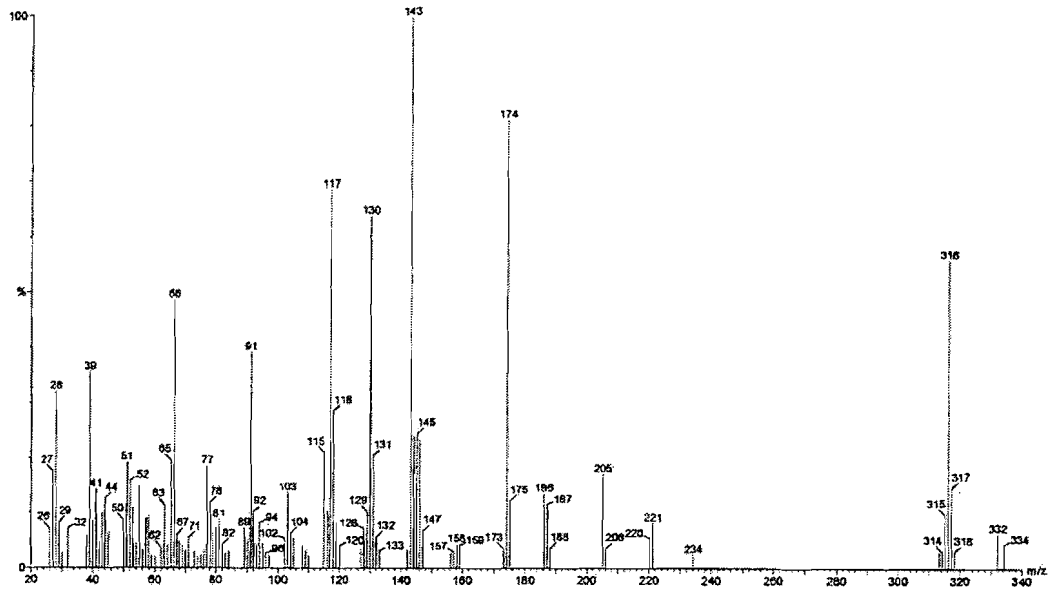

Spectrum 1: Mass spectrometry of **1**.

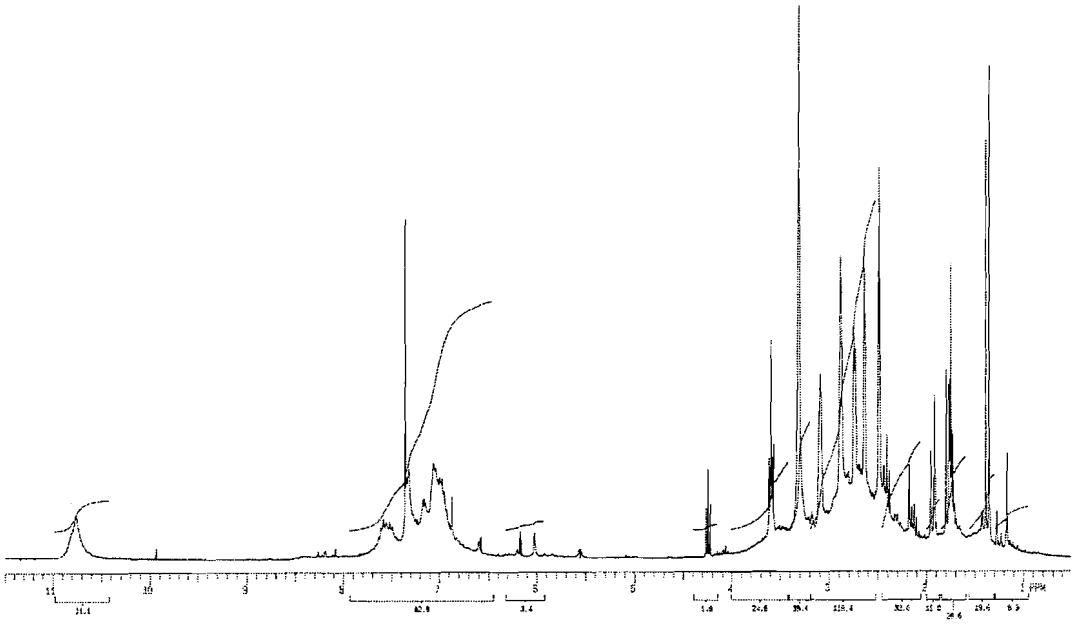

Spectrum 2: ^{1}H NMR of **1**.

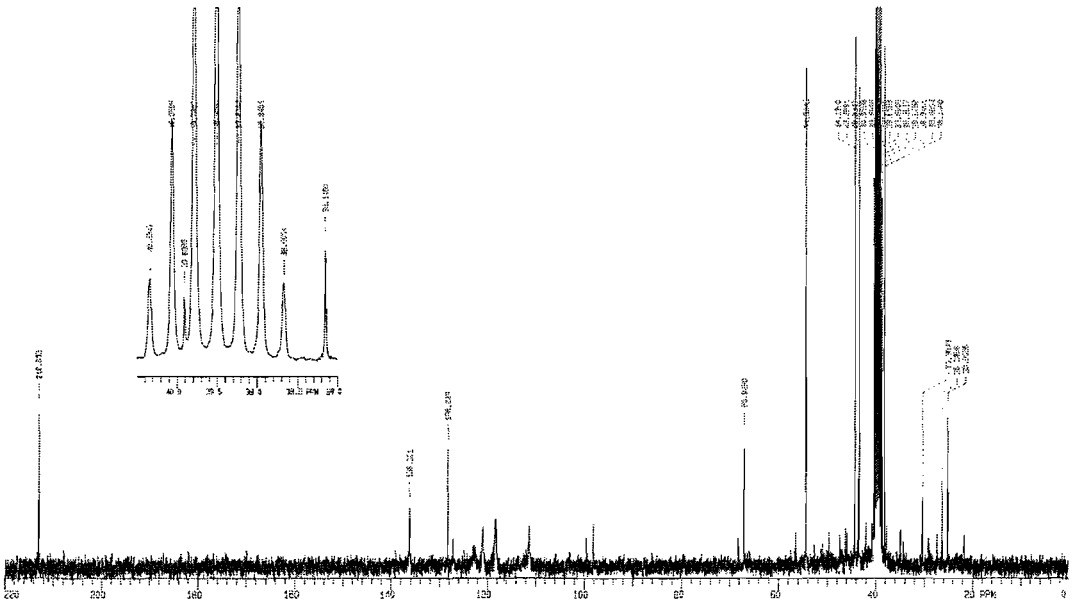

Spectrum 3: ^{13}C NMR of **1**.

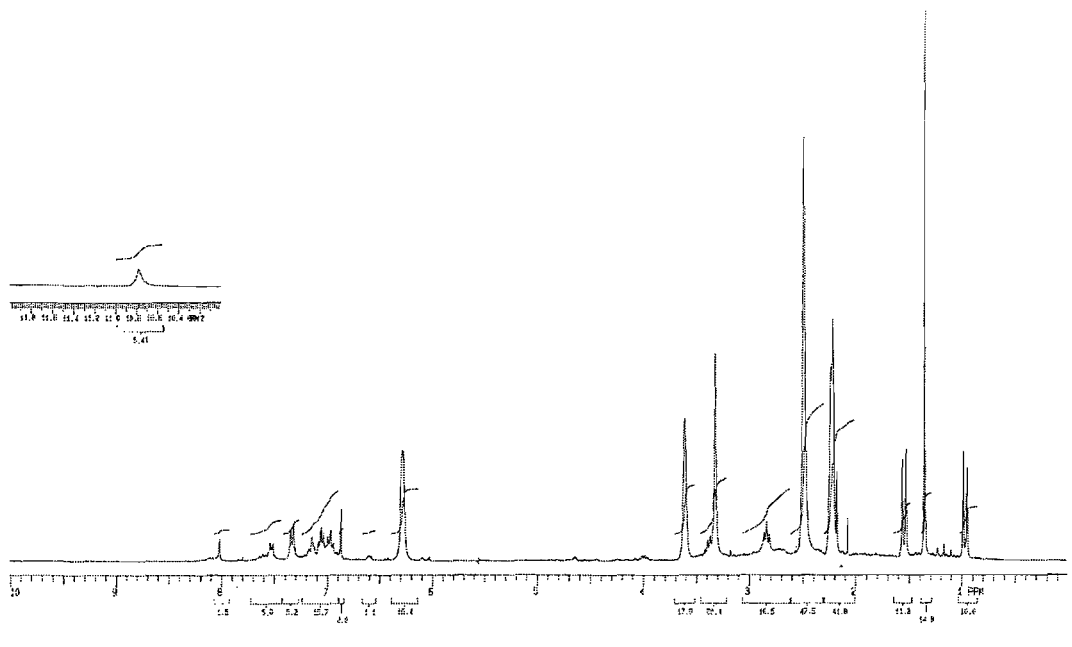

Spectrum 4: ^{1}H NMR of **2**.

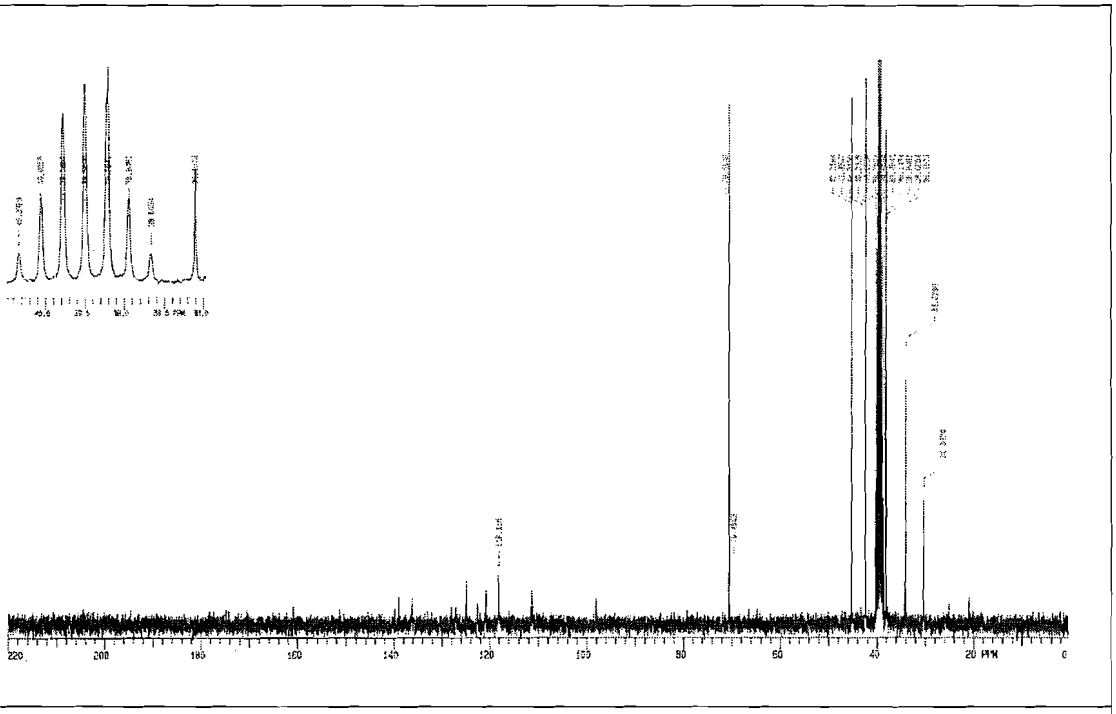

Spectrum 5: ^{13}C NMR of **2**.

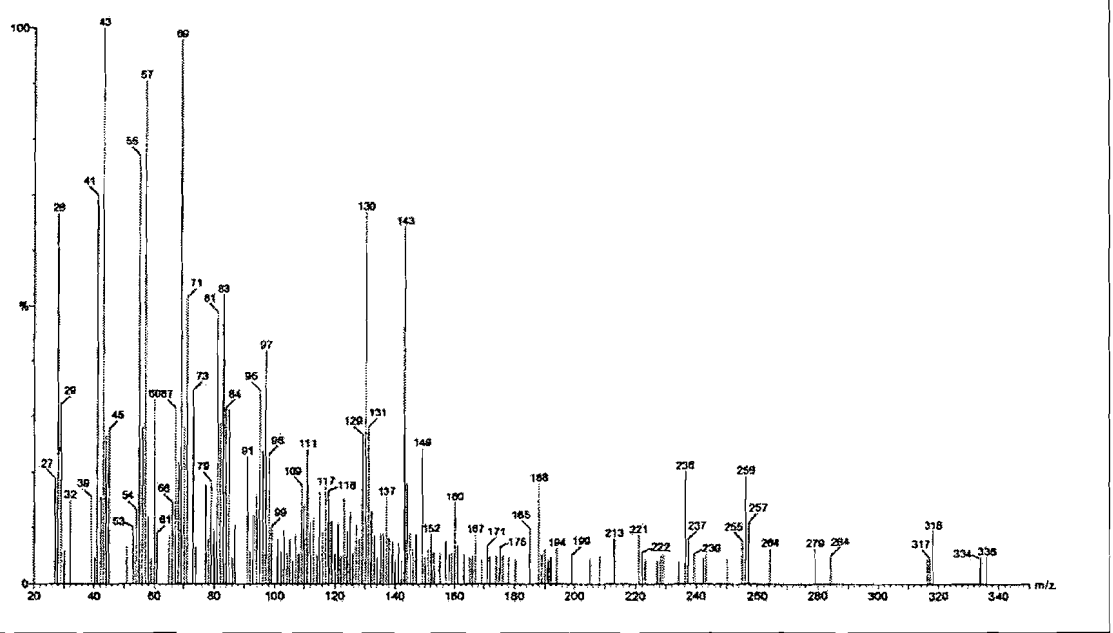

Spectrum 6: Mass spectrometry of **3**.

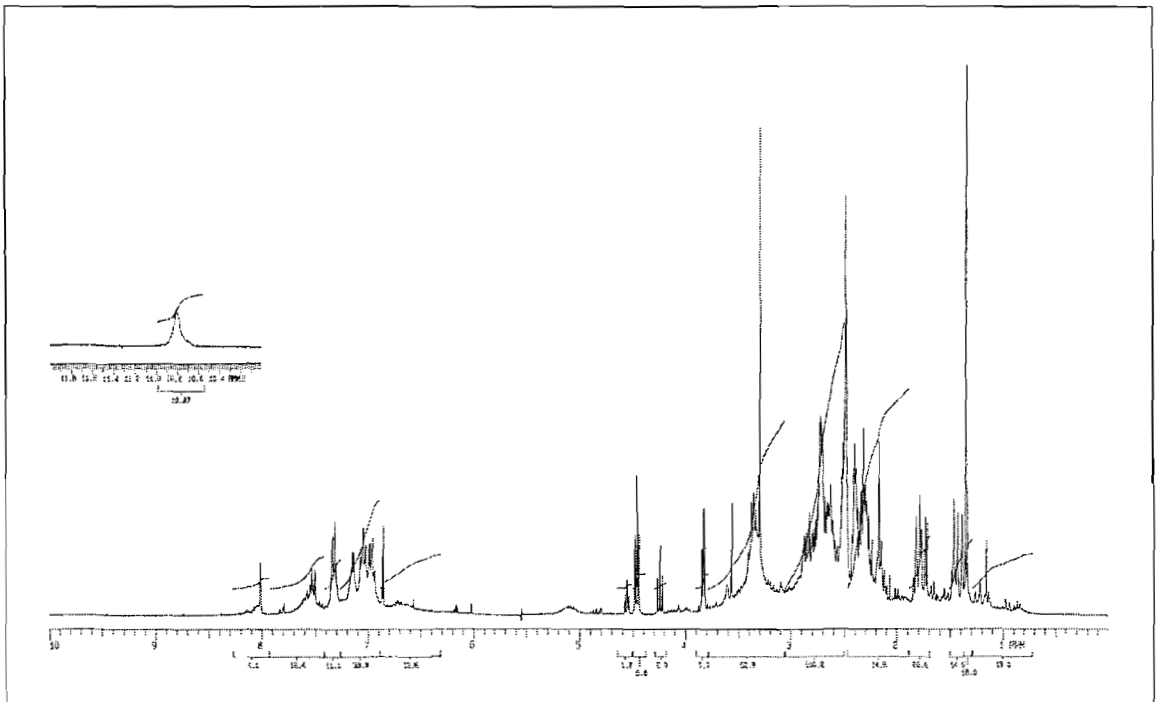

Spectrum 7: ^{1}H NMR of **3**.

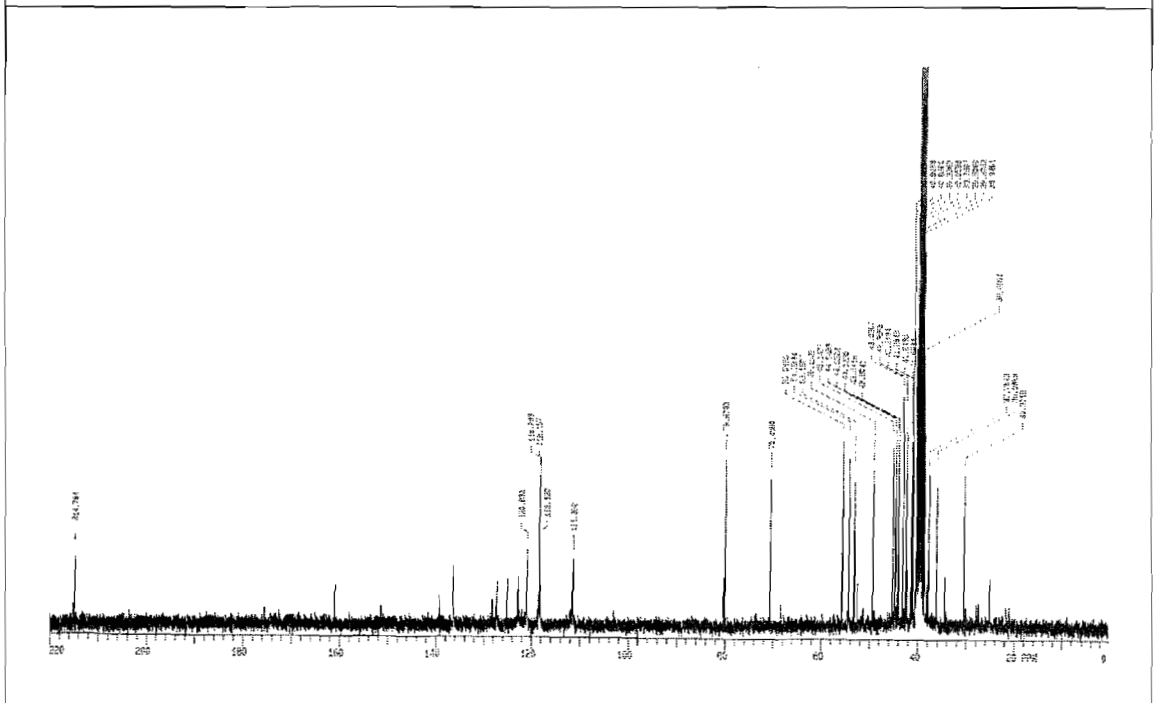

Spectrum 8: ^{13}C NMR of **3**.

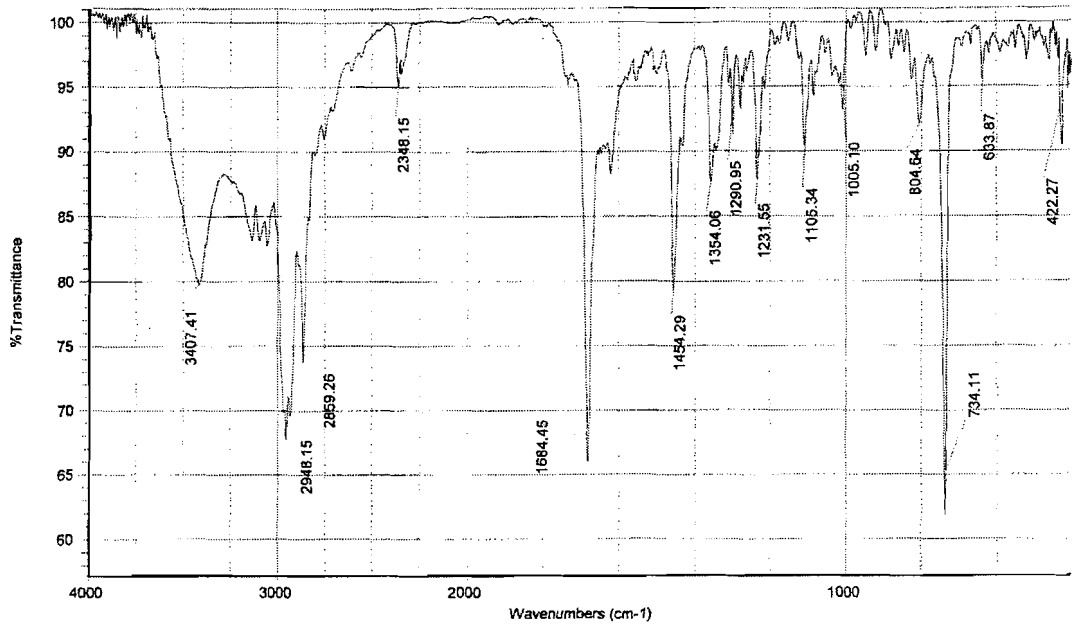

Spectrum 9: Infrared absorption spectrum of **4**.

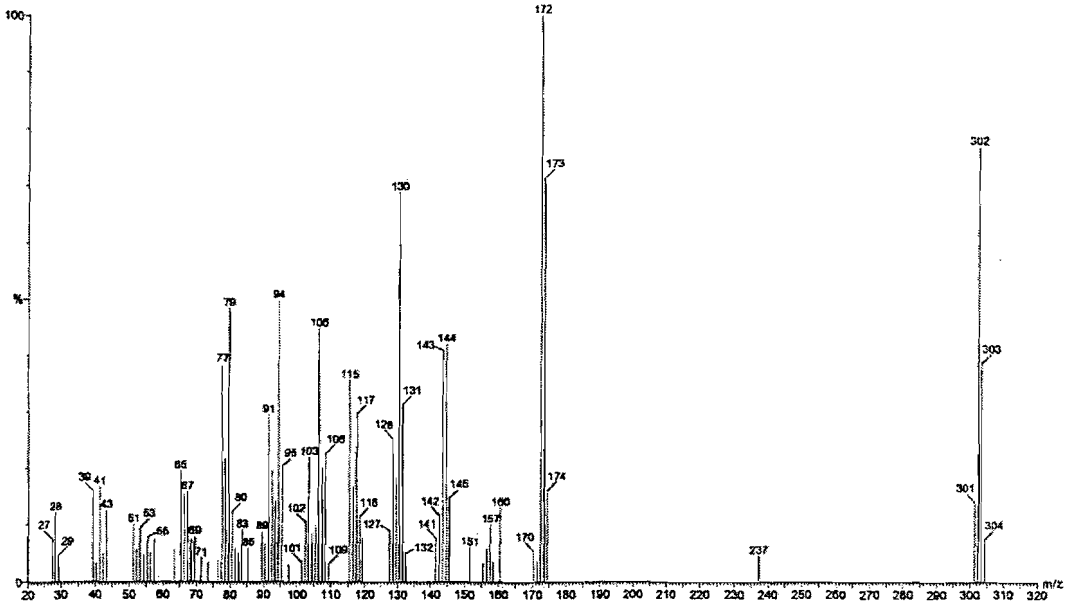

Spectrum 10: Mass spectrometry of **4**.

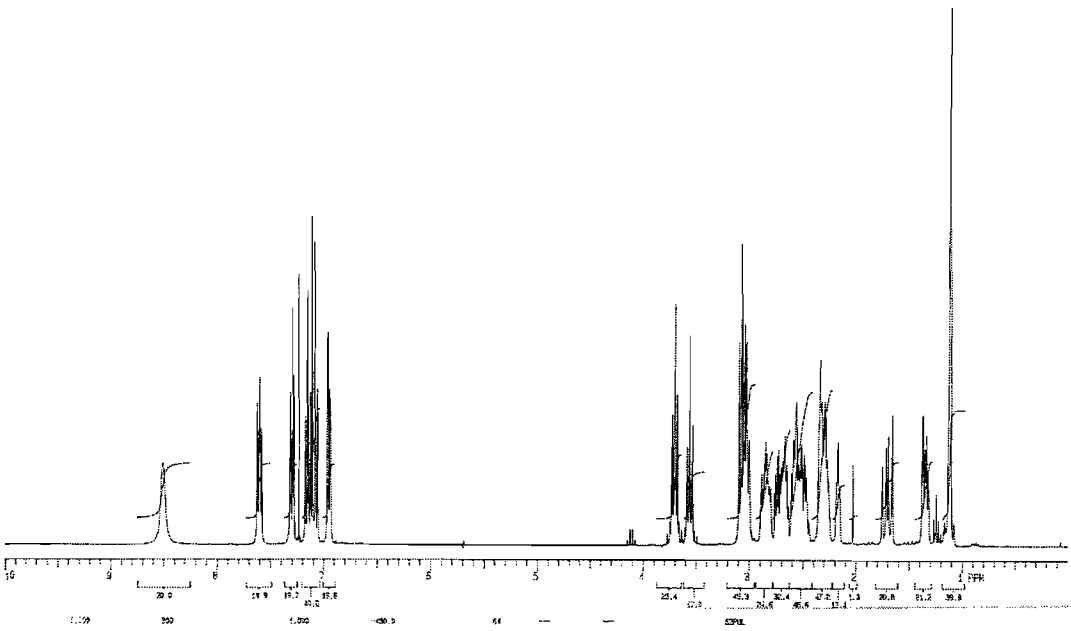

Spectrum 11: ^{1}H NMR of **4**.

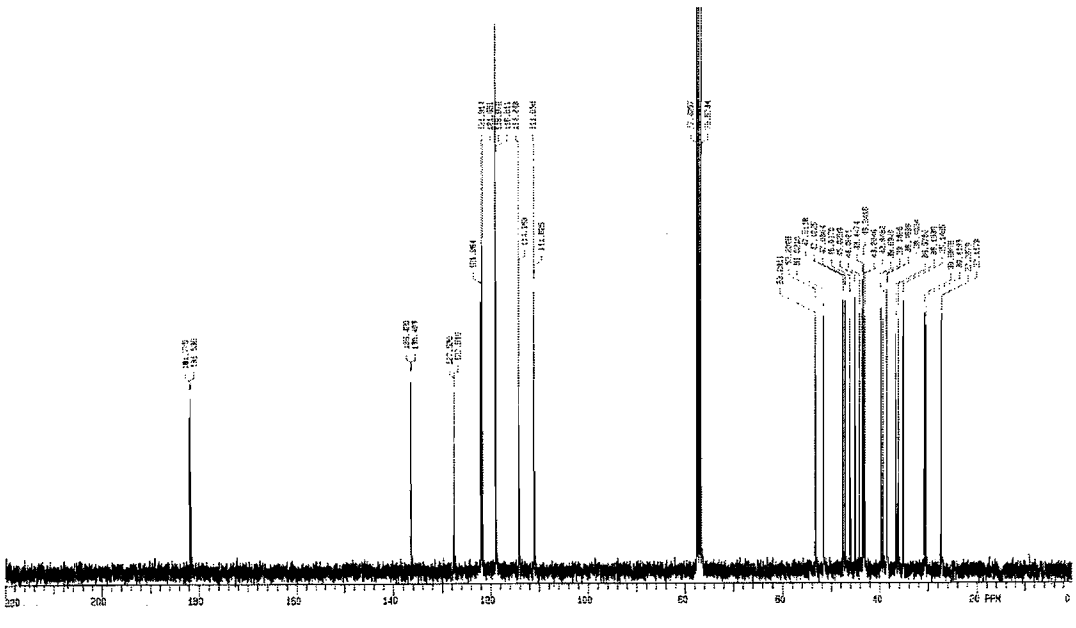

Spectrum 12: ^{13}C NMR of **4**.

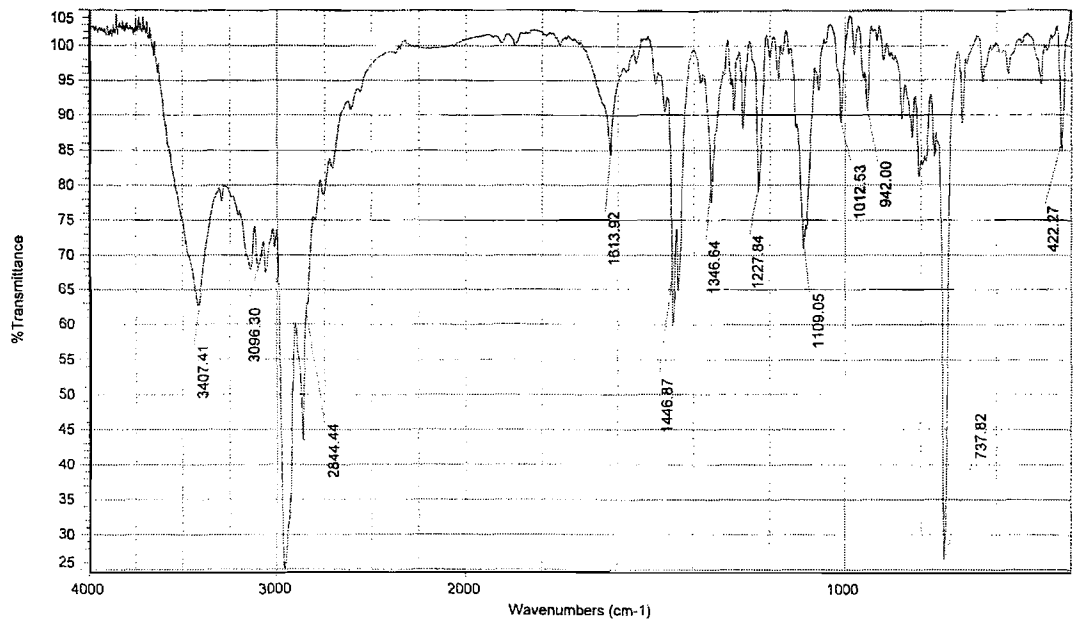

Spectrum 13: Infrared absorption spectrum of **5**.

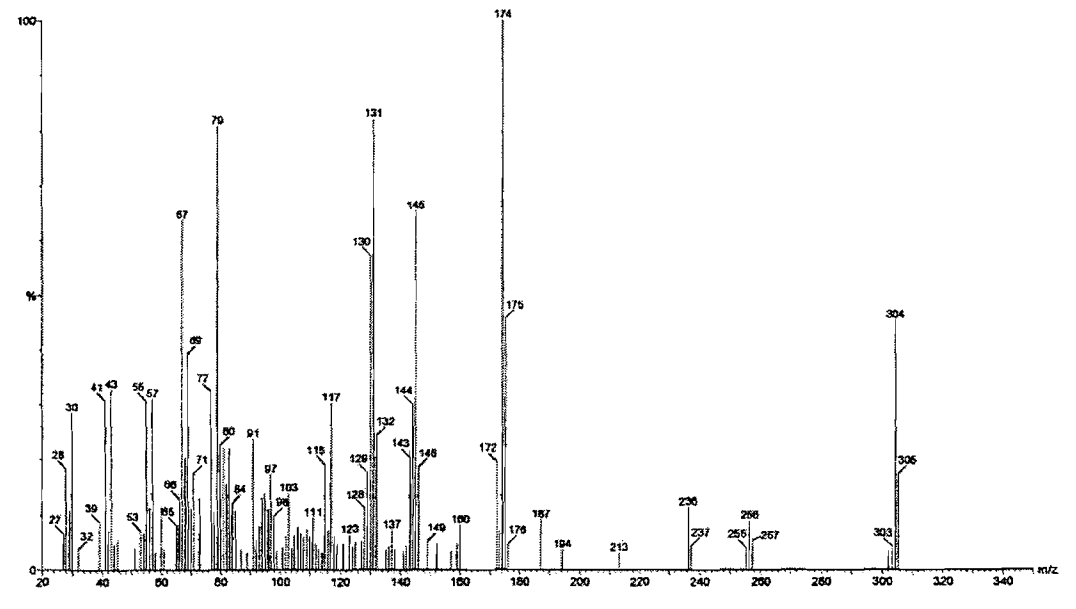

Spectrum 14: Mass spectrometry of **5**.

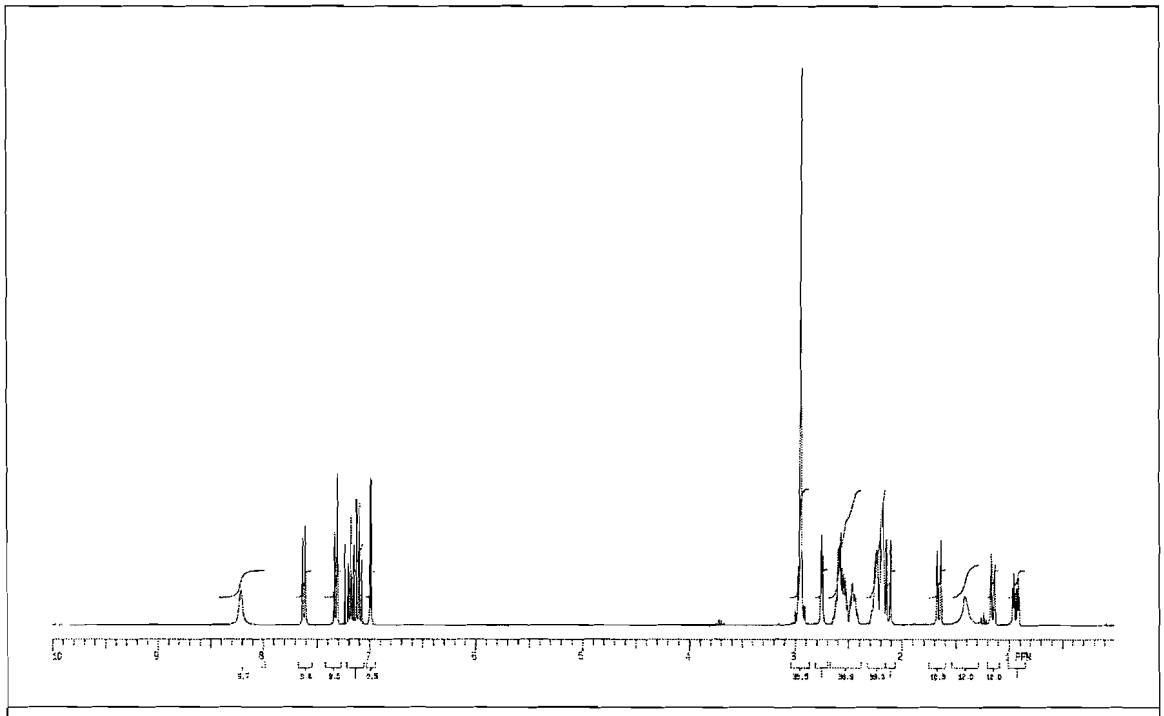

Spectrum 15: ^{1}H NMR of **5**.

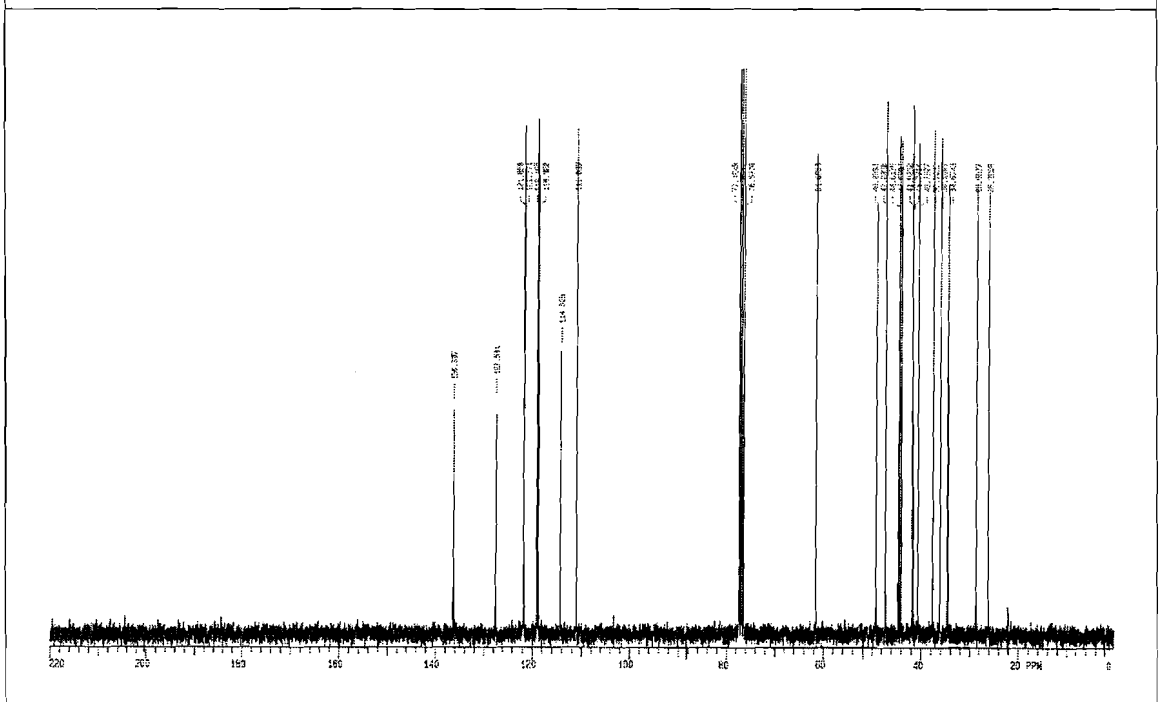

Spectrum 16: ^{13}C NMR of **5**.

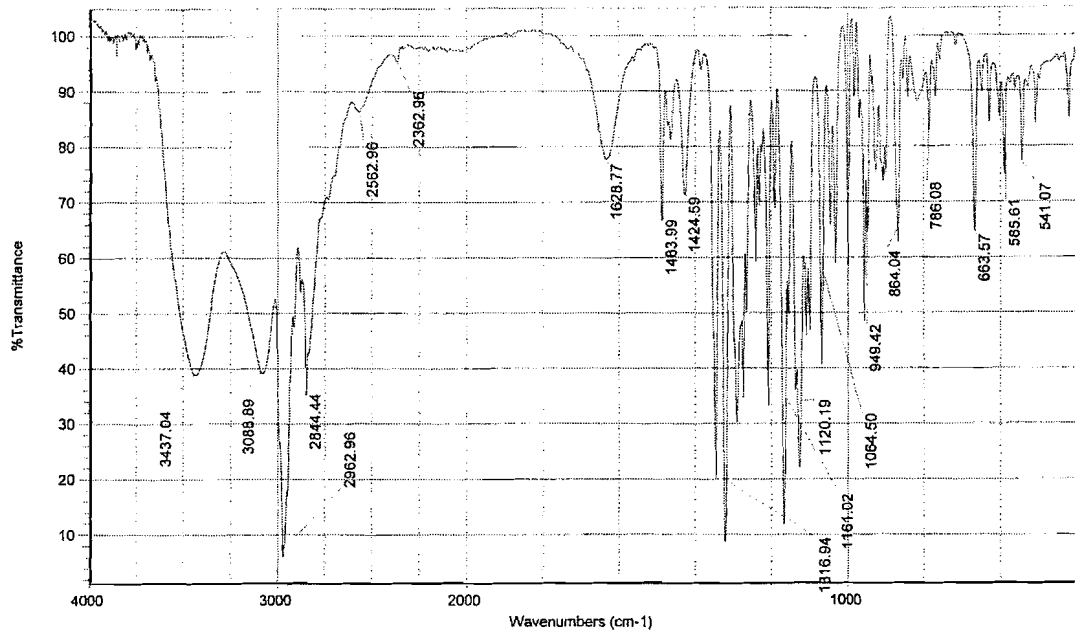

Spectrum 17: Infrared absorption spectrum of **19**.

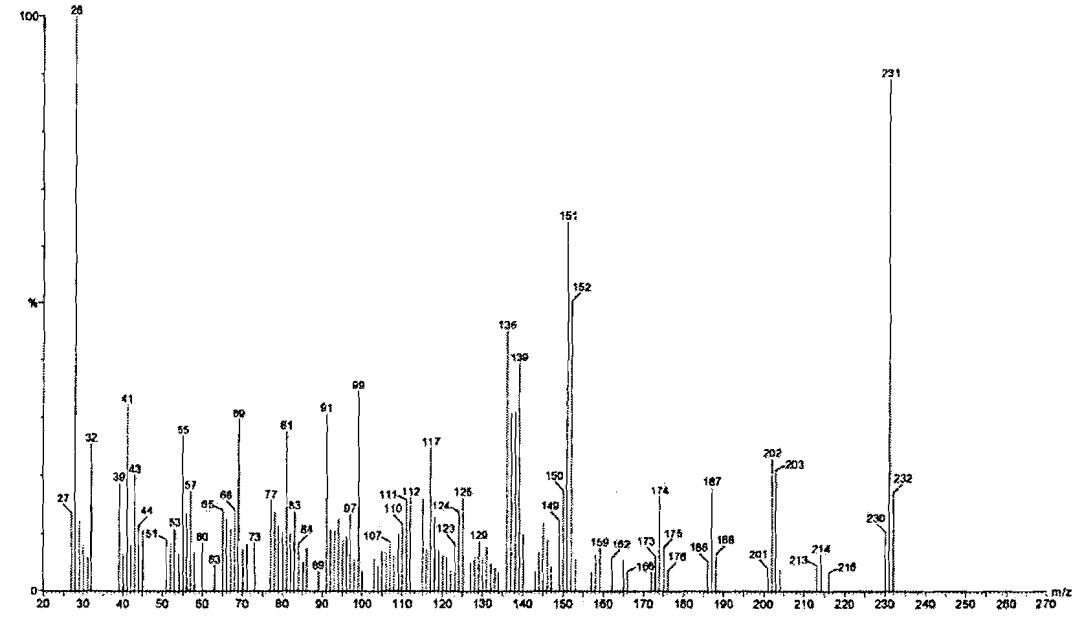

Spectrum 18: Mass spectrometry of **19**.

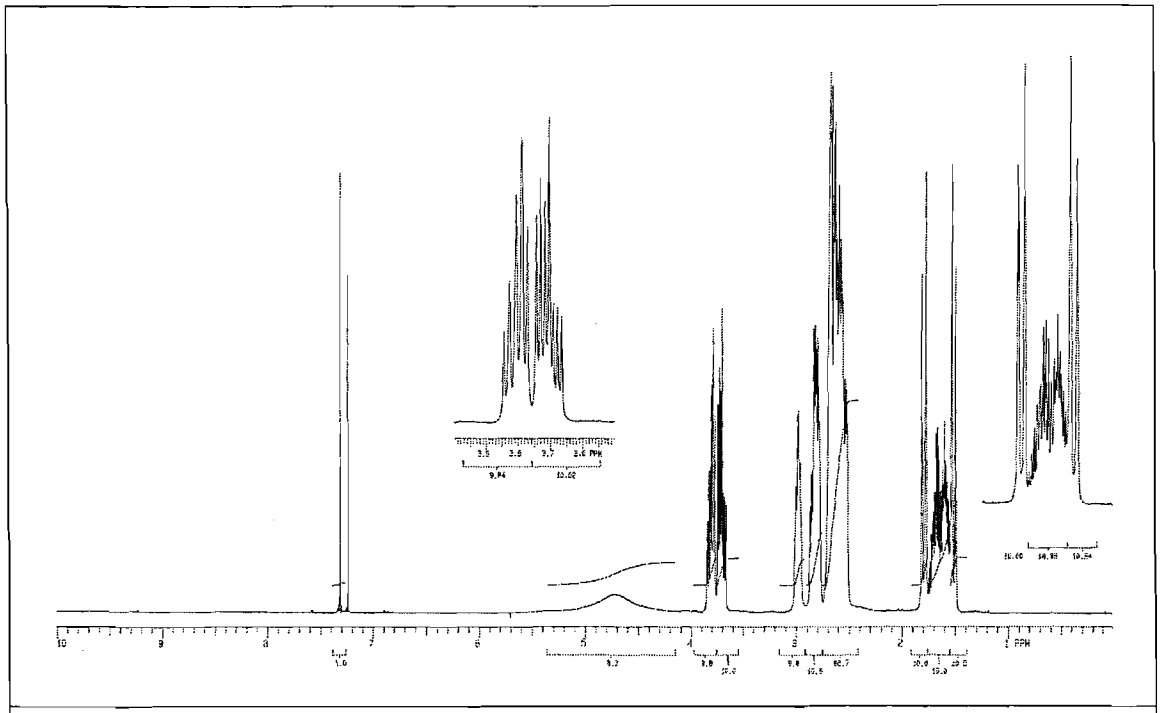

Spectrum 19: ^{1}H NMR of **19**.

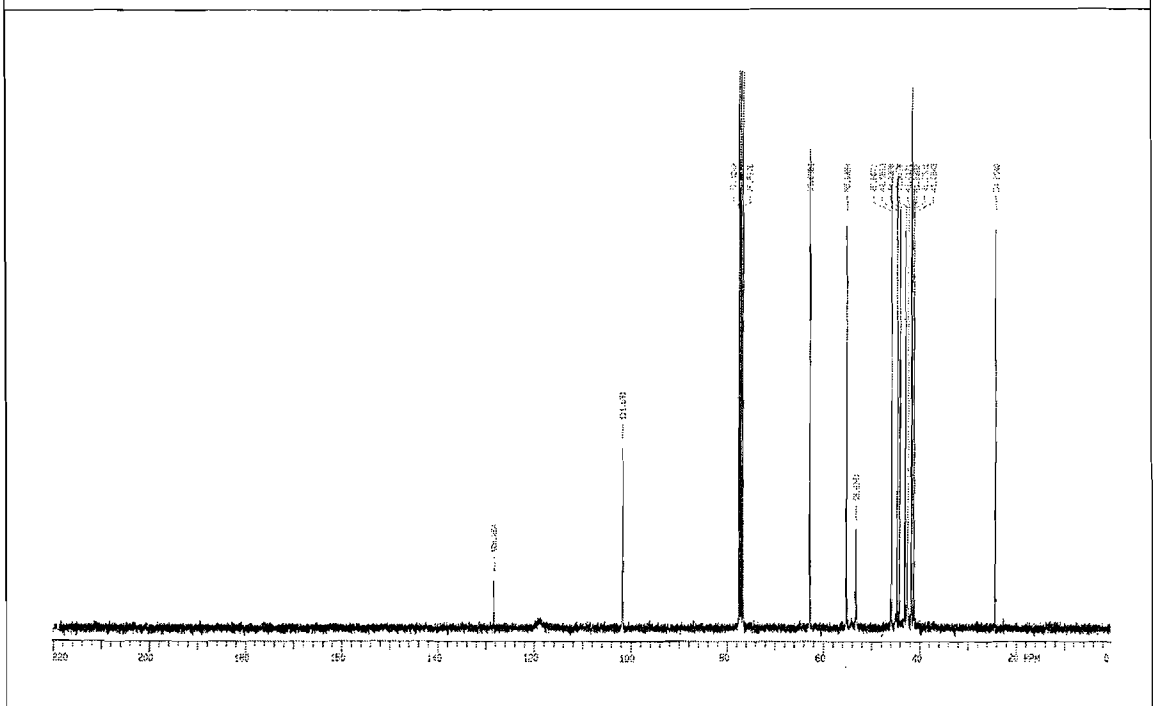

Spectrum 20: ^{13}C NMR of **19**.

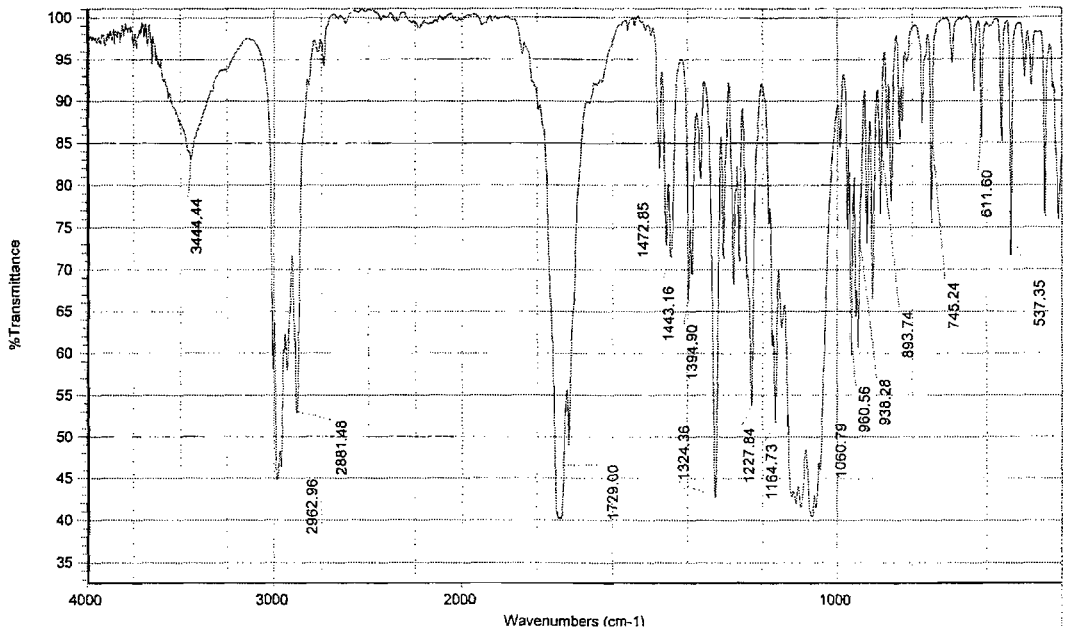

Spectrum 21: Infrared absorption spectrum of **21**.

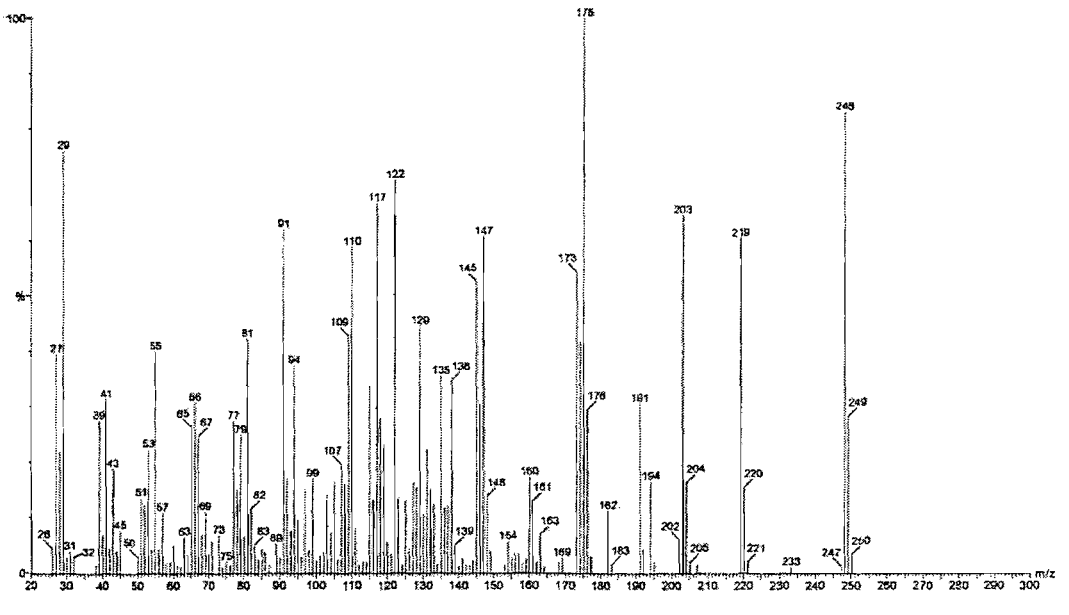

Spectrum 22: Mass spectrometry of **21**.

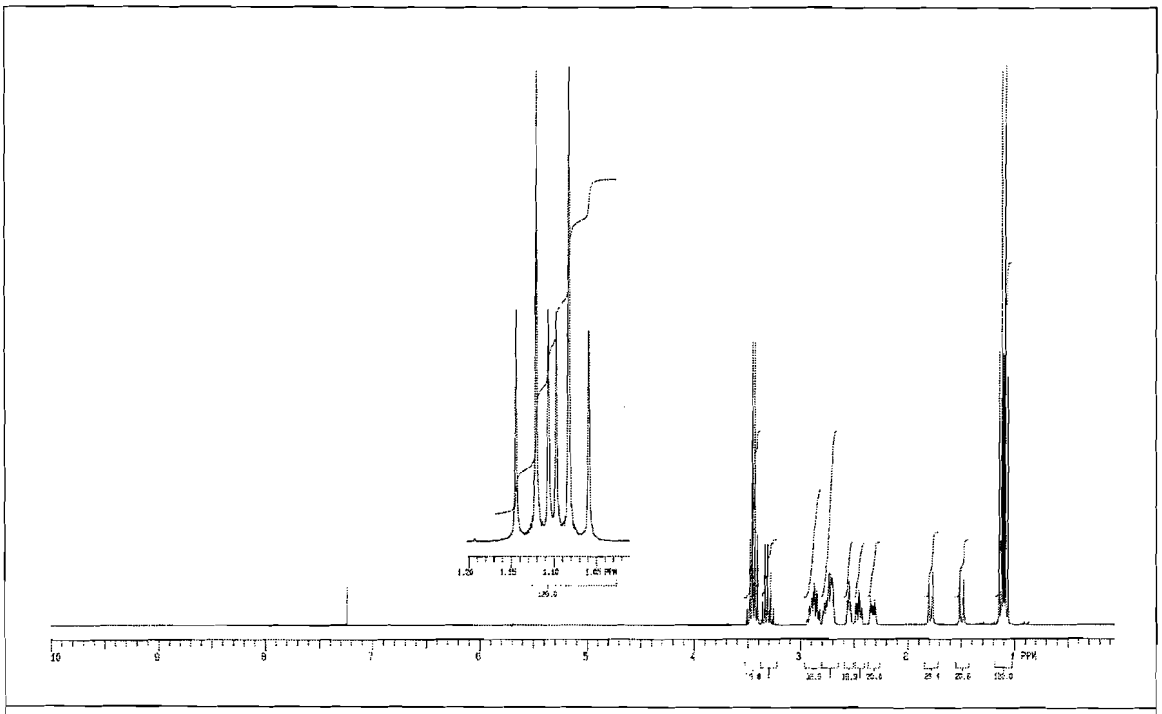

Spectrum 23: ^{1}H NMR of **21**.

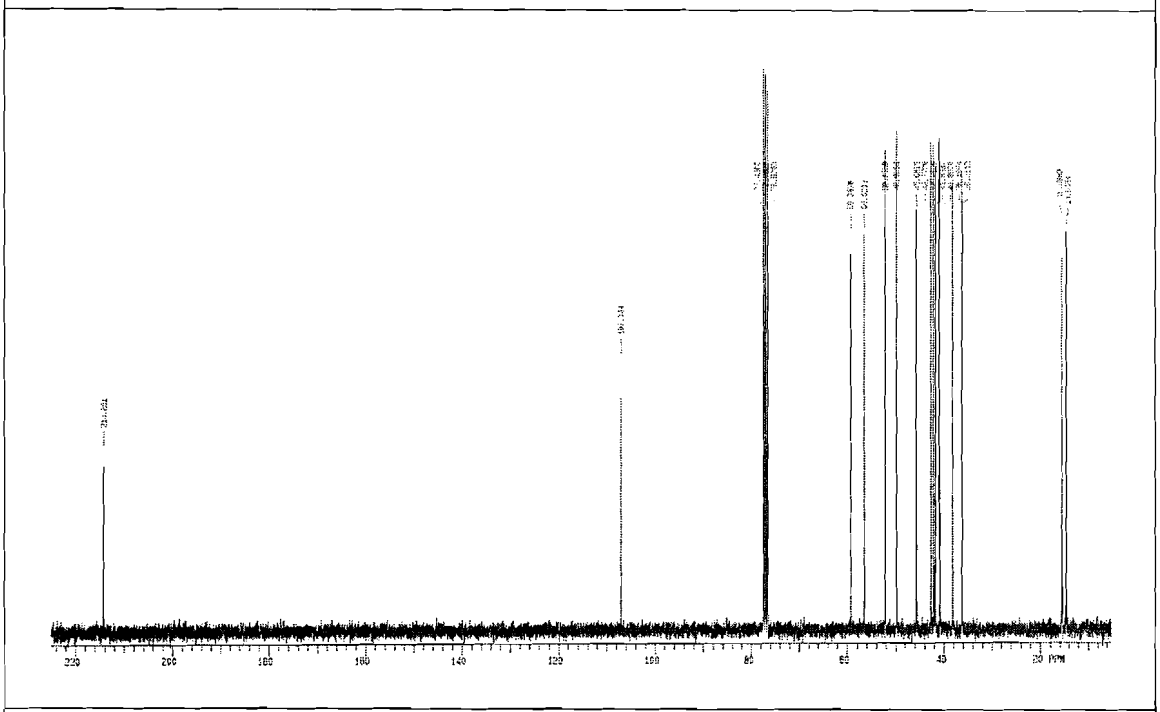

Spectrum 24: ^{13}C NMR of **21**.

- I would like to thank the Lord for His blessing and grace and for granting me the ability and opportunity. All the praise to Him.
- A special thanks to my study leader, Prof. S.F. Malan; my co-study leader, Prof. D.W. Oliver for your assistance and motivation. Without you, this study would not have been possible.
- My parents, Henk and Marie Oets and brothers – thank you for all your prayers and support. I'm proud to have you as my parents.
- My beautiful wife, Stephanie – thank you for your support, love and motivation.
- Dennis Wilkes for his guidance with the NOS assay.
- A special word of thanks to Prof Mino R Caira, University of Cape Town, Department of Chemistry for the x-ray analysis.
- Melanie van Heerden and Nellie Scheepers for their guidance and help with the lipid peroxidation assay.
- Dr. Jacques Petzer for his enthusiasm for chemistry and always willing to help.
- My lab partner, Louis Prins, for listening and motivation.
- A. Joubert and J. Jordaan for their help with the MS and NMR analysis.
- CENQAM for the use of their laboratory and spectrophotometer.
- The National Research Foundation for financial support.
- Kagisho Sempe for always being friendly and helping with chemicals.
- Mr. Cor Bester of the Animal Research Centre at North-West University (Potchefstroom Campus) for your assistance in handling and care of the animals.
- The Department of Pharmaceutical Chemistry and all personnel for friendliness and support.

- I would like to thank the Lord for His blessing and grace and for granting me the ability and opportunity. All the praise to Him.
- A special thanks to my study leader, Prof. S.F. Malan; my co-study leader, Prof. D.W. Oliver for your assistance and motivation. Without you, this study would not have been possible.
- My parents, Henk and Marie Oets and brothers – thank you for all your prayers and support. I'm proud to have you as my parents.
- My beautiful wife, Stephanie – thank you for your support, love and motivation.
- Dennis Wilkes for his guidance with the NOS assay.
- A special word of thanks to Prof Mino R Caira, University of Cape Town, Department of Chemistry for the x-ray analysis.
- Melanie van Heerden and Nellie Scheepers for their guidance and help with the lipid peroxidation assay.
- Dr. Jacques Petzer for his enthusiasm for chemistry and always willing to help.
- My lab partner, Louis Prins, for listening and motivation.
- A. Joubert and J. Jordaan for their help with the MS and NMR analysis.
- CENQAM for the use of their laboratory and spectrophotometer.
- The National Research Foundation for financial support.
- Kagisho Sempe for always being friendly and helping with chemicals.
- Mr. Cor Bester of the Animal Research Centre at North-West University (Potchefstroom Campus) for your assistance in handling and care of the animals.
- The Department of Pharmaceutical Chemistry and all personnel for friendliness and support.